Figure III.6.3-3(a) shows typical autoradiograph of cross-section of iron metal under the exposure time of 16 days. White line, which is across the middle of Fig.III.6.3-3(a), corresponds to grain boundary of iron metal. White small spots, which can be seen everywhere, corresponds to Ag grain whose diameter is 0.1 μm, and it shows the location of tritium. There is no concentrated spot or area of Ag grains, so tritium is distributed homogeneously in pure iron metal. Figure III.6.3-3(b) shows the typical autoradiograph of surface of oxide at the water-oxide interface under the exposure time of 100 days. In this photograph, the octahedron corresponds to iron oxide and it's had been identified the magnetite with XPS analysis. No Ag grain can be observed in this photograph, even the exposure time for oxide surface was much longer than that for iron metal. This result indicated that the oxide contained very low concentration of tritium. From the comparison with the permeation experiment, it was suggested that tritium would mainly diffuse other path except the oxide lattice [6.3-3].

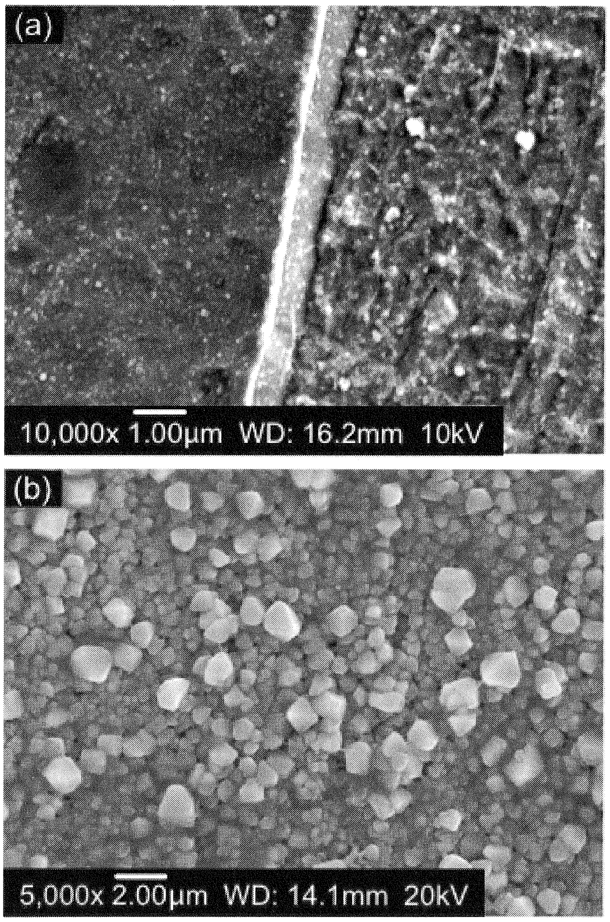

Fig.III.6.3-3 Typical autoradiograph: (a) cross-section of iron metal, (b) surface of iron oxide (magnetite).

In order to establish the effective surface decontamination methods for the ITER construction materials, so-called 'soaking' effect is important, and more systematic data of tritium sorption and desorption for various materials are required under actually considerable conditions. This effect is based on sorption of tritiated water on the materials and subsequent desorption from them. In 2007, the decontamination experiment was carried out as a function of water vapor concentration in the purge gas (N_2) for the organic materials [6.3-4]. When several hundreds ppm of water vapor was added in the chamber after the desorption by purge gas of N_2 for 5-6 hrs, 30-70 % of the tritium sorbed on the materials was quickly removed by the isotope exchange reaction between the water vapor and the tritium sorbed on the materials. It became clear from this result that it was effective to add water vapor to purging gas for the tritium removal on the surface of the organic materials.

In order to accumulate the data for the tritium safe handling system, various experiments were also performed using Caisson Assembly for the Tritium Safety study (CATS) and the other Glove Box under the collaboration with some Japanese universities. Main subjects are follows;

1) Interaction between the various materials and tritium (Kyushu Univ., Shizuoka Univ. and Toyama Univ.),
2) Development of low-level tritium monitor that separated HT/HTO/tritiated hydrocarbons (NIFS, Nagoya Univ. and Niigata Univ.),
3) Tritium behavior in the room (Kyushu Univ.).

Particularly, in the collaboration study with NIFS, Nagoya Univ. and Niigata Univ., the monitor system which was able to measure the low level tritium of each chemical species in the exhaust gas was developed [6.3-5]. The system was composed of a water vapor condenser, a fiber membrane module and ion chambers. The HT/HTO/tritiated hydrocarbons were separated in this system by using tritium.

References

6.3-1 Iwai, Y., *et al.*, "Experimental Durability Studies of Electrolysis Cell Materials for Water Detritiation System," to be published to *Fusion Eng. Des.*

6.3-2 Hayashi, T., *et al.*, "Safe Handling of a Tritium Storage Bed," to be published to *Fusion Eng. Des.*

6.3-3 Isobe, K., *et al.*, "Observation of tritium distribution in iron oxide with tritium micro autoradiography," to be published to *Fusion Sci. Technol.*

6.3-4 Kobayashi, K., *et al.*, *Fusion Sci. Technol.*, **52**, 696 (2007).

6.3-5 Sakuma, Y., *et al.*, "Development of a low-level tritium monitor," to be published in *Fusion Sci. Technol.*

6.4 Successful Operation Results of Tritium Safety Systems in TPL

The safety system of the TPL consists of the Glove Box Gas Purification System (GPS), the Air Cleanup System (ACS), the Effluent Tritium Removal System (ERS) and the Dryer Regeneration System (DRS). The GPS was operated for about 7,900 hours by controlling tritium concentration in the glove boxes. The ACS was operated for cleaning 66,400 m^3 of air during the experiments of Caisson Assembly and maintenance of the glove boxes, experimental apparatus and other tritium operations. The ERS removed about 10 TBq of tritium mainly out of the exhaust gas from the experimental apparatus. The DRS removed 176 liters of tritiated water (41 TBq) from the GPS and ACS dryers.

The tritium safety system of TPL has been in service to support operations with use of tritium since 1988. Some maintenance works such as the periodical inspection or the replacement of superannuated equipment have been carried out in 2007. Figure III.6.4-1 shows monthly environmental tritium release from the stack of TPL during this fiscal year. Total amount of released tritium was 57 GB, which is sufficiently lower than the target value at TPL.

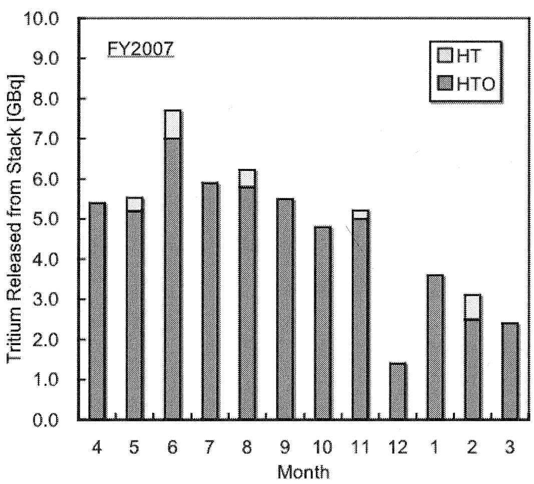

Fig.III.6.4-1 Monthly environmental tritium release at FY2007. Total amount of released tritium was 57GB, which is sufficiently lower than the target value at TPL.

7. Fusion Neutronics

7.1 Blanket Neutronics Experiments

7.1.1 Analyses of Blanket Neutronics Experiments

So far a series of neutronics experiments has been performed at FNS with partial mockups relevant to Japanese solid breeder water cooled TBM; (1) beryllium and enriched Li_2TiO_3 breeder mockup experiments with and without a reflector of SS316 [7.1-1], (2) Li_2O pebble bed mockup experiment [7.1-2], (3) mockup experiment with water panels [7.1-2]. Detailed distributions of tritium production rates (TPRs) were measured in the blanket mockups in the previous studies.

In the present study, these experiments have been analyzed using Monte Carlo code MCNP-4C with the latest nuclear data libraries FENDL-2.1 JENDL-3.3, ENDF-BVII.0 and JEFF-3.1 to evaluate prediction accuracy of the TPR [7.1-3].

Figure III.7.1-1 shows the ratio of the calculation result to the experimental one (C/E) in the first layer of the mockup with water panel. Most of the calculation results agree well with the experimental ones within the experimental error of 7 %. Calculation results of the tritium productions integrated over the diagnostic pellets in each layer agree well with the experimental ones within 5 % in all libraries, and prediction accuracy can fully satisfy design target of 10 %.

In the experiment with the neutron reflector of SS316, the calculation results overestimate the experimental ones by more than 10 %. This suggests that there are some problems on the back-scattering cross section data of nuclei included in SS316. In the pebble bed mockup, the calculation results of local TPR around the boundary between the rear part of the breeder layer and beryllium layers also overestimate the experimental ones by more than 10 %. This also suggests that angular distributions to rear directions in the nuclear data libraries have some problems on the beryllium.

We tentatively reduced the differential cross section of the elastic scattering for backward directions in ^{56}Fe and ^{9}Be of FENDL-2.1 and investigated its effect [7.1-4]. The angular distributions in the backward direction for the elastic scattering were reduced by 20 % respect to the original data. A slight improvement (about 3 %) of the C/E ratio was found in the experiment with the neutron reflector of SS316 when the above cross section variation of ^{56}Fe was applied to incoming neutrons from

0.5 MeV up to 15 MeV. The overestimation of the local TPR around the boundary between the rear part of the breeder layer and beryllium layers was lowered by 5 % in the pebble bed mockup, when the above cross section variation of ^{9}Be is applied to incoming neutrons from 0.62 MeV up to 15 MeV. But underestimation was also found at the front part of the breeder layer. We will investigate effects of angular distributions of reactions other than the elastic scattering, e.g. inelastic scattering and (n,2n) reactions.

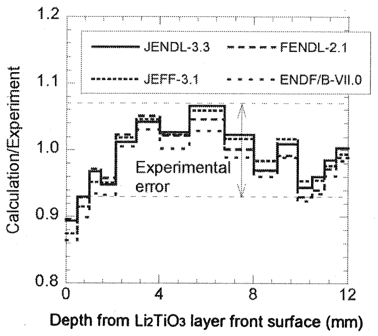

Fig. III.7.1-1 Ratio of calculation result to experimental one for local TPR in the first layer of the mockup with water panel.

7.1.2 Neutron Measurement for ITER-TBM

The test Blanket Module (TBM) of water cooling solid breeding type is planned to be set up into ITER equatorial port plug to test the nuclear performance (tritium production, nuclear heating and shielding property) and other engineering performances of the TBM. Neutron field measurement in the ITER-TBM is a key issue for the TBM test. Because the TBM will be high-temperature, neutron measurement systems should remain unaffected by high temperature. Thus we have proposed the multi-foil activation method as the neutron measurement system in the ITER-TBM.

We have investigated availability of the multi-foil activation method in a DT neutron experiment with a beryllium assembly to simulate the inside of the TBM. Figure III.7.1-2 shows the experimental arrangement of multi-foils activation method. Al, Ni, Zr, Nb and In foils have been used to measure neutron above 1MeV and Au foil has been used to measure slow neutron flux. The foils were inserted at the points of 0, 50.8, 101.6 and 152.4 mm in depth of the beryllium assembly and irradiated with DT neutrons. After adequate cooling, we measured gamma-rays from radioactive nuclei generated by ^{27}Al(n,α)^{24}Na, ^{48}Ti(n,p)^{48}Sc, ^{58}Ni(n,p)^{58}Co, ^{90}Zr(n,2n)^{89}Zr, ^{93}Nb(n,2n)^{92m}Nb ^{115}In(n,n')^{115m}In and ^{197}Au(n,γ)^{198}Au reactions with a germanium detector and each reaction rates were deduced.

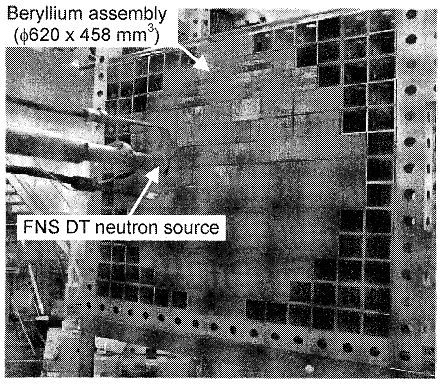

Fig III.7.1-2 Experimental arrangement.

The neutron flux was deduced from the measured reaction rates and an initial guess neutron flux with the SAND-II code. The initial guess neutron flux was calculated with the Monte Carlo calculation code MCNP4C and the nuclear data library FENDL-2.1. JENDL Dosimetry file 99 was used as the response function of the reaction rates.

Figure III.7.1-3 shows the obtained neutron flux at 152.4-mm depth in the beryllium assembly. From our evaluation, it was shown that the multi-foil activation method was a promising method to measure the neutron field in the ITER-TBM.

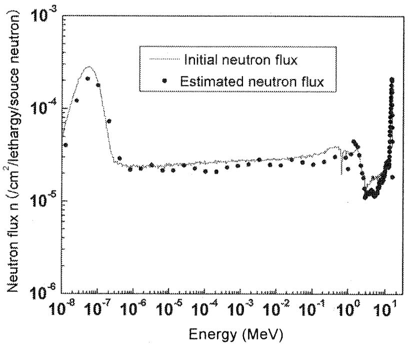

Fig III.7.1-3 Estimated neutron flux at 152.4-mm depth in the beryllium assembly.

References

7.1-1 Sato, S., *et al.*, *Fusion Sci. Technol.*, **47**, 1046 (2005).
7.1-2 Sato, S., *et al.*, *Nucl. Fusion*, **47**, 517 (2007).
7.1-3 Sato, S., *et al.*, "Monte Carlo Analyses of Blanket Neutronics Experiments at FNS with Latest Nuclear Data Libraries," *Proc. International Conference on Nuclear Data for Science and Technology 2007,* 995 (2008).

7.1-4 Sato, S., *et al.*, "Impact of reflected neutrons on accuracy of tritium production rate prediction in blanket mockups for fusion reactors," *Proc. 8th International Symposium on Fusion Nuclear Technology*, ISFNT-8 (2007), to be published to *Fusion Eng. Des.*

7.2 Basic Study on Fusion Neutronics

7.2.1 Development of CAD/MCNP Conversion System

An automatic conversion system from CAD drawing data to MCNP input data is under developing. In this fiscal year, the function of this system has been greatly improved as follows.

(1) In order to convert the CAD data to MCNP input data, partial shape splitting was required for very complicated components such as a divertor in the previous conversion system. In the present system, the MCNP input data can be automatically created without the partial shape splitting.

(2) A large number of microscopic geometrical errors can be removed by increasing the significant digits of the conversion system.

(3) Limitation on numbers of material data for CAD data is eliminated.

Using this system, the CAD data of the ITER 40 degree benchmark model were successfully converted to MCNP input data.

7.2.2 Modification of MCNP Program for Eliminating Unstable Answers in Cases with Hard Biasing Technique [7.2-1]

Some of MCNP users have been expressing that they have had inconvenient experiences in MCNP calculations, in which different answers were provided depending on applied weight window values. Such inconvenient case was also encountered in the analysis of the benchmark problem for ITER CAD/MCNP conversion system development. The biasing method, including weight window, can enhance calculation speed, but it should not give different answers depending on the strength of bias. Mechanism to cause unstable results in MCNP calculations is clarified in the case of ITER CAD/MCNP benchmark problem. It is caused by the combination of the following two facts;

(1) Algorism of 'lost particle' handling in MCNP program is curious and unreasonable. When one of particles in a history gets lost, MCNP cancels all tallies calculated during the history and all banked particles are thrown away.

(2) When input data have distributed micro geometry errors, important histories, which give significant contribution to results, have many splitting and have 'lost particles' with higher probability in the case of hard biasing.

These two facts lead to selective canceling of important histories and give significantly underestimated results. MCNP has been modified to eliminate this inconvenience, by correcting the algorism of subroutine "hstory". The modification has been made successfully not to cancel all tallies of the history but to neglect only 'lost particle'. It is confirmed by test calculations that the modification eliminated the large underestimation, giving the same answer independently from applied weight window values.

7.2.3 Analyses of Fusion Benchmark Experiments at FNS with Recent Nuclear Data Libraries [7.2-2]

Recently several nuclear data libraries, JENDL-3.3, FENDL-2.1, JEFF-3.1 and ENDF/B-VII.0, were newly released. It is essential to verify these libraries through analyses of integral benchmark experiments. Many integral benchmark experiments for nuclear data verification have been carried out at FNS. Thus we analyzed these experiments with the MCNP4C code and these nuclear data libraries (JENDL-3.3, FENDL-2.1, JEFF-3.1 and ENDF/B-VII.0) in order to compare calculation results with these libraries and to shed light on problems in these libraries.

The following typical results for iron, SS316, copper, beryllium and lithium oxide are obtained.

1) Iron : Figure III.7.2-1 shows the ratio of calculated neuron flux from 0.1 keV to 1 keV to measured one. ENDF/B-VII.0, JEFF-3.1 and FENDL-2.1 are good, while JENDL-3.3 is not good.

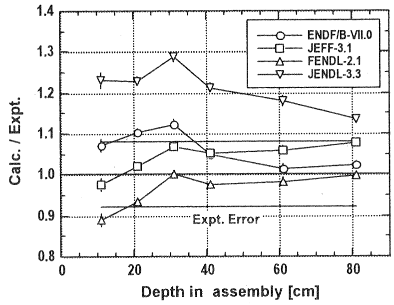

Fig. III.7.2-1 Ratio of calculation to experiment on neutron flux from 0.1 keV to 1 keV.

2) SS316 : All the libraries for nuclei included in

SS316 seem to be good except for molybdenum, which may have some problems for low energy neutrons.

3) Copper : All the libraries are not good, particularly for low energy neutrons.

4) Beryllium : JEFF-3.1 is slightly better. All the libraries cause overestimation of low energy neutrons.

5) Lithium oxide : All the libraries are good.

7.2.4 Problem on Unresolved Resonance Data in Recent Nuclear Data Libraries [7.2-3]

At the international conference on nuclear data for science and technology held in 2001, we pointed out that the leakage neutron spectrum from a niobium sphere of 0.5 m in radius with a 20 MeV neutron in the center, which was calculated with ANISN, MCNP4C and JENDL-3.3, had a large strange bump around 100 keV as shown in Fig. III.7.2-2, which was considered to be originated from self-shielding correction for the unresolved resonance data.

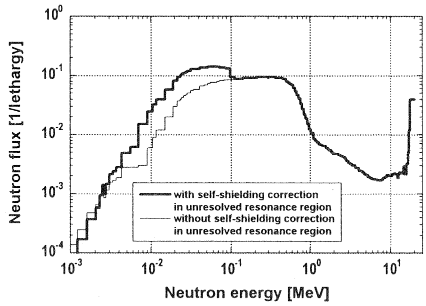

Fig. III.7.2-2 Calculated leakage neutron spectra from a niobium sphere of 0.5 m in radius with a 20 MeV neutron in the center by using ANISN.

As a result of the detail investigation, it is found out that the self-shielding correction for the unresolved resonances is too large around the upper boundary energy of the unresolved resonance region in ^{93}Nb of JENDL-3.3. It is confirmed that this issue can be solved by increasing the upper boundary energy of the unresolved resonance region from 100 keV to 600 keV. More than half of nuclei with unresolved resonance data in JENDL-3.3 and ENDF/B-VII.0 have the same issue. It is noted that probably other nuclear data libraries such as JEFF-3.1 also have the same problem for unresolved resonance data. In evaluation for unresolved resonance data, the upper boundary energy of the unresolved resonance region should be set to be high enough by considering self-shielding correction.

7.2.5 Attila Validation with Fusion Benchmark Experiments at FNS [7.2-4]

The three-dimensional Sn code Attila of Transpire, Inc. can use CAD data as a geometrical input directly and deal with assemblies of complicated geometry without much effort. The ITER organization has a plan to adopt this code as one of the standard codes for nuclear analyses. However validation of calculations with this code is not carried out in detail so far.

In order to assess the Attila code in fusion neutronics field, we carried out Attila analyses of fusion neutronics experiments at FNS and compared them with DOORS (DORT and TORT) and MCNP analyses and measured data.

As for the bulk experiments on iron and SiC, agreement between Attila and DORT or TORT calculations was excellent. Multigroup libraries with adequate background cross section should be also used for Attila. In the ITER streaming experiment as described in IV.3.10, last collided source calculation with forward bias is essential for Attila.

Through the Attila analyses, it is also found out that Attila is very attractive but Attila requires much more calculation time than DOORS.

References

7.2-1 Iida, H., *et al.*, *JAEA-Research* 2008-050 (2008).

7.2-2 Konno, C., *et al.*, "Analyses of Fusion Integral Benchmark Experiments at JAEA/FNS with FENDL-2.1 and Other Recent Nuclear Data Libraries," *Proc. 8th International Symposium on Fusion Nuclear Technology*, ISFNT-8 (2007), to be published to *Fusion Eng. Des.*

7.2-3 Konno, C., *et al.*, "Problem on Unresolved Resonance Data in Recent Nuclear Data Libraries," *Proc. International Conference on Nuclear Data for Science and Technology 2007,* 713 (2008).

7.2-4 Konno, C., *et al.*, "Attila Validation with Fusion Benchmark Experiments at JAEA/FNS," *Proc. 11th International Conference on Radiation and Shielding*, ICRS11 (2008), submitted to *Nucl. Technol.*

7.3 Operation of the FNS Facility

The operation of the Fusion Neutronics Source (FNS) has been carried out to execute a variety of experiments under collaboration with JAEA and domestic universities, responding to various requests for operation pattern. The total operation time was 353 hours in this fiscal year. In these experiments, fixed tritium and deuterium targets were changed several times for the various experiments at the target room I. Rotating tritium targets were also changed for material irradiation experiments and neutron instrument developments using the pencil neutron beam at the target room II.

A total amount of 2.02 TBq tritium in vacuum exhaust gas was processed with the Tritium Adsorption Processor (TAP) system. The oil-free vacuum pumps and CRYO pump for the 80 degree beam line were overhauled after the periodic check-up. The control circuit of the accelerator was inspected every six months.

FNS uses two types of titanium tritium targets for fusion neutronics experiments. One is a small target of 30 mm in diameter with about 200 GBq tritium and the other is a large one of 310 mm in diameter with about 30 TBq tritium. So far we imported the tritium targets, but the cost increased every year. In 2006 we started the development to manufacture tritium targets for ourselves in JAEA. In November of 2007 we successfully produced a small tritium target of 400 GBq tritium for the first time at the Tritium Process Laboratory (TPL). The produced tritium target performance was examined at FNS. The tritium distribution in titanium was almost flat. Figure III.7.3-1 shows change of the DT neutron generation rate of this target and previously imported targets with bombarded deuteron beam quantity. The initial DT neutron generation rate was 1.7×10^{11} n/s/mA. The attenuation rate of the neutron generation rate was better than those of the previously imported targets. The DT neutron generation performance of the manufactured target was very good.

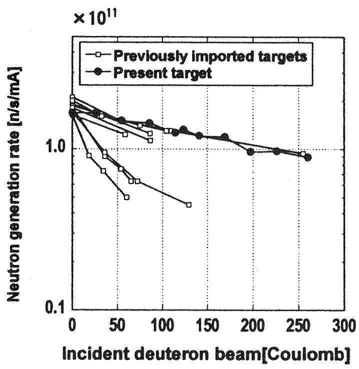

Fig. III.7.3-1 DT neutron generation rate.

IV. ITER

1. Overview of the ITER Program and Activities

1.1 Progress for the ITER Program

After the signing ceremony of (1) the ITER Organization Establishment Agreement [1] and (2) the ITER Organization Privileges and Immunities Agreement[2] in Paris on November 21, 2006, the interim ITER Organization (IIO) was granted French legal personality and started concluding contracts, providing employment and other activities necessary to launch the ITER Project on the basis of the Arrangement on Provisional Application of the ITER Organization Establishment Agreement[3]. Meanwhile each Member of IIO started domestic procedure for the ratification, acceptance or approval of (1) and (2) aiming at the official establishment of the ITER Organization. Japan deposited the instrument of acceptance of (1) and (2) on May 29, 2007 after getting approval of the Diet on May 9, 2007 during its 166th ordinary session.

On July 11-12, 2007 the second meeting of the interim ITER Council was held in Tokyo. The Management Advisory Committee (MAC) and the Science and Technology Advisory Committee (STAC) were provisionally held twice in 2007, respectively.

The Agreements (1) and (2) entered into force on October 24, 2007 after all the Members of IIO deposited instruments of ratification, acceptance or approval of them. The ITER Organization (IO) was established on the same day. On November 27, 2007 the first meeting of the ITER Council (IC) was held in Cadarache. The IC elected Sir Chris Llewellyn Smith as the Chair. Then the IC appointed Mr. Kaname Ikeda as the Director-General (DG) of the IO. The Principal Deputy Director-General and Deputy Director-Generals of the IO were also appointed by the IC. The IC appointed the Chair and Vice-Chair of MAC as well as STAC. The IC approved the internal rules of IO such as Project Resource Management Regulations and the Staff Regulations. The IC also approved the conclusion of the agreement with CERN and the partnership arrangement with the Principality of Monaco as proposed by DG.

1.2 ITER Organization

1.2.1 Formal Establishment of ITER Organization

ITER Joint Implementing Agreement (JIA) took into force on October 24, 2007 after the ratification by all ITER Parties and the ITER International Fusion Energy Organization (the ITER Organization) has been established formally since that day (Fig.IV.1.2-1). After that, the 1st ITER Council (IC-1) which is top level government body for the implementing of ITER JIA was held on November 27-28, 2007 at Cadarache, France as the headquarters of ITER Organization. Mr. Kaname IKEDA and Mr. Nobert HOLTKAMP were appointed formally as Director-General and Principal Deputy Director-General by the ITER Council, respectively. The ITER Organization was extended to have total of 194 staff, as 153 professional staff, 41 support staff, as of October 31, 2007. A total of 300 staff would be expected by spring of 2008.

The DAC (Demonde d'Autorisation de Creation) files which include the Preliminary Safety Report (RPrS) were prepared by ITER Organization and subsequently submitted to French Nuclear Authorities on January 28, 2008. These are main documents supporting the application for licensing of ITER Construction and operation. Also, the Construction Permit application was submitted to the regional authority on January 29.

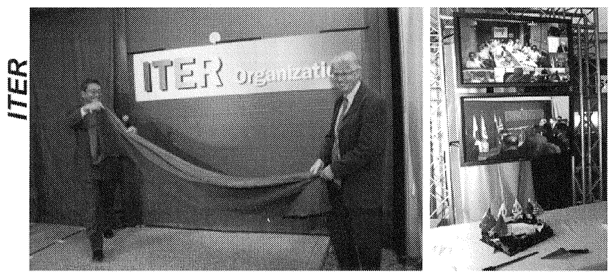

Fig.IV.1.2-1 Formal establishment of ITER Organization on October 24, 2007.

1.2.2 ITER Site Preparation

The preparation of the ITER site started since January 2007 and is progressing as planned which are undertaken by the Agence ITER France. The site preparations including the platform leveling for 75 hectares, contractor areas, temporary and permanent access roads and temporary construction offices are

[1] Agreement on the Establishment of the ITER International Fusion Energy Organization for the Joint Implementation of the ITER Project

[2] Agreement on the Privileges and Immunities of the ITER International Fusion Energy Organization for the Joint Implementation of the ITER Project

[3] Arrangement on Provisional Application of the Agreement on the Establishment of the ITER International Fusion Energy Organization for the Joint Implementation of the ITER Project

underway. Also road improvement between the nearest harbor and ITER site is underway.

1.2.3 New Baseline Document and Design Review

The ITER Organization set up the Design Review to fixed the baseline design of ITER since 2001 Final Design Report. The design review report was submitted to ITER Council and its subsidiary bodies by the ITER Organization. It was confirmed that the overall ITER design is sound and most of the design change requests that have resulted by the Design Review is acceptable. However, this activity is still required more careful examination. The Science and Technology Advisory Committee as subsidiary bodies of the Council asked ITER Organization to reexamine the 13 technical issues by the next ITER council which are related in, 1)Plasma vertical stability, 2) Plasma shape control, 3) Flux Swing in OH operation and Central Solenoid, 4) ELM (Edge localized mode) control, 5) Remote handling, 6) Load specification on vacuum vessel and in-vessel components, 7) Diverter material strategy, 8)Capability of 17MA discharge, 9)Coil cold tests, 10)Heating and current drive strategy, 11)TBM (Test Blanket Module) strategy, 12) Hot cell, 13) Continued involvement of science and technology communities.

On the other hand, "Project Specification" as one of the top level baseline documents which is described the technical scope of ITER was submitted to ITER council by IO and provisionally approved. And it will be submitted with the other top level baseline documents related the schedule, cost and project plan on the next Council.

1.2.4 Establishment of TBM Ad-hoc Group and Financial Audit Board

Tritium breeding blanket testing is a critical element in the ITER. Test Blanket Module (TBM) program at ITER is an activity that is considered necessary for contributing to the demonstration of technical feasibility of fusion energy. The members of TBM Ad-hoc Group were appointed from the government officials of all 7 Parities and convened by ITER Organization to make the proposals for the implementation of TBM program at ITER regarding with the following specific areas; 1) Legal basis, 2) Port sharing, 3) Cost sharing, and 4) Treatment of Intellectual Property Right. The proposal for the implementation of TBM program at ITER will be submitted to ITER Council by the summer 2008.

Accountability for the responsible budgetary and financial procedure is essential for ITER Organization. The first meeting of Financial Audit Board (FAB) was held on March 13, 2008 chaired by Prof. Nagano from Japan. The on-site audit will be carried out and its report will be issued soon.

1.2.5 External relations – Partnership Agreement with Principality of Monaco

Partnership Arrangement between ITER Organization and the Principality of Monaco was signed by DG Ikeda and Minister of State, Jean Paul Proust in the presence of Prince Albert II on 16 January 2008. The Arrangement includes a contribution by the Principality of 5.5 M€ for a ten-year period, which will be used to establish a program of five post-doctoral fellowships and annual International ITER-related Conferences.

1.2.6 International School Manosque

The International School was opened in September 2007 at the Lycée des Iscles in Manosque with 89 pupils, 30 teachers and 3 administration staff. 6 language sections are open: Japanese, German, English, Chinese, Italian, and Spanish; 50% of the teaching is in French. The first phase of the new school building is planned to be finished in 2009.The International Advisory Council for the International School with experts from each Member was established and its first meeting was held on 8 November 2007 at Manosque.

1.3 Contribution for the ITER program

JAEA has continued administrative activities to support Japanese candidates who apply for the professional and support staff of the ITER Organization. The number of the Japanese professional staff has been increased to fifteen by the end of March, 2008, which is 8 % of the total number of the professional staff of the ITER Organization. The number of the Japanese support staff has also been increased to four, which is 7.5 % of the total support staff.

In addition to these directly employed staff, JAEA has continued the secondment of researchers and engineers to the ITER Organization in FY 2007, which amounts to eighty-five man-month approximately.

Most of the ITA (ITER Transitional Arrangement) tasks have been completed in FY 2007. As shown in Table IV 1.3-1, seventy-two tasks have been completed and two tasks will be finalized in 2008. In addition, thirteen ITER non-credited tasks have been undertaken to cooperate the design review and to finalize technical specifications for the procurement of ITER components, and two tasks have been completed so far. Furthermore, three credited task agreements have been concluded and tasks are going on.

JAEA has also contributed to the participation in the various technical meetings with the ITER Organization and other participating members. 136 technical meetings were held and a total of 429 JA members were present at these meetings in FY 2007.

Table IV 1.3-1 Status of task agreement as of 31 March, 2008.

	On-going	Completed	Total
ITA Task	2	72	74
ITER Non-credited Task	11	2	13
Credited Task	3	0	3

2. Activity of Project Management

2.1 Overview

Until the formal establishment of ITER Organization (IO) in October 2007, project management group performed the preparation activities such as quality assurance (QA) and documentation management system in order to start the procurement of ITER components smoothly. Following the nomination of Japanese Domestic Agency (JADA) on October 24th in 2007, the project management group started the quality assurance activities of JADA and supported the procedure for the conclusion of procurement arrangement of Toroidal Field (TF) conductor between IO and JADA.

2.2 Configuration Management

According to the recommendations of ITER Management Advisory Committee (MAC) at the meetings held in November 7, 2007, the Configuration Management Working Group has been organized in December 2007 by the member from ITER Organization (IO) and 7 Domestic Agencies (DAs) to establish the project management procedure to ensure that the DAs are involved in the process of configuration change on technical baseline, cost baseline and schedule baseline. JADA member participated in four WG meetings (video conference) organized by the IO in FY2007, and the WG performed a) review of the Configuration Management Plan (CMP) proposed by the IO, b) discussion to formulate proposals concerning the definition of the roles and responsibility of the IO and DAs and the methods to assess the impacts of changes, and c) discussion to prepare the proposal for the establishment of threshold levels for the approval of changes. The draft proposal of WG on the change control procedure has been prepared for the approval by the MAC and ITER Council schedule in FY2008.

2.3 Schedule Management

The planning and scheduling of the in-kind Procurement Arrangement in the ITER project is one of the most important procedure as well as the budget management. The ITER organization has started in 2007, but an accurate process of the whole plan was not drawn up. Especially, it made most preferential topic of the ITER project in 2007 that schedule to the first plasma which is definition of constructive period is raised. Process meetings were held at Cadarache for four times in October, December, January and February, to stack the procurement arrangement process of the individual equipment, was performed. As a result as for the process which was drawn up, to stack the detailed process which the person in charge of each domestic agency draws up from the top down level one schedule which is put out in the ITER council, it was the great opening in the bottom-up level three schedule which it drew up. Because of that, squeezing in the individual equipment, to pierce the problematical point thoroughly, scheduling acceleration initiation (SAI) meetings were held frequently from February extending through March. After all, a new integrated project schedule (IPS) for the next ITER Council was completed for the procurement arrangement of including ten years construction and one year preparation for the first plasma in 2018.

2.4 CAD Management

For implementing the CAD work required for the finalization of technical specification of the component, CAD work, CAD data and CAD drawing management instructions were issued and implemented. CAD environment was also improved by acquiring 3 64bit PCs with 8GB RAM where ITER standard CAD software (CATIA) is installed including definition files for handling increasingly large amount of data and a smooth collaboration with ITER Organization design office. A 64bit server was also implemented to manage the CAD data. Considering a collaboration with ITER Organization three CAD Working Group work-shops and a videoconference were held in Cadarache and discussed design collaboration protocol and CAD data exchange methodology. ITER CAD Manual where ITER standard CAD methodology is described was translated to Japanese and started implementing the rules. A Design Collaboration Coordinator was appointed and started exchanging CAD data between JADA and ITER Organization for design collaboration.

2.5 Procurement Management

In advance of other Domestic Agencies, the Procurement Arrangement (PA) of TF conductor has been signed between IO and JADA after the establishment of JADA. For the agreement of the PA, the contents of the PA were finalized through the negotiation to the IO in cooperation with the Superconducting Magnet Technology Group and the Research and Development Co-ordination and Promotion Office. The Nb_3Sn strands for TF coils, Cable for TF coils and TF conductor based on the PA have been contracted with four suppliers. Procurement activities have started. A series of procedures concerning various procurement activities from finalizing the PA to awarding the supplier contract were confirmed over the course of this year.

2.6 QA Activity

In preparing to start quality assurance activities in JADA, the Quality Assurance Program has been created and approved by the IO. Drafts of 12 kinds of procedures and 4 kinds of instructions have been prepared as documents related to the quality assurance of JADA. These documents were formally enacted and the quality assurance system was created immediately after the establishment of JADA. The quality assurance activities have proceeded smoothly. The establishment of a quality assurance system was one of the requirements in the PA contracts. The Following activities have been performed : (1) convene the Quality Assurance Committee; (2) convene the Quality Assurance Review Meetings; (3) convene the Unit Exchange Meetings; (4) perform education and training activities, and approve the qualifications of the DA personnel, personnel engaged in design, fabrication, testing and inspection, personnel engaged in quality assurance activities and personnel engaged in internal audit and supplier audit, and (5) initiate the management of documents which are produced and received by JADA.

3. Preparation for ITER Construction

3.1 Superconducting Magnet

JAEA is responsible for the procurement of 25% of TF conductors, all CS conductors, 9 TF coil winding packs (WP), 19 sets of TF structures, which include one set for a spare, and the assembly of WP and the structure for 9 TF coils. The procurement of the TF conductor started in FY2007 and activities to prepare for the procurements of the TF coil WP and structures are under way. In addition, the installation of the PF Insert Coil was successfully performed in FY2007. The aim of the PF Insert Coil project is to demonstrate the performance of the Nb-Ti conductor for the ITER PF coils. The results of these activities were described below.

3.1.1 TF Conductor Development

The TF conductor is a circular cable-in-conduit conductor (CICC) with a central spiral, cooled by supercritical helium, as shown in Fig. IV.3.1-1. The conductor consists of 920 Nb_3Sn and 522 copper strands with 0.82 mm in diameter. The strands are cabled to a five stage cable with the final 6 fourth-stage subunits twisted around the central spiral. The central spiral, which is essential to reduce pressure drop, is a tube formed from a stainless steel strip to allow good convection of helium between cooling channels in the central spiral and at annular cable space.

To qualify the manufacturing processes of the TF conductor, JAEA developed a prototype TF conductor and fabricated 3.6-m long samples to be tested at the SULTAN test facility in Switzerland. Current sharing temperature (T_{cs}) of the conductors was measured at an operating condition of the ITER TF coil, namely 68 kA at 11.8 T. A typical result of the T_{cs} measurement is shown in Fig. IV.3.1-2 [3.1-1]. In the measurement, an electric field of the conductor was measured while increasing the temperature of the coolant helium. T_{cs} is defined as a temperature at which the electric field reaches 0.1 μV/m. As can be seen in this figure, T_{cs} is evaluated to be 6.3 K. T_{cs} was also measured after 800 cyclic charges up to 68 kA at 11.8 T and no degradation was observed. These results satisfy the ITER requirement that T_{cs} should be higher than 5.7 K for the TF conductor. Based on these technical achievements, JAEA launched contracts for the TF conductor procurement in early 2008.

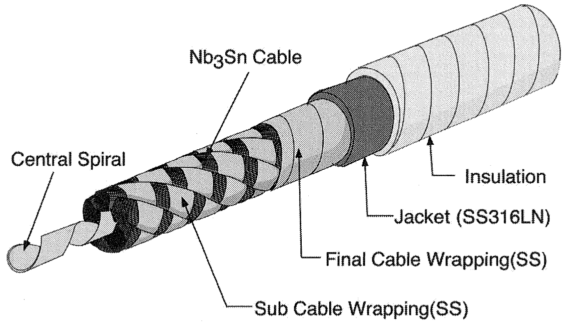

Fig.IV.3.1-1 Nb_3Sn cable-in-conduit conductor with central spiral for TF coil.

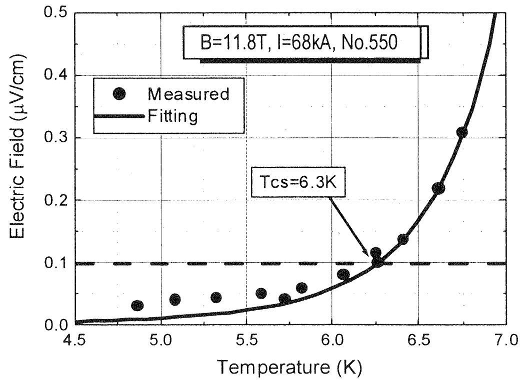

Fig.IV.3.1-2 Typical result of current sharing measurement at 68 kA and 11.3 T.

3.1.2 TF Coil Winding Pack Development

In the manufacturing of the TF coil WP, a heat-treated conductor is wound into a D shape with a height of about 14 m and a width of about 9 m and is then inserted into a radial plate groove without causing damage on the conductor critical current performance and turn insulation around the conductor. Tolerances between the radial plate groove wall and turn insulation are ±2.9 mm at the top and bottom of the winding and ±1.9 mm at the outboard. To enable the insertion of the winding into the radial plate, the conductor length of a single turn, which is about 36 m, should be controlled within ±16 mm. This corresponds to a tolerance of ±0.045%, which seems challenging from the manufacturing point of view. Furthermore, the conductor length changes due to the heat treatment of Nb_3Sn formation. Winding dimensions before the heat treatment should therefore be determined by taking into account this elongation or shrinkage of the conductor.

To precisely evaluate the change in a conductor length during the heat treatment was one of the key issues and JAEA developed a new apparatus for this purpose. Figure IV.3.1-3 shows schema of the apparatus [3.1-2]. Measurements were performed for the conductors using bronze and internal tin route Nb_3Sn strands. Results are shown in Fig. IV.3.1-4. The bronze conductor showed an elongation of 0.03% and the internal tin route conductors showed a shrinkage of 0.02% due to the heat treatment [3.1-2,3]. Based on these values, the winding dimensions can be determined. An error in the prediction of the winding dimension can conservatively be assumed to be a half of these values, *i.e.* ±0.015%, and this number is sufficiently small compared to the allowable tolerance of the conductor length, ±0.045%. It can therefore be concluded that the change in the conductor length due to the heat treatment is not a critical issue.

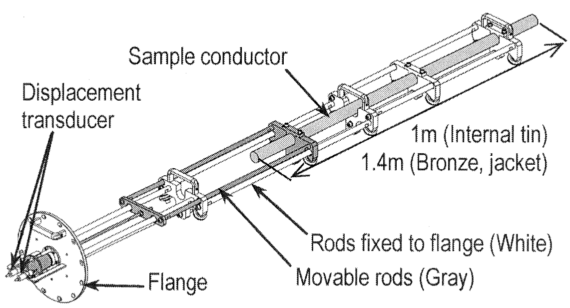

Fig.IV.3.1-3 Apparatus to measure elongation of conductor during heat treatment.

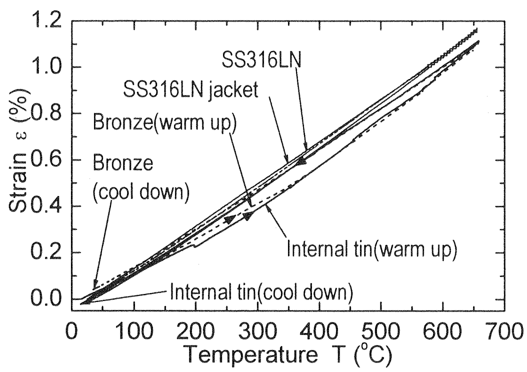

Fig.IV.3.1-4 Thermal strain of the prototype TF conductor using bronze and internal tin route strands, and SS316LN jacket. The thermal strain of SS316LN is shown for comparison.

3.1.3 TF Coil Structure Development

Since high fracture toughness of more than 180 $MPa{\cdot}m^{1/2}$ at liquid helium temperature (4K) is required for the TF structure, the full austenitic wires, which contain no δ-ferrite, will be used for welding of TF structures. However, full austenitic wires have high susceptibility to hot cracking compared with conventional wires, which usually contain a few percent δ-ferrite. Therefore, applicability of the full austenitic wires for welding with a narrow gap TIG welding was studied by performing trial welding of 40 and 100 mm thick plates. The tested wires are as the follows:

(1) DIN 1.4455: 0.03C-7Mn-19Cr-16Ni-3Mo-0.15N
(2) JJ1: 0.03C-10Mn-12Cr-14Ni-5Mo-0.14N

Weldability is the identical between these two materials. Both welded joints had yield strength and tensile strength of more than 300 MPa and 600 MPa, respectively, and satisfied the ITER requirements. The joint welded by the JJ1 wire showed good results in bending tests and no serious cracks were found after bending. On the other hand, several cracks, which might be caused by micro cracking during weld operation, were observed in bending test specimens taken from the joints welded by DIN 1.4455 wire, as can be seen in Fig. IV.3.1-5 [3.1-4]. It has therefore been decided that JJ1 wire is used for the welding of the TF structures to mitigate a risk for hot cracking during weld operation.

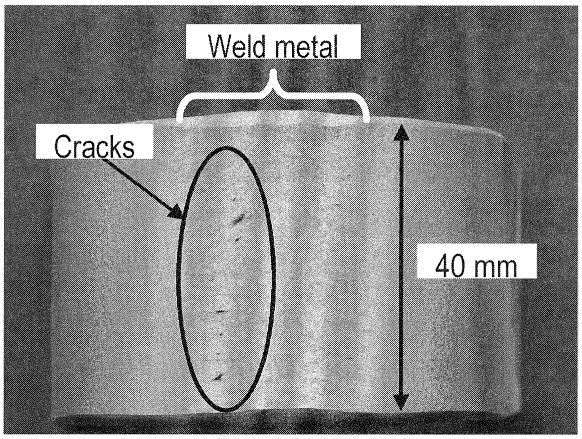

Fig.IV.3.1-5 Cracks observed after a bending test of a specimen taken from the joint welded using DIN 1.4455 wire.

3.1.4 Preparation of the PF Insert Coil Test

The ITER PF Insert Coil was developed by European Fusion Development Agreement (EFDA) to demonstrate the performance of a Nb-Ti conductor for the ITER PF coil under relevant operating conditions. The PF Insert Coil is a single-layer solenoid, wound from about 50 m of a prototype PF conductor, including a conductor joint located at high magnetic field (about 4T) to simulate its operating conditions. It has an outer diameter of 1.6 m, a height of 3.4 m and a weight of 6 tons. Its nominal current is 45 kA at 6 T and 6 K.

The PF Insert Coil was successfully installed in the facility at JAEA Naka which has the largest capability in the world for testing large superconducting coils, as shown in Fig. IV.3.1-6. Test will be carried out under the background field from the CS model coil that can provide a maximum magnetic field of 13 T. The major items of the test program are: 1) T_{cs} and critical current (I_c) measurements to clarify operation limit; 2) joint resistance measurement; 3) stability test against artificial perturbation and 4) AC loss measurement in the conductor and joint. The effects of cycling electromagnetic load on the T_{cs} and I_c, as well as on the AC loss, are also evaluated by 10,000 cyclic charges of the PF Insert Coil up to 45 kA at 6 T. The test will be performed from June to August in 2008 under the collaboration of the IO, EU and JAEA.

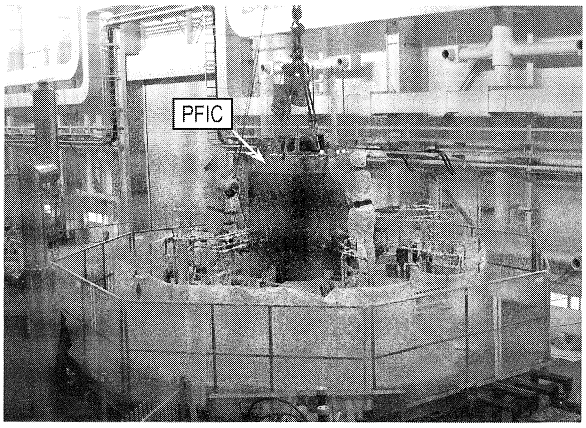

Fig.IV.3.1-6 PF Insert Coil being installed into the bore of the CS model coil.

References

3.1-1 Takahashi, Y., *et al.*, *IEEE Trans. ASC* **18**, 471 (2008).

3.1-2 Matsui, K., *et al. Cryog. Eng.* **42**, 311 (2007) (in Japanese).

3.1-3 Koizumi, N., *et al.*, *IEEE Trans. ASC* **18**, 475 (2008).

3.1-4 Niimi, K., *et al.*, Abstracts of CSJ conference, **76**, spring, 97 (2007) (in Japanese).

3.2 Blanket and Divertor

3.2.1 Blanket

As for preparation of the procurement of the blanket first wall, design of the first wall and evaluation of qualification mock-up for the first wall were performed, as in the following.

1) EM analysis for the first wall and shield block of #18 blanket module.
2) Evaluation of strength concerning with CuCrZr, SS/CuCrZr and Be/CuCrZr joints of qualification mock-up for the first wall.
3) Ultrasonic examinations, helium leak tests and pressure tests of the fabricated qualification mock-up.

The FW includes the Be amour tiles joined to CuCrZr heat sink with stainless steel cooling tube and backing plate. These joints must withstand the thermal and mechanical loads caused by the plasma and electromagnetic force. Qualification tests for the first wall fabrication technology are planed using the representative mock-ups to prove the soundness of the first wall. The qualification tests include heat flux testing and mechanical testing of the mock-ups to qualify the joining technologies required for the first wall. Figure IV.3.2-1 shows the fractured tensile specimens after the mechanical testing of the joints. The tensile properties of the joints fulfilled the ITER specifications. The specimens of SS/CuCrZr joint fractured at the CuCrZr region apart from the interface. The tensile strength of SS/CuCrZr was the same as CuCrZr base. However, the Be/CuCrZr joint fractured at the interface because of large stress concentration near the interface caused by discontinuity of materials properties at the interface.

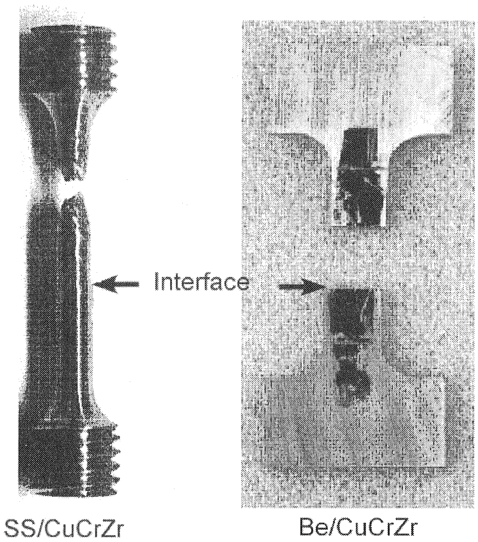

Fig. IV.3.2-1 Fractured tensile specimens after mechanical testing of joints.

3.2.2 Divertor

JAEA is going to procure the entire outer vertical target (OVT) of the ITER divertor, which corresponds to the 60.5 divertor cassettes (0.5 cassettes as a prototype, 54 cassettes as real components and 6 cassettes as spares). In the procurement of the OVT, the ultrasonic testing and the infrared thermography testing are mandatory as non-destructive testing. As one of the provisional procurement activities of the OVT, non-destructive test facility based on the infrared thermography has been developed in JAEA. Figure IV.3.2-2 shows the schematic diagram of the facility. This facility uses hot water (95°C) and cold water (5°C) to inspect the braze defects of the OVT components which consists of Carbon Fiber Composite (CFC) blocks brazed onto the copper alloy cooling tube. During the inspection, the hot water is continuously fed into the cooling tube, and then the hot water flow is instantaneously switched to the cold water flow within 1s. The transient thermal response of the OVT component is recorded by the infrared camera. By comparing this response to that from the "sound" component, the integrity of the braze interface is identified. Figure IV.3.2-3 shows the infrared image obtained from the OVT mockups at a time. The mockup with braze defects clearly shows slower thermal response than the "sound" mockup. This infrared test facility will be used as an acceptance test facility of the ITER OVT components.

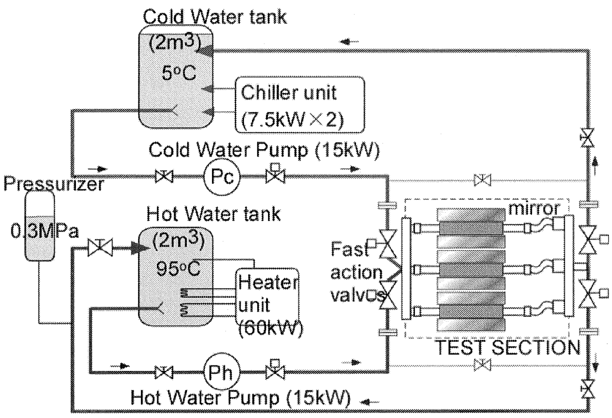

Fig. IV.3.2-2 Schematic diagram of the infrared thermography test facility

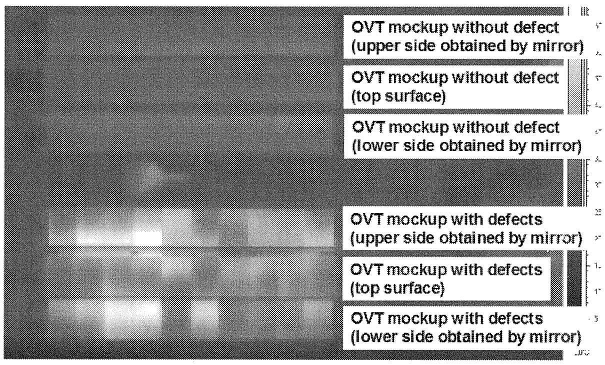

Fig. IV.3.2-3 Infrared image obtained from the mockups with/without braze defects

Reference

3.2-1 Nishi, H., *et al.*, "Stress Singularity at Interface Edge of Dissimilar Materials Joints for High Heat Flux Components," to be published in *J. Nucl. Mater.*

3.3 Remote Maintenance

3.3.1 Dry Lubricant

It is essential to prevent the lubricant oil such as grease from spreading in the vacuum vessel because it makes a problem on the plasma. Therefore, a solid lubricant for IVT system is also being developed using Diamond-Like-Carbon (DLC) coating as a candidate instead of liquid lubricant to keep cleanness in the VV. Based on the result of seizure test [3.3-1], test was also performed using the gears with combination of soft DLC and SNCM420, as shown in Fig. IV.3.3-1. The result shows that the life time of the gears with combination of soft DLC and SNCM420 (base material) has more than 30100 cycles beyond the requirement of 10000 cycles under required contact pressure of 1.5 GPa. The feasibility of DLC has therefore been demonstrated for the application to the transmission gears of the IVT.

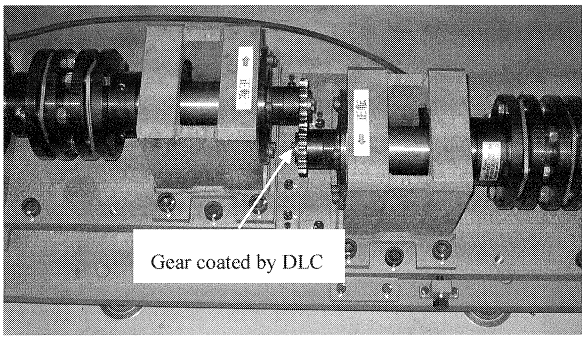

Fig. IV.3.3-1 Performance test apparatus

3.3.2 Connection of Rail Joint and Cable Handling

Connection and disconnection of the rail joint for rail deployment/storage in the transfer cask are critical issues. Therefore, the feasibility of the connection and disconnection of the rail joint have to be demonstrated to finalize the design. The test facility for rail joint connection and disconnection consists of three rail segments, lock mechanism of the rail joint, hinge connection, connection and disconnection of the rail joint for rail deployment/storage, as shown in Fig. IV.3.3-2(a). Cable handling technology is also one of the most critical issues for movable robot. The length of cable is estimated about 70 m and the over-tension of the cable should be avoided for stable movement of the vehicle manipulator along the rail. The feasibility of a new idea of the cable handling system with a drum type cable winding mechanism has to be demonstrated for compact storage of long cable in the cask. The test facility for cable handling consists of two drums (one for simulation of vehicle), multi-cable, guide mechanism for cable winding arrangement, simulated cable route with guide mechanism at the corner in front of maintenance port, as shown in Fig. IV.3.3-2(b). These test facilities are under fabrication and assembled by the end of March 2008, and the performance tests will be carried out from April 2008.

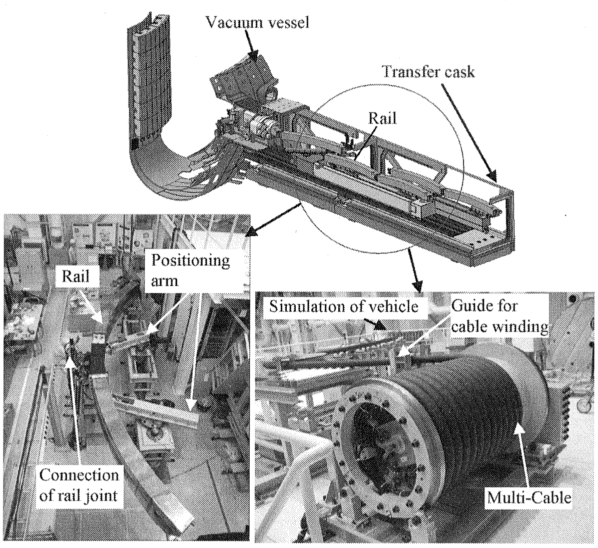

(a) Connection of rail joint (b) Cable handling (Drum type)

Fig. IV. 3.3-2 Performance test facility for rail connection and cable handling

Reference

3.3-1 Takeda N., *et al., Plasma Fusion Res.*, **2**, 052 (2007) / *Letters*.

3.4 EC Heating System

There were three JA tasks relating to the ITER ECH&CD system. Two of them were issued by the working group 6 during the design review meeting in 2007. The rest one was the procurement support task.

(1) Tritium release prevention

A tritium permeation though the inconel cuffs is prevented by Cu coating at the disc edge. A gate valve does not prevent tritium release since the time to close the valve is normally one second. Therefore, a tritium detector should be installed close to the window to minimize the release.

(2) Launcher performance

The poloidal 5° tilting of RF beams could be applied without degradation of transmission efficiency, which is more than 99%. Flipping off of only one beam row (8 MW) of three is the solution for the counter injection of RF beams, although injection power to the co-direction is decreased less than 16 MW.

(3) Launcher compatibility with 2 MW/line

The critical components is the steering mirror because Be coating on the reflection surface has been assumed. The maximum handling power for the mirror coated by Be is 1.63MW and the present mirror is not adequate for the 2MW transmission. A countermeasure is nickel coating (thickness of 50~100 μm) of the cooling channel in the mirror. However, if carbon comes from a divertor deposits on the mirror surface, the mirror with the nickel coated channel is not any more compatible with 2 MW/line.

(4) Start up RF beam injection

The maximum heat load on the fixed focusing mirror and the steering mirror are 1.74 MW/m^2 and 0.84 MW/m^2, respectively, for the start-up frequency of 127 GHz. The power transmission efficiency of the equatorial launcher optimized for 170 GHz is 99% at a slot exit for 127GHz without the significant degradation.

(5) Gyrotron procurement

Tables for specification and interface were introduced to be used in the procurement of the 170 GHz gyrotron. A preliminary draft of technical procurement document for JA 170GHz gyrotrons was prepared and required items such as the intellectual property and the guarantee were identified to be inserted in the procurement document.

3.5 NBI Heating System

The NBI Power Supply (PS) for ITER is a dc, ultra-high-voltage (UHV) PS to accelerate negative ion beams of 40 A up to 1 MeV, for duration of 3600 s at the maximum. The JAEA at present assumes to share the procurement of the UHV main components of the PS which include a dc -1 MV generator, a -1MV insulating transformer, transmission lines, a high voltage deck for water and gas supply, and a core snubber for surge suppression. The JAEA and EU together with the IO have discussed the specification of the PS system periodically. So far, the JAEA and EU jointly developed the Integrated Design Document (IDD) and submitted to the IO as a reference document for the technical specifications to be annexed to the procurement arrangement. Preparation for the Procurement Arrangement of the PS is now in progress.

In the UHV PS for the ITER NBI, surge suppression against electrical breakdowns in the accelerator is extremely important to protect both the beam source and the PS system. Considering constrains of layout inside the tokamak building, the PS building and the PS yard, major components of the PS have been designed. Based on this design, circuit analysis using EMTDC code has been performed to determine a most effective arrangement of the surge suppression devices. After optimization in the simulation, a series resistor of 50 ohm has been adopted in the return line of the PS to protect the high voltage rectifiers. It was confirmed that the intermediate electrode protection resistors can be moved to upper side of the High Voltage Deck 2 (HVD2) which supplies water and D_2/H_2 gas with 1 MV insulation. The core snubber distribution has been also designed so as to fit within limited space inside the transmission line. A result of the simulations is shown in Fig. IV.3.5-1. An upper graph shows the inflow energy from -1MV line of the PS to the accelerator at the breakdown. A lower graph shows the input energy at the grounded grid side. From these simulation, the input energy from the PS into the beam source was confirmed to be around 20 J which is less than the ITER design value <50 J.

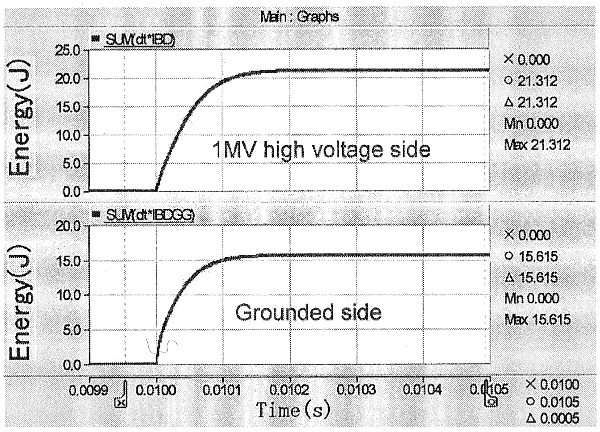

Figure IV.3.5-1 Inflow of energy to the accelerator during a simulated breakdown

3.6 Tritium Plant

3.6.1 Design Studies of Tritium Removal System

A series of design studies for the tritium removal systems of ITER and tritium retention studies of in-vessel materials for ITER have been carried out, as the most significant activities for ITER tritium plant by JAEA. We undertake 50% of the procurement of the tritium removal systems of ITER, as a work transferred from the EU. Recently, the design of the system has significantly changed to address site requirements at Cadarache. The following is the present concept for the tritium removal systems of ITER, which are still under discussion. The tritium removal systems of the tokamak building (TKC) are composed of 8 modules. These 8 modules are set in 4 fire sectors. Further, the systems are composed of the ADS (Air Detritiation System) and the VDS (Vent Detritiation System). The tritium in the atmosphere of the buildings is removed by the ADS in a circulation mode, therefore, ADS is not the SIC (Safety Important Component) system. An amount of the building air is exhausted from a stack though the VDS to keep the building at a negative pressure. Hence, the VDS is a SIC system. A water scrubber (SC) may replace the molecular sieve bed of the VDS, since a set of valve systems with the molecular sieve beds (MS), which is usually used in fusion facilities in the world, does not have adequate reliability. We will carry out the design work of the above system to support ITER activities under close discussion with an ITER tritium group [3.6-1, 2].

3.6.2. Tritium Retention Studies of In-Vessel Materials

The temperature dependence of blistering and deuterium retention in recrystallized tungsten (W) irradiated with 38 eV D ions at high flux of 10^{22} D/m^{2}s to fluences of 10^{26} and 10^{27} D/m^2 was examined with scanning electron microscopy and thermal desorption spectroscopy. After irradiated of the W samples to a fluence of 10^{26} D/m^2 at temperatures below 400 K, the blisters with size of 0.5-1 μm appear on the surface. At around 500K the blisters become much denser, and at 500-560K small cone-shaped blisters are observed in addition to large flattened blisters. As the ion fluence increases to 10^{27} D/m^2 at the irradiation temperatures below 400 K, the blisters become much denser. Some of the blisters increase in size up to 10μm. At irradiation temperatures above 520K, the increase of ion fluence from 10^{26} to 10^{27} D/m^2 does not change significantly the surface morphology. The blisters are not formed the irradiation temperature above 600K. Figure IV.3.6-1 shows the Deuterium retention in tungsten irradiated with different fluences. For an ion fluence of 10^{26}D/m^2, the D retention is about 2×10^{20} D/m^2 at T_{irr}=320 K and, as the irradiation temperature increases, rises to its maximum of about 5×10^{21} D/m^2 at T_{irr}=530 K and then decreases down to about 8×10^{18} D/m^2 leads to significant increase of the D retention at the irradiation temperatures below 500 K, whereas at higher temperatures the D retention increase is proportional to the square root of the fluence. The possible reason of the temperature dependence of the D retention on the ion flux is a balance between the incident flux and temperature dependent D atom diffusion rate out of the implantation zone [3.6-3].

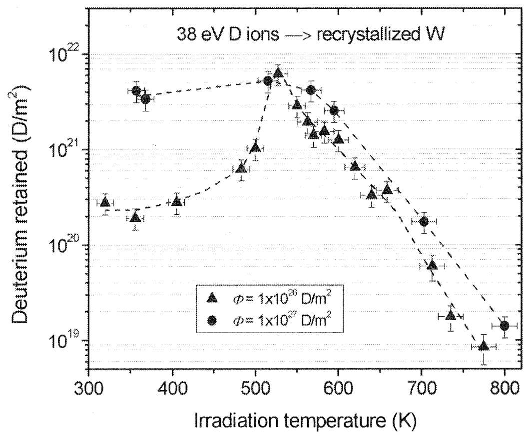

Fig.IV.3.6-1 Deuterium retention in recrystallized tungsten irradiated with 38 eV at ion flux of 10^{22} D/m^{2}s to fluence of 10^{26} and 10^{27}D/m^2, as function of the irradiated temperature.

References

3.6-1 Yamanishi, T., *et al.*, "Tritium research activities under the broader approach program in JAEA," to be published in *J. Fusion Sci. Technol.*
3.6-2 Yamanishi, T., *et al., IFERC-R-T-07-JA (3).*
3.6-3 Alimov, V., *et al.*, "Deuterium retention in tungsten and molybdenum exposed to low-energy, high-flux deuterium plasma," submitted to *Advanced Materials Research.*

3.7 Plasma Diagnostics

Design works on Impurity Influx Monitor (divertor), Microfission Chambers, Thomson Scattering (edge) System, and Poloidal Polarimeter have been carried out. Prototypes of the diagnostic components have been developed and tested. The design and analyses of the upper port plug have been performed.

3.7.1 Impurity Influx Monitor (divertor)

The optical components with a high reliability and a capability of the remote maintenance are being developed for the impurity influx monitor (divertor) system withstanding the harsh environment [3.7-1]. Because the optical path from the collection optics to the front-end optics is about 10 m long, the remote optical alignment system is necessary for keeping viewing fans. The double vacuum windows are placed at the end of port plug, which are arranged the optical path as the labyrinth structure by using two mirrors. The design of a gimbal type mirror holder for these mirrors with the adjustable range of 5° and the resolution of less than 0.01° is carried out [3.7-2]. In this design, the selection of materials of a bearing, an actuator and a feedthrough is important to get a sufficient alignment capability and to use in the higher gamma-ray irradiation, the high vacuum condition, the higher magnetic filed and the higher temperature. In the present, a sliding bearing made of zirconia, a piezo-motor and a linear feedthrough made of stainless steel 304 are used, respectively.

An in-situ calibration system using a newly developed micro retro-reflector array has been developed because the installation of a light source in the vacuum chamber of ITER is not feasible [3.7-3]. A standard light is set behind the bio-shield or in the diagnostic room and the light is applied to the micro retro-reflector array mounted on a shutter through the same optics for plasma measurement with the collection optics. The reflected light is measured with a spectrometer to evaluate the sensitivity change of the optics. During plasma measurement, the micro retro-reflector array, mounted on the shutter plate, retracts into a sheltered area to prevent particle bombardment and deposition. The proto-type micro retro-reflector array made of nickel shown in Fig.IV.3.7-1 is

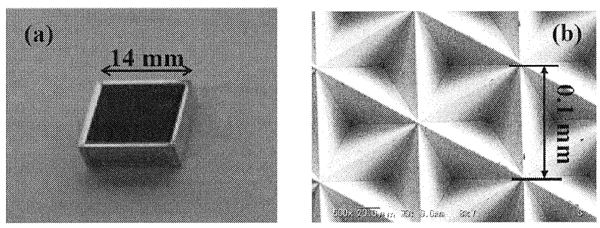

Fig.IV.3.7-1 Photograph of prototype micro retro-reflector array (a) and photo by SEM (b)

manufactured by an electro-forming method. Detected signals have been estimated by using the measured spectral reflectivity of the micro retro-reflector array. As a result, a signal-to-noise ratio of more than 1000 is expected.

3.7.2 Microfission Chamber

Microfission chambers (MFCs) provide time-resolved measurements of the global neutron source strength and fusion power (Required measurement range: 100 kW - 1.5 GW).

Though MFCs have been used as power monitors in Boiling Water Reactors (BWRs), operating environment is different between the BWRs and ITER. Since MFCs have not been used in vacuum, airtight and/or leakage test was needed. Mockup of the MFC without Uranium was made to test airtight and leakage performance (Fig.IV.3.7-2). High-pressure helium gas (18 atm) was filled for the test instead of the working gas (Argon 14 atm), and gas leakage was not detected.

Design of the MFCs and MI cables in the vacuum vessel has been carried out. To decide detail position of the MFCs between the blanket module and the vacuum vessel, the ratio of streaming neutrons at the installation position was evaluated. Neutron fluxes at various distances from the rear of the gap between the blanket modules have been calculated based upon a neutron Monte Carlo calculation using a MCNP version 5 code. The result shows that the effect of streaming neutrons should be taken into account when the MFC is installed closer than 20 cm to the rear of the gap between blanket modules [3.7-4].

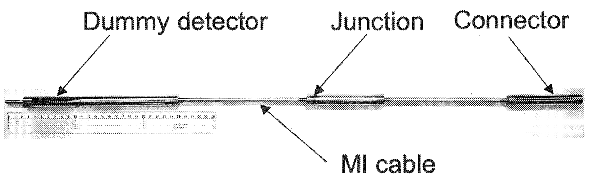

Fig.IV. 3.7-2 Trial manufacture of the Microfission chamber for gas leakage test without Uranium in the detector.

3.7.3 Thomson Scattering (edge) System

In ITER edge Thomson scattering diagnostic system, spectrometers (polychromators) consist of optical band-pass filters and avalanche photodiodes are planned to be used for the detection system. Design study of the polychromator for ITER edge Thomson scattering diagnostics system has been performed. Transmission wavelength ranges of filters for the polychromator are proposed by minimizing the numerically calculated errors in the electron temperature. To eliminate the laser stray light and the strong emission of D_α (656 nm), the two wavelengths are set to be the segment points of the filters. It has been found that the filter below 656 nm is important for evaluating the electron density and temperature because the required temperature range extends to 10 keV, in which the tail of the spectrum is broadened around 400 nm. It has been revealed that the emission, whose wavelength is shorter than 500 nm, is not important for the measurement. This is because only the tail part of high temperature spectrum appears in the wavelength range, while the shot noise due to bremsstrahlung radiation increases as expanding the transmission wavelength range. The characteristics of four configurations, i.e. case (i) transmission wavelength of 656-1064 nm, case (ii) one filter is added below 656 nm, case (iii) two filters are added below 656 nm, and case (iv) one filter below 656 nm and another above 1064 nm are added, are compared. It has been found that case (iv) becomes better than the others if the filter number is more than six. The optimized wavelength ranges for the filter number M = 7 are presented as shown in Fig.IV.3.7-3 [3.7-5].

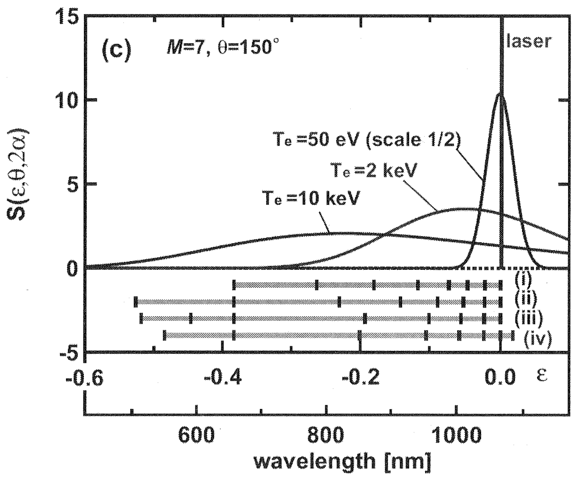

Fig.IV.3.7-3 Segment points of the filters in cases (i)-(iv) and spectral density functions at 50 eV, 2 keV and 10 keV. The transmission wavelength range of the case (i) is 656-1064 nm. Single and double filters are added below 656 nm in case (ii) and (iii), respectively. In case (iv), filters are added below 656 nm, and above 1064 nm. In all the cases, M = 7.

3.7.4 Poloidal Polarimeter

The viewing chord arrangements of the Poloidal Polarimeter have been optimized for various equilibria of ITER operation scenario [3.7-6]. For this purpose, a magnetohydrodynamic equilibrium reconstruction code has been developed and applied. This code only uses the data from Poloidal Polarimeter and the shape of the last closed flux surface as inputs so that a conventionally used assumption of isotropic plasma pressure is not needed, thus the code can treat un-isotropic plasmas. Using this code, optimized viewing chord arrangement for the inductive operation scenario II at the start of the burn phase (S2-SOB) has been obtained. The accuracy of the central safety factor within 3% has been achieved. Furthermore, the optimized viewing chord arrangement for S2-SOB has been applied for other equilibria, i.e. non-inductive operation scenario IV at the start of the burn phase (S4-SOB) and limiter plasma during the current ramping up phase. The accuracy with optimized arrangement for S2-SOB has not been deteriorated drastically compared with the accuracy evaluated using the optimized arrangement for individual equilibrium. Consequently, the optimized viewing chord arrangement for S2-SOB is a promising candidate.

A conceptual design study of the Poloidal Polarimeter has been progressed. A designing study of transmission lines and mirror arrangement at the equatorial no.10 port plug has been carried out to adopt a concept of that several laser beams share a single vacuum window. As the result, CAD drawings are successfully created with twelve laser beams and four vacuum windows (3 beams per 1 vacuum window). With this concept, it is expected that space limitation at the back plate of the port plug is relaxed, risk of vacuum leakage is reduced, and cost is reduced. A new design of a retro reflector has been made. A cylindrical and tapered mirror housing is proposed instead of the box type housing that is previously proposed by ITER organization. With this new concept, retro reflector design to be applicable to the various viewing chords can be simplified and standardized. This is also beneficial to simplify the interfaces between retro reflectors and the blanket modules.

3.7.5 Port Plug

Engineering analyses and studies have been performed for the representative diagnostic upper port plug of ITER [3.7-7]. An integration design has been also carried out for the diagnostic components to be installed in the upper port plug.

The displacement of the upper port plug induced by eddy currents during VDE was calculated at first. Maximum displacement of 3.2 mm has been observed at the top of the port plug in the circumferential direction. Dynamic amplification factor have been estimated to be 1.5 in the preliminary result. Here, the gap between the VV port and port plug is designed to be 20 mm. The fabrication and assembly tolerance is designed to be ± 5mm. It seems that the displacement of the port plug would be less than this tolerance. For the stress on the port plug, high stress concentrations are produced at the joint points between side plate/rib and manifold. Maximum stress of 230 MPa is obtained at the manifold/side plate. These stresses can be reduced by small design changes such as additional supports structure and change of joints configuration.

Maintenance scenario for the upper port plug has been studied to complete the design. The gripping mechanism and load transfer for the upper port plug was focused because these two are key issues of the cantilevered structure. A 14 steps removal procedure was established to satisfy these functions. Here, an additional low body roller was proposed in order to support the weight of the upper port plug and load transfer process. The integration of diagnostics into the port plug has been studied for the Upper Port Plug No.11. An additional inner frame has been considered to fix the optical equipment accurately as shown in Fig. IV.3.7-4. Moreover, it will assist an easy maintenance for the diagnostic components. These studies and designs have established the design basis of the diagnostic upper port plug.

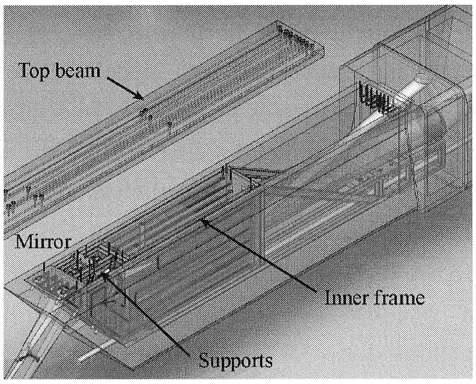

Fig. IV.3.7-4 Integration of diagnostics into upper port plug No. 11 with inner support frame

References

3.7-1 H. Ogawa, *et al.*, *Plasma and Fusion Res.* **2,** S1054 (2007).

3.7-2 Ogawa, H., *et al.*, "Engineering Design and R&D of Impurity Influx Monitor (divertor) for ITER," to be published in Fusion Eng. and Design.
3.7-3 Sugie, T., *et al.*, "Spectroscopic Measurement System for ITER Divertor Plasma: Impurity Influx Monitor (divertor)," *Burning Plasma Diagnostics*, F.P.Orsitto, et al., ed., American Institute of Physics, New York, 218 (2008).
3.7-4 Ishikawa, M., *et al.*, "Detailed Design of Microfission Chamber for ITER ," to be published in *Rev. Sci. Instrm.* (2008).
3.7-5 Kajita, S., *et al.*, "Optimization of Optical Filter Design for ITER Edge Thomson Scattering Diagnostics," submitted to *Fusion Eng. Design*.
3.7-6 Yamaguchi, T., *et al., Plasma Phys. Control. Fusion* **50,** 045004 (2008).
3.7-7 Sato, K., *et al., Plasma and Fusion Res.*, **2**, S1088 (2007).

3.8 CODAC Design Activity

The ITER instrumentation and control (I&C) system, which controls ITER facility, consists of three systems; COntrol, Data Access and Communication (CODAC), interlock system and safety I&C system. The design of CODAC has been carried out by ITER organization (IO) with contributions from each party.

JAEA has contributed CODAC design continuously. The draft version of document "Plant System I&C Handbook" that is a guideline for each plant system of ITER to construct its instrumentation and control system was reviewed, and the problems concerning the software have been extracted. The data flowchart between each function of the CODAC was made based on the various CODAC documents, and the functions lacked in the current CODAC model were extracted. The codes and standards to be conformed for CODAC and plant systems of ITER were clarified. Moreover, the items to be described on the technical specification of CODAC were examined.

JAEA reviewed the conceptual design of CODAC as a member of CODAC working group. The suggestions for CODAC design were arranged and reported to the ITER IO from the working group.

3.9 Code and Standards

In order to cover the features of safety and mechanical design of ITER components and to introduce several new fabrication and examination technologies, the development of technical structural standard for ITER is being continued by the Japan Society of Mechanical Engineers (JSME) since 2003. The work had been focused on the structural standard development for Superconducting Magnets, because it is urgent to use for Japanese procurement of TF coil structure. In FY2007, the discussions to finalize the drafts of standards prepared by JAEA were continued in JSME nuclear fusion standard committee. Finally after the approval of the committee, the drafts of standards was submitted to the JSME Committee on Power Generation Facility Codes and approved in March 2008. The standards are expected to be approved in June 2008 after the process of public hearing. The publication of the standards is expected in August 2008.

3.10 Other Tasks

3.10.1 Neutronics

Under the ITER/ITA task, we have conducted a neutron streaming experiment simulating narrow and deep gaps at boundaries between ITER vacuum vessel and equatorial port plugs [3.10-1] in order to validate neutron transport calculations with the MCNP, Attila and TORT codes.

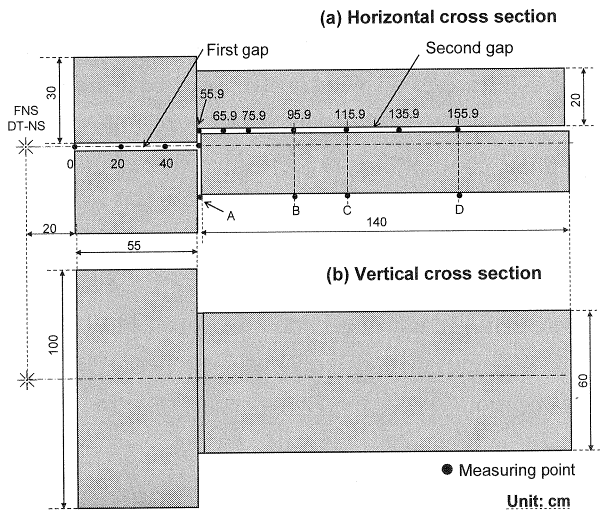

Fig. IV. 3.10-1 Experimental arrangement.

Figure IV.3.10-1 shows the experimental arrangement with a gap structure. The experimental assembly was prepared with two iron blocks of 100 cm in height, 30 cm in width and 55cm in thickness and two iron blocks of 60 cm in height, 20 cm in width and 140 cm in thickness. The widths of the first and the second gaps were 4 cm and 2 cm, respectively. A dogleg structure at the point of 56 cm in depth was provided and the distance of offset was 4.2 cm. The distance from the FNS D-T neutron source to the surface of the assembly was 20 cm.

^{238}U and ^{235}U Micro-Fission Chambers (MFC) and Nb, Al and In activation foils were used as detectors to measure fission rates and reaction rates along the gap as a function of the depth. $^{238}U(n,fission)$, $^{93}Nb(n,2n)^{92m}Nb$, $^{27}Al(n,\alpha)^{24}Na$ and $^{115}In(n,n')^{115m}In$ is sensitive to fast neutrons. Therefore, the fission and reaction rates show the relative MeV neutron fluence. On the other hands, $^{235}U(n,fission)$ is sensitive to slow neutrons, especially neutrons from thermal energy to 1 keV, and the fission rate shows relative slow neutron fluence. The experimental errors of the fission and reaction rates were within 6 %.

Analyses of the streaming experiment were carried out with the Monte Carlo code MCNP4C3 and FENDL/MC-2.1. We also performed analyses with the Sn codes TORT (forward biased angular quadrature) and Attila (last collided source). Multigroup libraries (21 group structure, P_5 Legendre expansion) were generated from the matxs file FENDL/MG-2.1 with the TRANSX2.15 code. The data for ^{238}U and ^{235}U fission cross sections and $^{93}Nb(n,2n)^{92m}Nb$, $^{27}Al(n,\alpha)^{24}Na$ and $^{115}In(n,n')^{115m}In$ cross sections were cited from JENDL Dosimetry File 91.

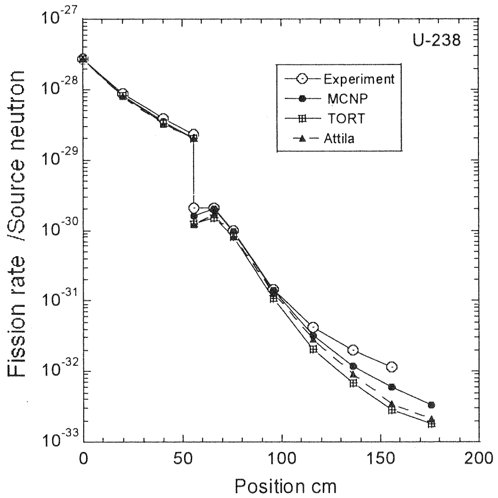

Fig. IV.3.10-2 Measured and calculated ^{238}U fission rate.

Figure IV.3.10-2 shows the measured and calculated ^{238}U fission rate. The calculated ^{238}U fission rate up to 95.9 cm in depth is close to the measured one. Especially, the calculation with MCNP agrees with the measurement well. The calculated reaction rates with Nb, Al and In also correspond with the measured ones up to 95.9 cm in depth. From the results, it is found that the evaluation of fast neutron transport by using MCNP, TORT and Attila is adequate up to about 100 cm in depth.

However, between 136 cm and 176 cm in depth, the measured ^{238}U fission rate tends to overestimate than the calculated ones. This overestimation is considered to be due to many background neutrons scattered in the experimental room wall.

3.10.2 Operation Scenario

IO tasks regarding the plasma operation scenario of ITER have been performed through analyses of poloidal field (PF) control and disruptions, making a significant contribution to the detailed design of ITER. Recent studies of the heat loads on limiter structures have pointed out that for real ITER operation an early transition from limiter to divertor configuration of plasma equilibrium is needed at the level of plasma current less than ~ 5 MA. This PF scenario of the early formation of X-point, however, retards penetration of inductive plasma current. Consequently, the plasma internal inductance, l_i decreases appreciably, making the plasma shape control more difficult. In this task, impacts of the low l_i operation on previous ITER inductive scenario were investigated in detail. Equilibria of full bore plasma were shown to exist under the engineering restrictions that arise from practice of the ITER PF system. It was verified that the lowest limit of l_i, i.e. 0.7, is attainable. In order to lower l_i further, it is recommended: 1) to increase the number of turns in PF6 and PF2 coils, 2) to raise the limit on separation force between the CS modules, 3) to extend allowable displacement of the separatrix legs towards the divertor dome. Simulations of several representative disruption scenarios were performed with the DINA code, using recently derived data of L/R time constant and geometry newly specified for the models of ITER blanket and divertor. These data are utilized as the data basis for determining the physics specification of heat loads on plasma facing components and designing the vacuum vessel as well as in-vessel components.

A comprehensive simulation of plasma current ramping-up was performed under the operation condition at a slow rate, based on the ITER 15 MA inductive Scenario 2. In tokamak fusion reactors with superconducting PF coil system, ramping-up of the plasma current for startup of discharges is essentially restrained at a rate much slower than the current tokamak with normal PF conductors. Therefore, the induced plasma current can penetrate deeply into the core region with higher electron temperature, i.e. low Ohmic resistivity, leading to a centrally peaked current profile. Consequently, such the high l_i, highly elongated configuration imperative to divertor formation has the dangerous property of causing vertical instability. Using the Tokamak Simulation Code (TSC), a self-consistent simulation, including a model for improved core energy confinement and non-inductive current sources, has been performed in consideration of the operational constraints, i.e. sawtooth free $q_0 \geq 1$, $q_{\min} \geq 2$ to avoid internal MHD activity in reversed shear plasmas and flux consumption that could seriously compromise the available duration of the burn phase. Additional heating at early phase of the ramp-up has been addressed as one of startup procedures that retard the penetration of plasma current. A potential drawback, however, is the substantial increase in the direct heat load to limiter. Therefore, phasing of the earliest possible formation of diverted plasma, formation of internal transport barrier (ITB) and transition from L to H-mode was investigated. Timing of the EC heating and non-inductive current driving using off-axis ECCD source was also optimized. Time-evolution of the safety factor q-profile was in reasonable agreement with those of JT-60U reversed magnetic shear discharges with high bootstrap current fraction. These simulation results provide an instruction basis to create the ramp-up scenario that best suits the ITER requirements: enhanced bootstrap current fraction, stable current profile, as well as the interests: how quickly the plasma current needs to be ramped up and how slowly it can be.

Reference

3.10.-1 Ochiai, K., *et al.*, “D-T Neutron Streaming Experiment Simulating Narrow Gaps in ITER Equatorial Port,” *Proc. 8th International Symposium on Fusion Nuclear Technology*, (2007), to be published in *Fusion Eng. Des.*

4. Contribution to International Tokamak Physics Activity (ITPA)

Contribution to the 7 topical groups is summarized below. In addition, large number of JAEA authors contributed to publication of 'Progress in the ITER Physics Basis' (Nucl. Fusion, **47**, S1 - S413 (2007)).

4.1 Transport Physics

Two group meetings were held and six JAEA staff participated. Intrinsic/spontaneous rotation values for enhanced confinement regimes in JET, C-Mod, Tore Supra, DIII-D, JT-60U, TCV and NSTX were used to form a database. The Mach numbers (both ion thermal and Alfven) were found to scale with β_N, with no dependence on collisionality or normalized gyroradius. Extrapolations to ITER, from both dimensionless and machine parameter scalings, predict rotation velocities of a few 100 km/s or $M_A > 2\%$ without external momentum input [4.1-1]. This should be high enough to suppress RWMs. In JT-60U, the relations among diffusive and non-diffusive terms in the momentum transport and heat diffusivity were investigated. In low beta plasmas the measured rotation agrees well with a diffusive model for rotation in response to the applied torque, but not in high beta plasmas where the pressure gradient contribution also becomes important. Modulation experiments showed that χ_ϕ increases with χ_i radially and locally, and both decrease as I_p is increased [4.1-2].

References

4.1-1 Rice, J.E., *et al.*, *Nucl. Fusion*, **47**, 1618 (2007).
4.1-2 Yoshida, M., *et al.*, *Phys. Rev. Lett.*, **100**, 105002 (2008).

4.2 Confinement Database and Modeling

Two group meetings were held and three JAEA staffs participated. Three working groups, i.e. global confinement WG, particle transport WG and IMAGE (Integrated Modeling – A Global Effort) WG, were organized. The impact of the new version (DB3) of Global H-Mode Confinement Database and its analysis on ITER was discussed [4.2-1]. Similar collisionality dependence of density profiles was found in multi machines. Status of integrated modelling in each party was introduced. CDBM-TG contributed to publication of Progress in the ITER Physics Basis, Chapter 2: Plasma confinement and transport [4.2-2].

References

4.2-1 McDonald, D.C., *et al, Nucl. Fusion* **47**, 147 (2007).

4.2-2 Doyle, E.J., *et al, Nucl. Fusion* **47**, S18 (2007).

4.3 Pedestal and Edge Physics

Two group meetings were held and four JAEA staffs participated. In JT-60U, effects of toroidal field ripple and edge toroidal rotation on the pedestal performance and ELM characteristics were investigated. Both pedestal pressure (p_{ped}) and ELM energy loss (ΔW_{ELM}) decreased with increasing the counter rotation. But, the reduction of p_{ped} with counter rotation is less sensitive than ΔW_{ELM}, normalized ELM energy loss to the pedestal stored energy ($\Delta W_{ELM}/W_{ped}$) can be reduced with increasing the counter rotation [4.3-1]. In order to examine the dependence of pedestal width on non-dimensional parameters, ELMy H-mode plasmas were compared between hydrogen and deuterium plasmas. When ν^* and β_p were fixed between H and D plasmas, similar profiles of n_e, T_e and T_i were obtained, indicating weak ρ_p^* dependence. On the other hand, when ν^* and ρ_p^* were fixed in comparison of D plasmas with different plasma current, wider pedestal width was observed in high β plasmas. Based on these dedicated experiments, the scaling of the pedestal with of the ion temperature was evaluated as $\Delta_{ped} = a\ \rho_p^{*0.2}\ \beta_p^{0.5}$ [4.3-2].

References

4.3-1 Urano, H., *et al., Nucl. Fusion*, **47**, 706 (2007).

4.3-2 Urano, H., *et al., Nucl. Fusion*, **48**, 045008 (2008).

4.4 Steady-State Operation

Two group meetings were held and two members participated. Results on joint experiment for ITER hybrid and steady-state scenarios were discussed. Simulation study in ITER advanced scenarios by CRONOS, GLF23, ONETWO and TASK were carried out and compared. Issues related to this group in the ITER design review were discussed. From JT-60U, results on measurement of off-axis NBCD current profile using N-NB were reported, and experimental research plan, hardware modification and new diagnostics for the ITER advanced scenario study was explained and discussed. Benchmarking study of codes for electron heating and electron cyclotron current drive under ITER conditions was summarized and published [4.4-1]. Section related to this group in Progress of ITER Physics Basis was published [4.4-2]. Group papers for the 21st Fusion Energy Conference were published [4.4-3 (in collaboration with the ITPA pedestal topical physics group), 4.4-4]

References

4.4-1 Prater, R., *et al., Nucl. Fusion* **48**, 035006 (2008).

4.4-2 Gormezano, C., *et al., Nucl. Fusion* **47**, S285 (2007).

4.4-3 Maggi, C.F., *et al., Nucl. Fusion* **47**, 535 (2007).

4.4-4 Kessel, C.E., *et al., Nucl. Fusion* **47**, 1274 (2007).

4.5 MHD

Meetings of this Topical Group were held at San Diego in May, Garching in October, and Naka in February. Three members from JAEA attended at the all three meetings. Issues discussed were experimental and theoretical results on resistive wall mode (RWM), neoclassical tearing mode (NTM), high-energy particle induced instabilities such as Alfvén eigenmode, vertical instability, and disruption. Also discussed were the issues in the ITER Design Review, such as the effect of the resonant magnetic perturbation coils on ELM and RWM stability and the effect of ferritic steel tiles and test blanket modules on fast ion loss. From JT-60U, results of NTM experiment and comparison with TOPICS simulation were presented. In addition, results from experiments on the critical velocity for RWM and stability analysis using the MARG-2D code were presented. Specification of newly installed external magnetic perturbation coils was also shown. As contribution to the ITER Design Review, results of simulation on fast ion loss using the OFMC code under various installation conditions of ferromagnetic materials in ITER were presented [4.5-1].

Reference

4.5-1 Shinohara, K., *et al.,* "Effects of ferromagnetic components on energetic ion confinement in ITER," submitted to *Fusion Eng. Design*.

4.6 Scrape-Off-Layer and Divertor Physics

Three and two members participated in the 9th IPP Garching (Germany) meeting and in the 10th Avila (Spain) meeting, respectively. Experiment results of JT-60U contributed to the ITPA research. ELM filament dynamics such as propagation velocity and filament size were presented [4.6-1], and it contributed to a review of the 11th IAEA TCM on H-mode physics and transport barriers in Tsukuba (Japan) [4.6-2]. Comparison of the particle retention in the series of long-pulse discharges under 150 and 300 degree baking temperatures was presented. Impurity transport of the dominant radiator, i.e. C^{3+}, in the X-point MARFE was carefully determined [4.6-3]. Evaluation of dust generation in tokamaks was recently focused due to limitation of the ITER tritium retention. Dust correction result (~7% of the carbon erosion from the outer divertor tiles [4.6-4]) will reduce estimation of the tritium retention in the ITER.

References

4.6-1 Asakura, N., *et al.*, "ELM propagation in the low- and high-field-side Scrape-off Layer of the JT-60U tokamak," to be published in *J. Phys.: Conf. Ser.* (2008).

4.6-2 Kirk, A., *et al.*, "Comparison of the spatial and temporal structure of type-I ELMs," to be published in *J. Phys.: Conf. Ser.* (2008).

4.6-3 Nakano, T. *et al.*, "Radiation process of carbon ions in JT-60U detached divertor plasmas," *submitted to J. Nucl. Mater.*

4.6-4 Masaki, K., et al., *et al., J. Nucl. Mater.* **337-339** 553 (2005).

4.7 Diagnostics

A group meeting was held in Chengdu, China. Two scientists of JAEA participated the meeting. Progress in developments for ITER diagnostics was presented. A concept of absolute calibration of Impurity Influx Monitor utilizing a micro retro-reflector array was proposed and the expected signal level at the calibration was evaluated. Designing study of Micro Fission Chamber was carried out so that the chamber and the MI cable are separable for easier installation in the ITER vacuum vessel. Optimized viewing chord arrangements of Poloidal Polarimeter were obtained for various ITER operation scenarios, which satisfy the requirement of accuracy of q(r) measurement. From JT-60U, it was reported that the proof of principle test of Thomson scattering diagnostic utilizing Fourier transform spectroscopy was successful.

V. Broader Approach

1. Overview of the Broader Approach

1.1 Progress of the BA Programe

The Agreement between the Government of Japan and the European Atomic Energy Community for the Joint Implementation of the Broader Approach Activities in the Field of Fusion Energy Research (referred as "the BA Agreement" hereafter), which provides the legal framework of the implementation of the Broader Approach, was signed in February 2007[1.1-1]. The Agreement entered into force in June 2007 after the completion of internal procedure for conclusion of the Agreement in Japan and EURATOM. JAEA was assigned as the Implementing Agency in Japan and Fusion for Energy, which is also the Domestic Agency of ITER, was assigned as the one in EU.

The Broader Approach Agreement comprises three large research projects to be jointly implemented, aiming at supporting the ITER project and at an early realization of fusion energy as a clean and sustainable source of energy for peaceful purposes, and will be open to participation of other ITER Parties.

The three projects are 1) the Engineering Validation and Engineering Design Activities for the International Fusion Materials Irradiation Facility (IFMIF/EVEDA), 2) the International Fusion Energy Research Centre (IFERC), and 3) the Satellite Tokamak Programme. The first two projects will be carried out at Rokkasho, Aomori; the third project will be carried out at Naka, Ibaraki.

After the entry into force of the Agreement, 1st Steering Committee on the Broader Approach Activities was held in Tokyo on 21 June 2007 as shown in Fig. V.1.1-1. The Parties discussed the work program, structural framework etc. On 15 November 2007, the second meeting of the Steering Committee was held in Barcelona. The Steering Committee took note of the progress in each project and took decisions on the IFMIF/EVEDA, IFERC and the Satellite Tokamak Programme projects. To initiate activities of the both Implementing Agencies, a template for the Procurement Arrangement was made and approved by the Steering Committee and procurements of "in-kind" contributions were started.

Fig. V.1.1-1 The 1st BA Steering Committee

Reference

1.1-1 http://www.mofa.go.jp/policy/s_tech/b_approach/index.html

1.2 BA Organization

The general principles governing the Broader Approach Activities are specified in the BA Agreement [1.2-1]. The principles specific to each project of the Broader Approach Activities are specified in its Annexes I, II and III, which form an integral part of the BA Agreement. Administrative structure of the Broader Approach Activities consists of one Steering Committee and its Secretariat, three sets of Project Committee, Project Leader and Project Team of the individual projects, and Japan and European Implementing Agencies. Relationship of the individual elements of the administrative structure is presented in Fig. V.1.2-1 and their main functions are as follows

1.2.1 Steering Committee

The Steering Committee, which has legal personality, is responsible for the overall direction and supervision of the implementation of the Broader Approach Activities. The Steering Committee shall meet at least twice per year, alternately in Europe and in Japan. Major functions of the Steering Committee are;

(a) appointment of a project leader for each project and the staff of the Secretariat,

(b) approval of a project plan, a work programme, an annual report of each project and the structure of a project team.

1.2.2 Project Committee

Project Committee established for each project of the Broader Approach Activities meets at least twice per year (in principle, in Japan).

Major functions of each Project Committee are:

(a) making recommendations on the respective draft Project Plans, Work Programs and Annual Reports to be submitted to the Steering Committee,

(b) monitoring and reporting on the progress of the project of the BA Activities.

1.2.3 Project Leader and Project Team

The Project Leader is responsible for the co-ordination of the implementation of the project. Each Project Leader is assisted by the respective Project Team in the exercise of his responsibilities and functions. The members of each Project Team shall comprise the Experts and other members such as visiting scientists. The structure of each Project Team shall be approved by the Steering Committee upon proposal by the respective Project Leader.

Major functions of each Project Leader are:

(a) organizing, directing and supervising the Project Team in the implementation of the Work Programme;

(b) preparing the Project Plan, the Work Programme and the Annual Report, and submitting them to the Steering Committee for approval after consultation with the respective Project Committee;

(c) reporting to the Project Committee on the progress of the respective project of the Broader Approach Activities.

1.2.4 Implementing Agency

Each Party designated an implementing agency, i.e., JAEA of Japan and Fusion for Energy of EU to discharge its obligations for the implementation of the BA Activities, in particular to make available the resources for their implementation.

JAEA host the Project Teams and makes available working sites including required office accommodations, goods and services. JAEA is also responsible for the management of agreed financial contributions to operational costs and of the financial contributions to common expenses of each Project Team, dedicated to each project of the BA Activities. In addition, JAEA takes the necessary steps to obtain all permits and licenses provided for in the laws and regulations in force in Japan and required for the implementation of the Broader Approach Activities.

Reference

1.2-1 Agreement Between the Government of Japan and the European Atomic Energy Community for the Joint Implementation of the Broader Approach Activities in the Field of Fusion Energy Research.

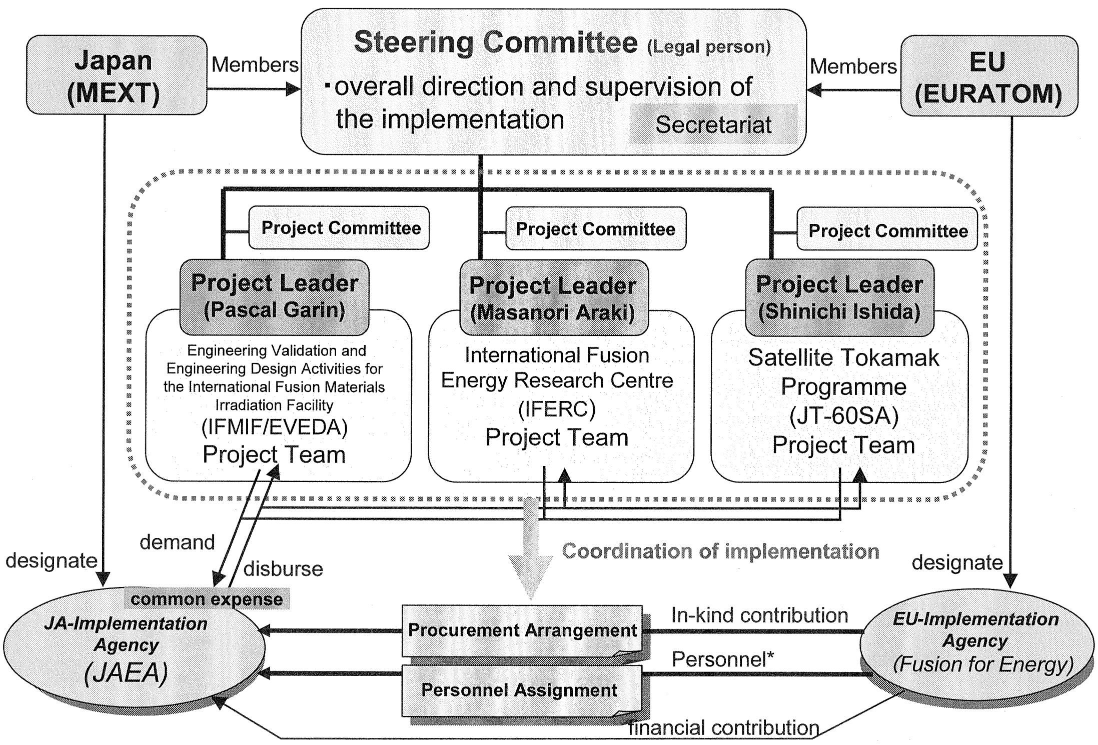

Fig. V.1.2-1 Administrative Structure of the Broader Approach Activities

2. Satellite Tokamak Programme

2.1 Overview

Based on the BA agreement entry into force, the Project Leader and the Project Team were nominated and started the activity. In order to expand the scope of the work towards the re-baselining of the design for the integrated design report, a single albeit distributed organization was established, constituting an integrated team working under the leadership of the Project Leader and of the JA and EU Project Managers. The integrated team proceeded the integration activities and design activities described in following sections.

2.2 Integration Activities

The Project Leader (PL) was nominated in the 1st Steering Committee (SC) Meeting. Executive summary of the Conceptual Design Report on JT-60SA (CDR) has been prepared based on the CDR and approved in the 1st SC Meeting.

Functional specifications of the components (FS) were agreed in the 1st Coordination Meeting between Japanese and European Implementing Agencies (JA- and EU-IAs) held on 23-26 July 2007 at the EFDA Garching under the coordination of the PL. The STP Project Committee (STP-PC) approved the FS submitted to the 1st STP-PC Meeting (remote meeting) held on 10 August 2007, and agreed to inform the SC. However, the functional specifications were not adopted by the SC through a written procedure as a consequence of concerns with respect to the cost estimates.

Proposal of the integrated organizational structure and actions for an Integrated Design Report (IDR) towards re-baselining of the design to meet the cost objectives was approved in the 2nd SC Meeting. Then, activities to organize the integrated organizational structure working under the leadership of the PL and of the JAEA and Fusion for Energy (F4E) PMs, and actions for the IDR were commenced.

Five experts were appointed for the Project Team (PT) in the 2nd SC Meeting, while they had already started activities with the PL from the beginning of the Project.

A Common Management and Quality Programme (CMQP) including necessary management structures and processes was agreed among the PL and the IAs. Based on CMQP, the JAEA JT-60SA Quality Assurance Programme based on ISO 9001:2000 and IAEA No. GS-R-3 (2006) was developed and also agreed.

In order to develop the "Codes and Standards", JAEA started discussions on applicable laws for the superconducting magnet and cryogenics system with the prefecture authority, and for the vacuum vessel with the governmental authority, respectively. Work Breakdown Structure (WBS) was developed by PT who incorporated inputs from each IA. Document management for integrated activities started operation with Documentation Management System (DMS) equipped by F4E based on ITER Documentation Management (IDM) system. Designated members of PT and both IAs started to use this tool for storage, review, and approval of common documents. The preparation of CAD management software (SmarTeam) has been started.

The re-baselining of the machine design has been developed as follows:

- Plasma performance has been changed in a limited way. Albeit some reduction of aspect ratio, in some sense some parameters have been improved.
- The toroidal field ripple has been further reduced.
- The flattop flux has been increased to provide a reasonable window of operation with long pulse and high current. About 4-5 Wb has been added.
- Design requirement of the maximum neutron rate was re-assessed to reduce nuclear heating in the magnet, jointly with F4E.
- Seismic analysis was started including soil property of the Naka site to identify seismic load at ground floor in collaboration with F4E.

2.3 Design Activities

Based on the provisional Work Programme 2007 approved in the 1st SC Meeting, the following activities were implemented.

2.3.1 TF Magnet

Current feeder and He coolant pipes of the TF coils in the cryostat were designed. Interface issues with the vacuum vessel were assessed jointly with F4E, requiring a down shift of the large horizontal ports of vacuum vessel, for the installation of inter-coil structure of TF magnet.

2.3.2 PF Magnet

The detailed design report of Central Solenoid and

Equilibrium Field Coils was submitted to the PL and F4E as the evolution of CDR. Considering the comments from F4E, the plasma operational boundary was developed from a viewpoint of experimental flexibility. The PA for superconducting conductors of CS and EF coils was signed by the IAs with the consent of the PL. Based on the PA, the tender documents for cable and EF jacket were prepared.

2.3.3 Vacuum Vessel

The geometrical shape of vacuum vessel was assessed, and a round shape in poloidal direction and polygonal shape (10 degree segments) in toroidal direction was chosen from a viewpoint of easiness of manufacturing. The detailed design report of the Vacuum Vessel was submitted to the PL and F4E, subject to revision after the submission of IDR to the SC. The PA for the vacuum vessel including the vacuum vessel body, ports, gravity supports, jigs and tools was proposed. The implementation of the PA is limited by appropriate milestones for possible revision of the design, including a hold point, such that manufacturing should not be started before the overall geometry, dimension and shape are finalized in the IDR.

2.3.4 In-Vessel Components

Technical R&D plans were discussed with the support of the ITER blanket laboratory. There are some possible candidates for fabrication of the CFC mono-block type divertor target. This activity will continue to the middle of 2008. The PA for raw materials (CFC) of divertor targets, domes and baffles was prepared.

2.3.5 Power Supply and Control

Plasma operation scenarios for ITER-shaped single null and low-A double null configurations were developed to meet cost objective on power supplies to be supplied by EU so that power supplies could be designed by using existing JT-60 transformers. Work continued in the area of Quench Detection System and the definition of the technical specifications of the power supplies for the EF system. Consorzio RFX staffs visited at JAEA-Naka to discuss the specifications on quench protection system (one stayed in October to December, one stayed for one week in October, and three stayed for one week in December). EU (RFX) and JAEA have jointly drawn up the basic document series with the joint work report to proceed the detail design activities. In cooperation with EU, JAEA proceeded to design the overall power supply systems consistently with the existing facilities and buildings.

2.3.6 Cryostat

Detailed drawings and analysis results of the gravity supports of the cryostat was provided to EU for the manufacturing design. The support work for the detailed design of the cryostat vessel body is ongoing to provide the design conditions, functional requirements and detailed drawings to EU. Three CIEMAT staffs stayed at JAEA in July and August (2 staffs for one month), and one JAEA staff visited CIEMAT in October for the detailed design of the gravity supports. Issues with respect to seismic loads coming from the vessel and magnet supports was identified, which gives a base for the detailed design of the gravity supports and the cryostat body done by EU.

2.3.7 Cryogenic System

The total heat load was evaluated in time to provide as design conditions for EU. Through the collaborative works with EU, the conceptual design definition of the cryoplant was conducted, including specific activities such as 1) pre-sizing of the main refrigerators, capacities storage and warm compressor sets, 2) synthesis of thermal heats loads/summary of cryoplant needs, and preliminary thermo hydraulic calculations, 3) definition of process flow diagrams for cryoplant and cryodistribution as well as the determination of the main cryogenic equipments.

2.3.8 ECRF

JAEA exchanged necessary information with EU to determine the detailed specifications, the outlines of construction and test schedule, device layout and interface design. The operational data and the general site conditions for the ECRF system were provided to EU. The procurement items for the gyrotron set, the superconducting magnet and the high voltage power supply were defined. The delivery boundaries, the JAEA contribution on-site, the site conditions are being revised and mutually agreed. The re-design of the JT-60SA magnet has a direct impact on the ECRF design, since the lowered main field should require, to maintain the same physics goals, a decrease of the

ECRF resonance frequency by an equivalent ratio. This ECRF design change is presently under consideration with EU-IAs.

2.4 Coordination and Review Meetings

The PL organized the 1st Coordination Meeting in July at Garching for the agreement of the functional specifications and the discussion of project management issues. The Project Coordination Meeting (PCM) had been regularly held seven times in which management and technical issues were discussed by PL and F4E-IA/JAEA-Project Managers.

2.5 Reporting

The following documents were reported to the Steering Committee (SC) and the Project Committee (PC).

2.5.1 Report to the SC

i) 1st SC Meeting (21 June, 2007);

a. "Structure of Project Team for the Satellite Tokamak Programme", BA SC 01-6.2.3.
b. "Executive Summary of Conceptual Design Report on JT-60SA", BA SC 01-6.3.3(a).
c. "Provisional Work Programme 2007 for the Satellite Tokamak Programme", BA SC 01-6.3.3(b).

ii) 2nd SC Meeting (15 November, 2007);

a. "Integrated Organizational Structure and Actions for Integrated Design Report", BA SC 02-7.2.
b. "Provisional Work Programme 2007-2008 for the Satellite Tokamak Programme", BA SC 02-7.2.1.

2.5.2 Report to the PC

i) 1st STP-PC Meeting (10 August 2007);

a. "Progress and Status", BA STP PC 01-6.
b. "Functional Specifications of Components", BA STP PC 01-7.1.
c. "Comparison of Functional Specifications with those of JA-EU Satellite Tokamak Working Group Report", BA STP PC 01-7.2.
d. "Record of Conclusions Minutes of the 1st Meeting of the Satellite Tokamak Programme Project Committee", BA STP PC 01-8.

ii) 2nd STP-PC Meeting (31 March 2008);

a. "2007 Annual Report", BA STP PC 02-4.
b. "Provisional Project Plan of the Satellite Tokamak Programme", BA STP PC 02-5.
c. "Update of Actions for Integrated Design Report", BA STP PC 02-8.
d. "Record of Conclusions of the 2nd Meeting of the Satellite Tokamak Programme Project Committee", BA STP PC 02-12.

3. International Fusion Energy Research Center

3.1 Overview

For DEMO design, information exchange to obtain common view of DEMO design concepts and discussion on the common issues for DEMO basic design was carried out. Regarding research and development for DEMO design, survey and design for experimental equipments, devices, etc., to be installed in the facility at the Rokkasho site, had been carried out. Also, Procurement Arrangement for the urgent tasks to be implemented for DEMO R&D was made with the EU Implementation Agency, and preliminary R&D had been initiated.

To realize selection of a "state-of-art" super computer for the Computational Simulation Centre, JAEA started examination of existing database for selection of a supercomputer and choice of appropriate benchmark codes with the Project Leader and the EU Implementation Agency, in order to facilitate discussion in the Special Working Group to be established by the Steering Committee.

Detailed design of the buildings had been completed in January 2008 and contracts for the constructions were made in March 2008 after all the processes including making a procurement agreement of the IFERC related buildings. Construction started in spring 2008 and will be completed in March 2010.

3.2 BA DEMO Design

In FY 2007, Japanese and European experts met twice to exchange their own views on DEMO design. In particular, the first BA DEMO Design Workshop held in 2007 July in Rokkasho, covered various topics including

- objectives and organization of DEMO BA activity,
- fusion development strategy and the definition of DEMO,
- key issues on DEMO physics, technology and engineering,
- proposals on DEMO R&D.

In the workshop, it was recognized that DEMO Design activity would be divided into at least two phases and that workshops and technical meetings would be held in Phase One (first three years). Other points of the discussion in the workshop are as follows:

1) DEMO physics basis and related issues were discussed on the basis of the understandings of the present experiments and computational simulations. Since the physics basis should be validated in the ITER first phase operation, the role of simulations for DEMO physics assessment is expected to expand during BA activity;

2) As to DEMO technology and engineering, it was recognized that study or assessment on "maintenance and blanket", "performance of heating and current drive system", "coolant", "magnet", and "divertor" would be beneficial to develop a common DEMO design basis.

Considering the results of the workshop, the design issues to be implemented as "Work Programme for 2008" were determined. Most of the issues are relevant to the "design drivers and constraints" discussed during the workshop. Amongst the other issues, which are related with "system design", the most critical design issues cover the assessment of pulsed DEMO and a parametric analysis of DEMO. The tasks are summarized as follows:

i) Design drivers and constraints

- Physics : plasma shaping, positional stability of shaped plasma, etc.
- Technology and engineering : magnet, CD system, EM forces, maintenance, etc.

ii) System design

- Feasibility of pulsed DEMO
- Sensitivity study of design parameters

In the second workshop, the background on why these issues were selected as tasks for 2008 was explained. Japanese and EU's stances on such tasks in Phase One are on a voluntary basis. Thus, each Party will contribute to every possible issue concerned with its domestic DEMO design activity.

On the Japanese side, JAEA, CRIEPI (Central Research Institute of Electric Power Industry) and universities have attempted to solidify cooperative ties. It was confirmed that effective use of cooperative activities under the Fusion Energy Forum and bilateral research cooperation between CRIEPI or a university and JAEA should be promoted.

3.3 BA DEMO R&D

BA DEMO R&D activities are planned to implement following 5 items;

1) R&D on Materials Engineering for DEMO Blanket
2) R&D on Advanced Neutron Multiplier for DEMO Blanket
3) R&D on Advanced Tritium Breeders for DEMO Blanket
4) R&D on Tritium Technology
5) R&D on Mechanical Properties of SiC/SiC

To effectively and smoothly start the DEMO R&D coordination activities as a part of the IFERC project, assessment and preparation of the activities as mentioned above have been completed based on the "Procurement Arrangement for the Initial Urgent Task for the DEMO R&D for the International Fusion Energy Research Centre". Also the assessment and preparation provided the information necessary to the DEMO R&D Centre Building design to be completed by early 2008.

3.3.1 R&D on Materials Engineering for DEMO Blanket

In R&D on Material Engineering for DEMO Blanket, the optimization of fabrication technology of reduced activation ferritic/martensitic steels (RAFM) is going to be conducted. In Japan, F82H (Fe-8Cr-2W-V,Ta) will be the material to be optimized.

In this R&D, impurity and inclusion control under large scale fabrication process would be one of the key issues to practically estimate achievable reduced activation level in DEMO. Thus, it is important to assess the currently available large scale fabrication technologies for RAFM production, in order to plan the detailed R&D activities.

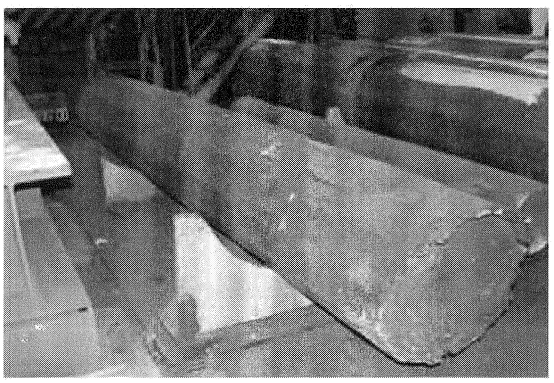

Fig. V.3.3-1 F82H ingot before ESR.

In FY 2007, the vacuum induction melting (VIM) of F82H in 5 tons followed by secondary refinement and forging was performed for this purpose as shown in Fig. V.3.3-1. It was found that Electro Slag Remelting (ESR) was required as for secondary melting process in order to control unexpected impurities. Three slabs were made as the wrought product as shown in Fig. V.3.2-2.

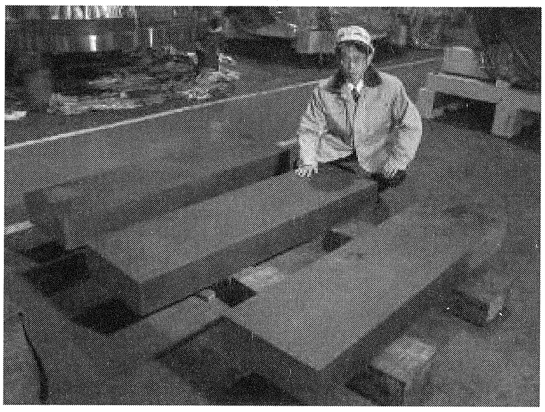

Fig. V.3.3-2 F82H slabs.

3.3.2 R&D on Advanced Neutron Multiplier for DEMO Blanket

In 2007, the conceptual design of the beryllium handling facility in the DEMO R&D Building was carried out on the following items; (1) survey of all regulations relevant to the beryllium (Be) handling facility, (2) preliminary design work of the Be handling facility, and (3) specifications of the Be handling facility.

The size of the Be handling facility is 8m×12m. The electrodes made of beryllides such as $Be_{12}Ti$ and $Be_{12}V$ will be fabricated in this facility. Be is a hazardous substance, and it is necessary to get the license to use it. Main items and values for the regulation were determined for the conceptual design of the Be handling facility. The maximum concentration of Be must be less than 0.002 mg/m^2 according to a Japanese law. This concentration is also adopted in the International Program on Chemical Safety (IPCS).

Fig. V.3.3-3 shows the plan view of the Be handling facility in the DEMO R&D building. The Be handling facility will be composed of three areas, namely, the controlled area for Be handling, the room of exhaust system, and the entrance area.

The devices for manufacturing of beryllide electrodes will be installed in this controlled area. The devices for the manufacturing will be of tightly closed structure. The frequency of ventilation in the controlled area will be set at 16 times per hour. On the other hand, the devices for the manufacture and the draft chambers installed in the controlled area will be connected to a local exhaust ventilation system. The local exhaust ventilation system will be arranged in the room of exhaust system. Beryllium will not be manufactured in this room, so that the frequency of ventilation in this room will be decreased to 4 times per hour. Entrance of researchers and engineers will be administered in the entrance area. This area shall not be contaminated by beryllium, and will be segregated by an air shower when the researchers and engineers go into the controlled area.

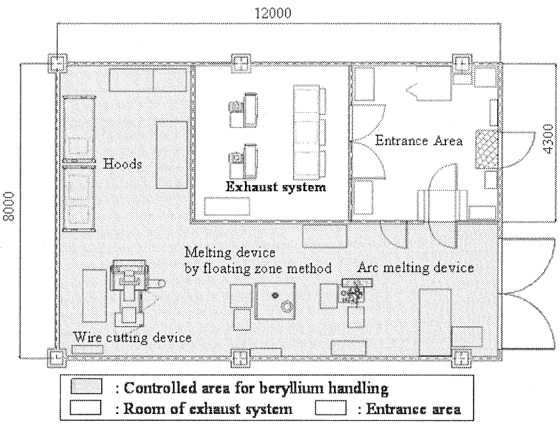

Fig. V.3.3-3 Plan view of the beryllium handling facility in the DEMO R&D building.

3.3.3 R&D on Advanced Tritium Breeders for DEMO Blanket

The equipment for production of advanced tritium breeder pebbles will be installed in DEMO R&D Building, in preparation for BA R&D works on lithium ceramic pebbles.

In FY2007, feasible processes were examined for dissolution, purification, raw-material preparation, composition adjustment and pebble-forming processes, in which 100 gram of spent lithium ceramic breeder pebbles are introduced as a raw material, and purified lithium ceramic pebbles can be eventually re-produced. Approximate specifications were also investigated by examining the dimension of apparatuses in these processes and by selecting appropriate apparatuses.

Fig. V.3.3-4 shows a conceptual diagram of lithium recovery process which is being studies in Japan. Step-1 (dissolving process) and step-2 (purification process) were investigated so far in preliminary experiments. Lithium recovery of more than 90% was attained by an aqueous dissolving method using HNO_3, H_2O_2 and citric acid. Furthermore, decontamination efficiencies of ^{60}Co were 97 – 99.9% using a new chemical adsorbent, i.e., activated carbon impregnated with 8-hydroxyquinolinol.

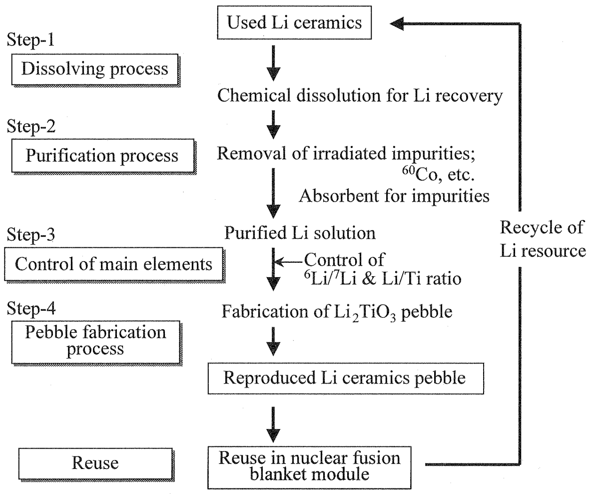

Fig. V.3.3-4 Conceptual diagram of lithium recovery process for the tritium breeder.

As for the pebble-forming process, conceptual investigations were carried out for a rotating granulation method to prepare the precursor of Li_2TiO_3 pebbles with a controlled Li/Ti ratio. The developed method should be realizable based on a new process with simple operation and reduced waste, and has a capability to replace the conventional sol-gel method. It is summarized at this stage that further experimental investigations on the production conditions are needed together with selection of apparatuses and equipment.

3.3.4 R&D on Tritium Technology

It is essential for the R&D on tritium technology to install the tritium handling equipment at Rokkasho. A part of structural design for construction of DEMO R&D Building was carried out by early 2008. To provide a set of information of the tritium handling equipment is one of the most urgent duties for the R&D on tritium technology. The present R&D activity in the field of tritium engineering is therefore focused on a series of conceptual design of the tritium handling equipment. As the result, a set of system concepts, brief system configurations of the tritium handling equipment have been decided through the design works: ventilation concepts; monitoring systems; hoods and glove boxes; tritium removal facilities; tritium waste water facilities; etc. The procedure and the schedule of the above-mentioned R&D tasks were also examined.

A conceptual layout of tritium handling equipment has been decided as shown in Fig. V3.3-5. There are a radio control area and a cold experimental area. In the cold area, a set of experiments of beryllium and breeder materials will be carried out. The radio control area is composed of a tritium handling area and some experimental rooms for material studies. The radio control and the cold areas are ventilated by two HVAC (heating, ventilation and air conditioning) systems separately. A conceptual layout of main components in the tritium area has also been decided. To handle tritium, there are glove boxes, hoods, a tritium removal system, and a liquid waste system. The conceptual flow diagrams of the HVAC and the tritium removal systems have been then decided.

Based on the result in 2007, a work of the detailed design of the equipment will be carried out in 2008. In the detailed design studies, a layout, flow diagram, and drawings of main components will be made. A preliminary application form for the licensing will be prepared as the results of this work.

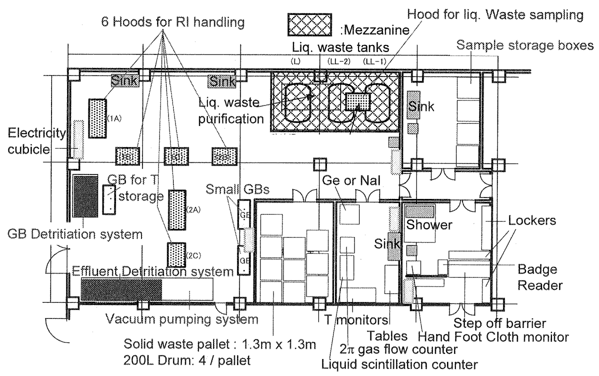

Fig. V.3.3-5 Conceptual layout of tritium handling equipment in the DEMO R&D building

3.3.5 R&D on SiC/SiC Composites

A silicon carbide fiber reinforced silicon carbide (SiC/SiC) composite is one of the attractive materials for the high-temperature operating advanced DEMO blanket. Of many composite types, a nano-infiltration transient-eutectic-phase sintered (NITE) SiC/SiC composites is specifically considered as a main target material in the R&D on SiC/SiC composites for the DEMO R&D for the IFERC project. This task aims to assess whether the NITE-SiC/SiC composite is sufficient to be used as a reference material throughout the project.

According to the literature survey on the "lab-grade" NITE-SiC/SiC composites, it is concluded that the latest "lab-grade" NITE-SiC/SiC composites can be satisfactorily utilized as reference materials in the project due to the exceptionally high-competitiveness. Based on this assessment, a preliminary specification of the reference NITE-SiC/SiC composites was decided. With this specification, two types of "pilot-grade" NITE-SiC/SiC composites: unidirectional and cross-ply plates were preliminarily produced and their fundamental material properties were evaluated. Figures V.3.3-6 and -7 show the outlook and the micro-structure of the unidirectional NITE-SiC/SiC composite prepared as a reference specimen.

Most fundamental requirements of these composites were found to be in acceptable level, though the results indicate that the present "pilot-grade" NITE-SiC/SiC composites need some minor modifications. Microstructural observation and tensile test results specified key directions in optimization of the process control from the following aspects: 1) fiber protection during processing, 2) intra-bundle matrix densification, and 3) control of fiber volume contents.

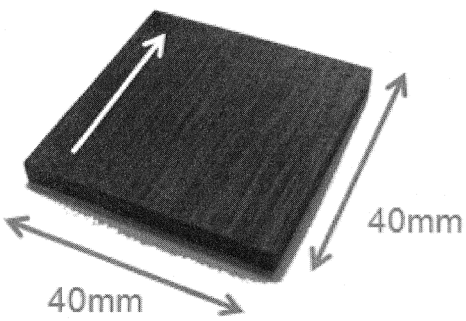

Fig. V.3.3-6 Picture of the unidirectional NITE-SiC/SiC composite prepared as a reference specimen.

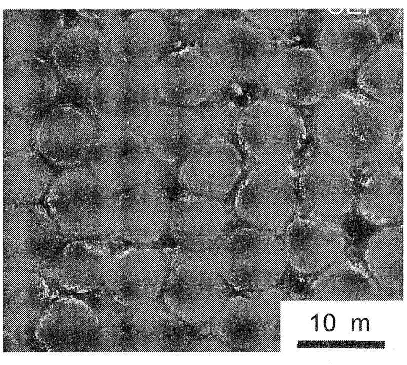

Fig. V.3.3-7 Micro-structure of the unidirectional NITE-SiC/SiC composite.

3.4 Fusion Computer Simulation Center

In FY 2007, a technical meeting on the CSC building was held (September 7, CEA-Saclay, France) to reach a consensus between Japan and Europe that the building should be a two-storied one for the protection of super computer system; the first floor is for the facility of air conditioning and power supply; the second floor is for the super computer with peripheral equipments. Also, it has been confirmed that an electric power of 4.5 MW and a space of 600 m^2 should be enough for a super computer with the peak performance of 1 Peta flops that becomes available in 2012.

The second technical meeting was held from December 10 to 12, 2007 at CEA-Saclay, and defined the detailed list of items, summarized in a table with appropriate future action items. Through the second meeting, the followings are confirmed:

(1) The UPS (Uninterruptible Power Supply) system is unnecessary for a super-computer since many present-day and future super-computers are designed so that they can shut down safely without UPS in case of the power failure.

(2) The assessment of cooling systems, both air cooling and liquid cooling, are continued so that they have enough performance for the CSC super computer and simultaneously meet the boundary conditions of the CSC building, such as necessary space and necessary electric power for itself.

3.5 Design and Construction of IFERC Buildings

In the fiscal year 2007, detailed design of the site development was carried out and construction was initiated. There are three buildings related to the IFERC project, which are Administration & Research Building, CSC&REC building and DEMO R&D Building. The construction schedule is shown in Figure V.3.5-1.

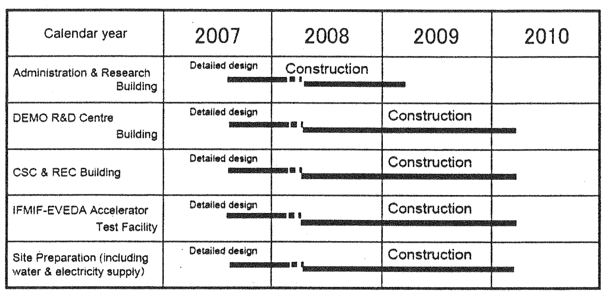

Fig. V.3.5-1 Design & construction schedule of Buildings and Site Preparation, at the Rokkasho BA Site.

Detailed design of the buildings and power station at the Rokkasho BA site have been carried out. The implementation design of the buildings started in Aug. 2007. Procurement Arrangement was concluded between the Implementation Agencies with the consent of the Project Leader. Site development (uprooting, flatting ground and construction of temporary road) was completed in Sept. 2007, succeeded by the foundation examination including boring core sampling/test. The Administration & Research Building will be completed in March 2009, and the other research buildings will be completed in March 2010. The completion image of the building of the DEMO R&D building is shown in Fig. V.3.5-2.

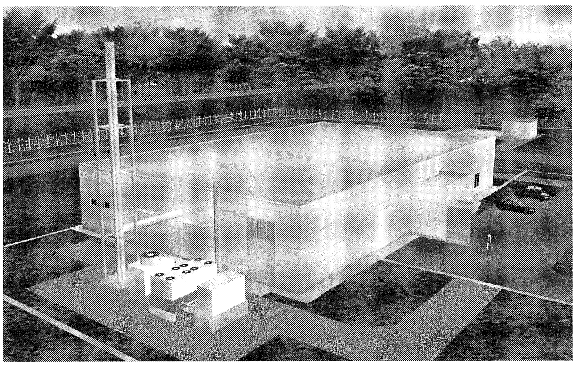

Fig. V.3.5-2 3D image of the DEMO R&D building.

4. IFMIF/EVEDA

4.1 Overview

In the first year of IFMIF/EVEDA, the project team consists of seven experts (4 expert from EU and 3 experts from Japan) and one support staff from Japan. To procure the facility, goods, etc., which will be required for the planned future activities, the following items were implemented under coordination with the EU Implementation Agency and the Project Leader.

1) Preliminary examination and detailed planning of engineering validation of the accelerator components (RFQ coupler and its control method),
2) Detailed design of the Prototype Accelerator building and its auxiliary components (mainly high voltage power supply),
3) Detailed plan for initial engineering research of the lithium target, and
4) Detailed plan for initial engineering research of the test cell.

Among those items, the implementation design of the Prototype Accelerator building was completed in January 2008.

4.2 Accelerator

4.2.1 Conceptual Design of an RF Input Coupler

RF input couplers using co-axial waveguide of a 4 1/16 inch and 6 1/8 inch were designed. The final size will be decided by a high RF power test using a high-Q load circuit. Configuration of the RF input coupler using the size of 4 1/16 inch indicates in Fig.V.4.2-1.

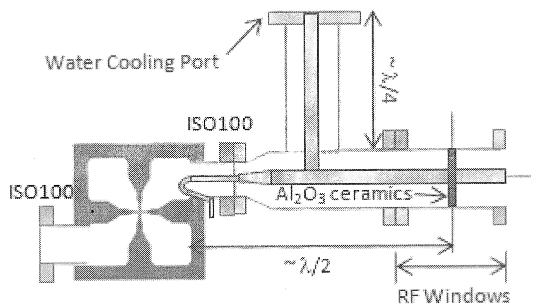

Fig. V.4.2-1 Configuration of an RF Input Coupler.

The RF input coupler consists of a taper waveguide, an RF window and a water cooling port, respectively. The taper waveguide length of less than $\lambda/4$ and the length of water cooling port of $\lambda/4$ were designed. If it is possible to get cool the antenna tip by double a water cooling circuit in the loop diameter, the water cooling port is not necessary. For the RF window, a ceramics disk made of Al_2O_3 was located at the $\lambda/2$, in order to suppress electric field at the disk on no beam loading.

4.2.2 Conceptual Design of Control System

Conceptual design of Personal Protection System (PPS), Machine Protection System (MPS) and Timing System has been started. In 2008, the detail design will be completed.

4.2.3 Design of IFMIF/EVEDA Accelerator Building

Implementation design of the accelerator building was carried out and completed by the end of July 2007. Discussion with EU Accelerator Sub-working Group (ASG) was performed on the layout and neutron shielding. It was concluded that the concrete thickness of 1.5m is reasonable with the conditions of using a local concrete shield of 0.5m-thickness and a water tank of a 1m-radius for beam dump. Layout of the accelerator building with a floor area of 2,020m^2 is shown in Fig.V.4.2-2. The accelerator building consists of Power supply area, Accelerator vault, Nuclear Heating, Ventilation and Air Conditioning Area (Nuclear-HVAC) system, Control room and so on. The building construction will be completed in March 2010.

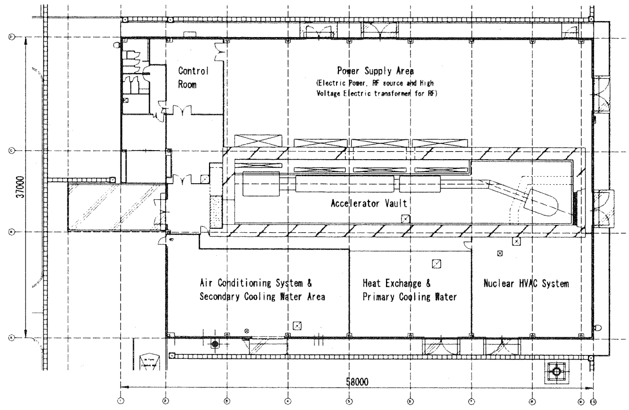

Fig. V.4.2-2 Layout of the IFMIF/EVEDA Accelerator Building.

4.3 Target Facility

In FY2007, the engineering validation tasks were started as conception phase including planning and conceptual design, and analytical estimations were carried out in the engineering design task, as follows.

4.3.1 Conceptual Design of EVEDA Lithium Test Loop

To validate safe stable long-time operation of a liquid Li loop simulating IFMIF Li loop from viewpoints of hydraulics and condition of impurities in Li, the EVEDA Lithium Test Loop is constructed and operated. The loop is operated for also other validation tasks for flow diagnostics and Li purification system. To meet the requirements, major specification of the loop were determined as shown in Table V.4.3-1 and a target assembly was conceptually design as shown in Fig. V.4.3-1 [4.3-1].

Table V.4.3-1 Major Specification of EVEDA Li Test Loop.

Item	Specification
Thickness of Li jet	25 mm
Width of Li jet	100 mm
Velocity of Li jet	20 m/s
Contraction of nozzle	250→62.5→25 mm
Curvature of back-plate	min. 250 mm
Temperature of Li	250-300 °C
Impurity control	10 wppm (each H, C, N, O)
Vacuum near Li flow	10^{-3} Pa (in Li operation) 10^{-4} Pa (without Li)
Materials	RAF (Back-plate), 316L (others)

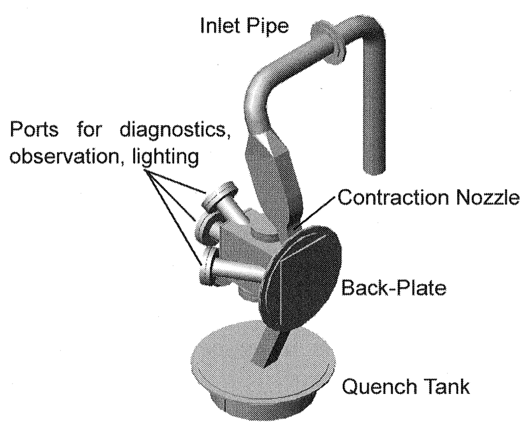

Fig. V.4.3-1 Target Assembly of EVEDA Li Test Loop.

4.3.2 Thermal-stress Analysis of Back-Plate

A thermal-stress analysis using ABAQUS code was performed for an engineering design of a back-plate of the IFMIF target, which should have enough low thermal-stress even under nuclear heating up to 25 W/cc by the neutrons in IFMIF operation. Allowable stress was 455 MPa for most part of the back-plate made of a reduced-activation ferritic martensitic steel F82H and 328 MPa for circumference part made of 316L stainless steel at 300 °C. In this analysis effect of thickness of stress mitigation part: t_{SM} was estimated.

Figure V.4.3-2 shows the von Mises stress of the back-plate in case of t_{SM} = 2, 5, 8 mm. In the F82H part, in any cases, the stress was < 170 MPa far less than 455 MPa. On the other hand, in the 316L part, maximum stress 208, 326, 500 MPa was respectively given at the stress-mitigation part with t_{SM} = 2, 5, 8 mm. The thickness: t_{SM} should be 5 mm or more [4.3-2].

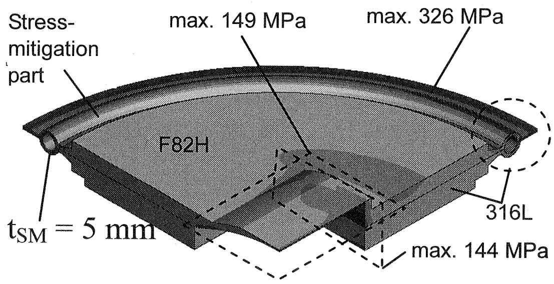

Fig. V.4.3-2 von Mises Stress of Back-plate (t_{SM} = 5 mm).

4.3.3 Dose Estimation of Lithium Loop

Behavior of beryllium-7 (^{7}Be, the dominant radioactive nuclide in IFMIF Li loop) was estimated considering temperature gradient in the loop. The result showed that most of ^{7}Be, 5.0 x 10^{15} Bq, would be deposited on most downstream 1/10-part of the heat exchanger. Subsequent estimation using QAD-CGGP2R code for dose equivalent rate showed that, without radiation shielding, the rate would be 8.5 x 10^7 μSv/h, far higher than a guideline of 10 μSv/h. Required thickness of radiation shield made of lead was 8 cm [4.3-3].

References

4.3-1 Nakamura, H.., *et al.*, "Latest Design of Liquid Lithium Target in IFMIF," *Proc. 8th ISFNT*, (2007), to be published in *Fusion Eng. Des.*.

4.3-2 Ida, M., *et al.*, "Thermal-Stress Analysis of IFMIF Target Back-Wall made of Reduced-Activation Ferritic Steel and Austenitic Stainless Steel," *Proc. 13th ICFRM*, (2007), to be published in *J. Nucl. Mater.*.

4.3-3 Ida, M., *et al.*, *Fusion Eng. Des.*, **82**, 2490 (2007).

4.4 Test Cell Facilities

In Japanese work program, there are three subjects correlated with each other.

4.4.1 Post Irradiation Examination Facility

Measurement equipments in Post Irradiation Examination (PIE) facility of IFMIF was summarized and analyzed. In basic conditions of design of PIE facility, it was thought that the PIE facility would treat mainly with small specimens and a rig of high flux test module (HFTM); In addition, the design of PIE facility needs to consider the time schedules and allotments of PIE tests inside and outside of IFMIF facility.

As described in Key Element Technology Phase, it can list the kinds of the equipments for the PIE tests which are necessary as below; cutter, welder, NaK processing and pouring equipments, universal testing machine, fatigue testing machine, slow strain rate testing machine, compact Charpy impact tester with thermostat, equipment for measurement of specimen dimension, periscope, laser profile meter, specimen preparation machines, optical microscope, micro hardness tester, Ge and Si-Li gamma ray spectrometer, immersion density equipment, furnace, other equipments (measurement of magnetic property of specimen, electric insulation of heater, electromotive force of thermocouple, etc), shielded storage containers. However, it should list furthermore the other important PIE equipments as below; reloading instruments of specimens and a rig of irradiation module, fracture toughness, creep, creep-fatigue, crack growth measurement, SP test, hardness, automatic radiography, micro γ-scanning, chemical analysis, extraction residue device, X-ray diffraction, FIB, etc. As a non-destructive inspection, there is appearance inspection, X-ray inspection, size measurement, γ scanning and eddy current flow detection, etc.

Conceptual design of the PIE facility will be performed from 2008 to 2009. In addition, some techniques of the PIE facility such as reloading process will be examined. Engineering design of the PIE facility will be performed from 2010 to 2013. In addition, some techniques of the PIE facility such as reloading process will be examined. Engineering design of the PIE facility will be performed from 2010 to 2013.

4.4.2 High Flux Test Module

The detailed engineering design of the High Flux Test Module (HFTM) and the objective was discussed. In Japan, the horizontal set-up HFTM was proposed as shown in Fig.V.4.4-1. This becomes very useful for the irradiation module at high temperatures about 1000°C. The summarized work program is described as below;

(1) Conceptual design of heater-integrated plate and capsule (H-I).
(2) Fabrication and basic performance tests of model of H-I.
(3) Engineering design of prototype of H-I.
(4) Performance tests of prototype H-I in gas loop.
(5) Engineering design of full scale HFTM.

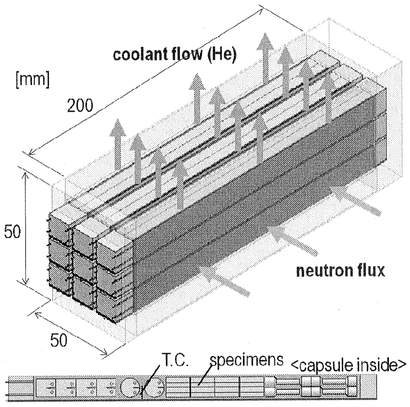

Fig. V.4.4-1 Horizontal set-up HFTM.

4.4.3 Small Size Test Technique

Work program of Small Size Test Technique (SSTT) and the objective was discussed. The summarized work program is described as below;

(1) Preparation for the standardization of test methodology of small size specimen for fracture toughness, fatigue and crack growth tests.
(2) Evaluation of extrapolating methodology of experimental data on small size specimens to standard size specimens.

VI. Fusion Reactor Design Study

1. Progress in Compact DEMO Reactor Study

The design study of fusion DEMO reactor based on a slim CS (center solenoid coil) concept has been continued and still now be in progressing way. The slim CS concept leads to low aspect ratio plasma. The lower aspect ratio plasma is considered to have higher plasma performance (high elongation plasma and high beta) and then is considered to be preferable from viewpoint of economical aspect. The size of CS coil (radius of 75cm) is decided from the minimum magnetic flux requirement of 20 volt-second.

The SlimCS reactor produces a fusion output of 2.95GW with a major radius of 5.5m, aspect ratio (A) of 2.6, normalized beta (β_N) of 4.3 and maximum toroidal field of 16.4T.

Among the design progress issues, two issues concerning a plasma profile consistency and a tritium breeding are given in the followings.

Since plasma parameters are determined by a systems code based on a point model, the parameters should be checked for correctness using a one-dimensional (1-D) code. For this purpose, an ACCOME code [1-1] was used to investigate the consistency between the assumed plasma profiles and key parameters such as P_{fus}, β_N, n/n_{GW}, HHy2 and f_{BS}. In the 1-D analysis, we attempted to find a solution with q-profile other than strongly reversed shear (RS). This is because strong RS does not seem to be appropriate as the standard operation mode of SlimCS from the points of view of disruptivity and the controllability of q in the central region. Figure VI.1-1 shows a solution for weakly RS [1-2]. Although the profile is not reasonably optimized because of a single ECRF beamline, the following information was obtained from the analysis:

1) Most of the design parameters by the point model are consistent with the 1-D calculation;
2) The location of NBCD is restricted to the peripheral region because of beam attenuation even for 1.5 MeV NB;
3) Use of ECRF as the main CD tool requires a high CD power due to its lower current drive efficiency than NBCD.

In addition, the calculation indicates that q-profile control in the central and peripheral regions is important to maintain the bootstrap fraction around the design value for various density and temperature profiles. For example, suppose that the BS current around an internal transport barrier is dominant. Then f_{BS} is strongly dependent on q-value around the ITB, i.e., the total current driven inside the ITB. For this sense, q-profile control can be key technology to maintaining f_{BS} at a design value in fusion plasma especially with high f_{BS}. In connection to this, the interplay between q-profile and pressure profile (including ITB structure) will be an essential issue governing the controllability on f_{BS}. A concern about the analysis is consistency between the obtained q-profile and the given density/temperature profiles. This is an open question to be resolved with further understanding on plasma transport. The result that even 1.5 MeV NB deposits in the peripheral region suggests the necessity to reconsider the role and beam energy of NBI. A possible idea for it is to use lower energy (e.g. ~0.5 MeV) NBI for driving plasma rotation as well as peripheral beam current.

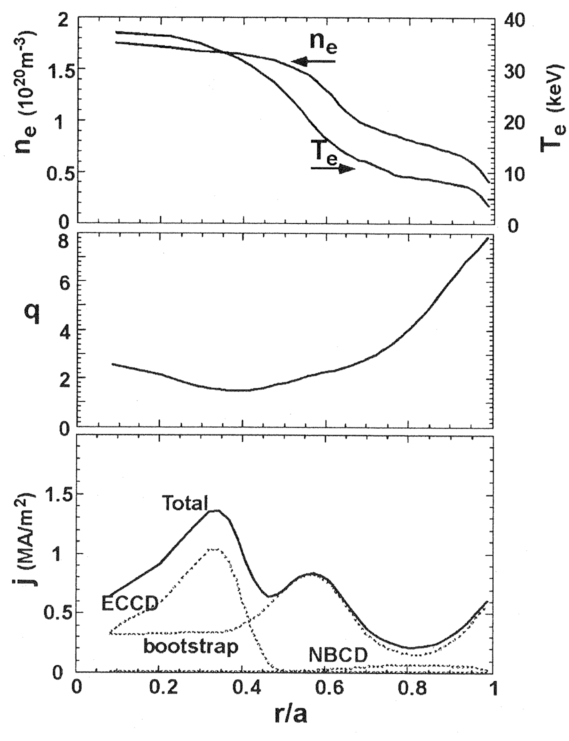

Fig.VI.1-1 Example of weakly RS with consistency between pressure and current profiles

Another issue is a systematic analysis of tritium breeding ratio (TBR) based on a one-dimensional neutronics code THIDA with FENDL2.0 library. Findings of the analysis are:

- The required TBR is satisfied when ^{6}Li is enriched to about 70% for water-cooled solid pebble breeding blanket consisting of Li_2TiO_3 and Be;
- When ^{6}Li is enriched up to 40% or more, there is no difference about TBR between Li_2TiO_3 and Li_2ZrO_3;
- Sector-wide copper conducting shell with 1cm in thickness, which is placed in between replaceable and permanent blanket for vertical stability and high beta access of plasma, can be replaced by 7cm-thick reduced activated martensitic steel (F82H) with a slight decrease in TBR. This means that the torus configuration of SlimCS can be simplified by a modification of the structure of permanent blanket made of F82H.

When the actual tritium production is larger than expected, for example by 5%, surplus production of tritium amounts to about 25 g/day, which will be extracted from the fuel cycle system and stored in the on-site fuel storage. Since the surplus production of tritium reaches 9 kg for one-year operation, an in-situ TBR control method will be required to avoid excessive production. Borated-water is promising for the purpose in that water borated with 0.7 wt% of H_3BO_3 reduces the local TBR by 0.07 as shown in Fig.VI.1-2, corresponding to a reduction of 0.05 in the net TBR. This indicates that borated-water injection into coolant is useful as in-situ TBR control.

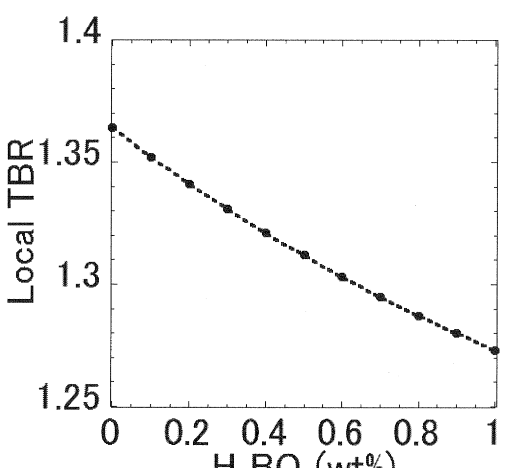

Fig.VI.1-2 Local TBR as function of the concentration of H_3BO_3 in coolant.

References

1-1 Tani K., *et al., J. Comput. Phys.* **98**, 332(1990).

1-2 Tobita K., *et al., Nucl. Fusion* **47**, 892(2007).

2. Numerical Study on Beta Limit in Low Aspect Ratio Tokamak

The critical beta of low aspect ratio tokamak for toroidal mode number n=1 is analyzed by using MARG2D code developed in JAEA, which solves 2-dimensional Newcomb equation as an eigen-value problem [2-1].

The maximum stable beta value is considered to be mainly limited by RWM mode that is induced by ideal kink ballooning mode, and we analyze the ideal kink ballooning mode as a first step. As for the equilibria, typical up-down symmetric configuration of SlimCS (elongation : κ=2.0, triangularity : δ=0.36) is used, and the profiles of plasma current and pressure are obtained from the correlation function using the experimental profile data of JT-60U plasma with ITB (Internal Transport Barrier) [2-2], where the minimum values of safety factor are set to be greater than 3. Critical normalized beta 2.7 is obtained in the case of no ideal wall. To obtain stable β_N=4.3 SlimCS plasma, the conformal ideal wall must be placed at the position of 1.2 times plasma minor radius (Fig.VI.2-1). Profile optimization is necessary to obtain higher critical normalized beta.

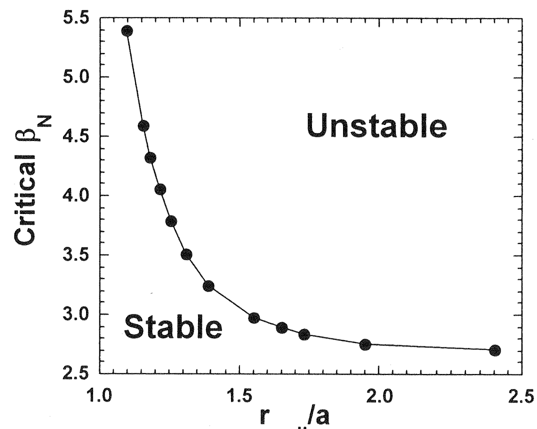

Fig.VI.2-1 Critical β_N vs. minor radius of conformal ideal wall for n=1 mode.

References

2-1 Aiba N., *et al., Comp. Phys. Commun.* **175** 269 (2006).

2-2 Kurita G., Nagashima K., *et al* 1998 *15th Annual Meeting of Japan Society of Plasma Science and NuclearFusion Research.*

Appendix

A.1 Publication List (April 2007 – March 2008)

A.1.1 List of JAERI/JAEA Report

1) Chida, T., Ida, M., Nakamura, H., et al., "Thermo-Structural Analysis of Backwall in IFMIF Lithium Target, 2," JAEA-Technology 2007-048 (2007) (in Japanese).

2) Fujieda, H., Sugihara, M., Shimada, M., et al., "Studies on Representative Disruption Scenarios, Associated Electromagnetic and Heat Loads and Operation Window in ITER," JAEA-Research 2007-052 (2007).

3) Hayashi, K., Nakagawa, T., Onose, S., et al., "Investigation and Design of the Dismantling Process of Irradiation Capsules Containing Tritium, 1; Conceptual Investigation and Basic Design," JAEA-Technology 2008-010 (2008) (in Japanese).

4) Ichige, H., Honda, M., Sasaki, S., et al., "Development of Pellet Injector Using Screw Type Pellet Extruder; Improvement of Pellet Extruder for High Frequency and Long Duration, and its Test Results," JAEA-Technology 2007-037 (2007) (in Japanese).

5) Ida, M., Nakamura, H., Chida, T., et al., "Review of JAEA Activities on the IFMIF Liquid Lithium Target in FY2006," JAEA-Review 2008-008 (2008).

6) Ishii, K., Seki, M., Shinozaki, S., et al., "Power Injection Performance of the LH Antenna Tipped with Carbon Grills in JT-60U," JAEA-Technology 2007-036 (2007) (in Japanese).

7) Ishikawa, M., Kondoh, T., Hayakawa, A., et al., "Detail Design of Microfission Chamber for Fusion Power Diagnostic on ITER," JAEA-Technology 2007-062 (2007).

8) Iwai, Y., Hayashi, T., Kobayashi, K., et al., "Application of Tritium Behavior Simulation Code (TBEHAVIOR) to an Actual-Scale Tritium Handling Room," JAEA-Research 2007-070 (2007).

9) Kajita, S., Hatae, T., Katsunuma, A., et al., "Design Study of the Optical System in the Port Plug for Edge Thomson Scattering Diagnostics for ITER," JAEA-Technology 2007-064 (2008).

10) Kakudate, S., Shibanuma, K., "Singular Point Analysis During Rail Deployment into Vacuum Vessel for ITER Blanket Maintenance," JAEA-Technology 2007-032 (2007).

11) Oshima, K., Okano, F., Honda, A., et al., "Development of Protection System for Power Supply Facilities in JT-60U P-NBI for Long Pulse Operation," JAEA-Technology 2007-044 (2007) (in Japanese).

12) Sakata, S., Kiyono, K., Oshima, T., et al., "Progress of Data Processing System in JT-60 Utilizing the UNIX-Based Workstations," JAEA-Technology 2007-039 (2007) (in Japanese).

13) Seimiya, M., and JT-60 Operation Team, "The Archives of Operational Achievements in JT-60," JAEA-Technology 2007-049 (2007) (in Japanese).

14) Seki, Y., Tanigawa, H., Tsuru, D., et al., "Studies on Tritium Breeding Ratio for Solid Breeder Blanket Cooled by Pressurized Water Through Nuclear and Thermal Analyses," JAEA-Technology 2007-067 (2008) (in Japanese).

15) Shimada, K., Omori, Y., Okano, J., et al., "Initial Design Study of a DC Power Supply System for JT-60SA," JAEA-Technology 2008-031 (2008) (in Japanese).

16) Shimada, K., Terakado, T., Kurihara, K., "Design Study of an AC Power System for Additional Heating Facilities in JT-60SA," JAEA-Technology 2008-022 (2008) (in Japanese).

17) Sueoka, M., Kawamata, Y., Kurihara, K., et al., "Development of the Plasma Movie Database System in

JT-60," JAEA-Technology 2008-021 (2008) (in Japanese).

18) Suzuki, S., Seki, M., Shinozaki, S., et al., "Improvement of the Protection Devices for JT-60U LHRF Antenna System," JAEA-Technology 2007-055 (2007) (in Japanese).

19) Takato, N., Tobari, H., Inoue, T., et al., "Spatial Uniformity of Negative Ion Beam in Magnetically Filtered Hydrogen Negative Ion Source; Effect of the H^- Ion Production and Transport Processes on the H^- Ion Beam Intensity profile in the Cs-seeded negative ion source (Joint research)," JAEA-Research 2008-031 (2008) (in Japanese).

20) Terakado, M., Shimono, M., Sawahata, M., et al., "Development of the Power Modulation Technique in JT-60U ECH System," JAEA-Technology 2007-053 (2007) (in Japanese).

21) Totsuka, T., "Development of the Java-Based Man-Machine Interfacing System for Remote Experiments on JT-60," JAEA-Technology 2007-034 (2007) (in Japanese).

22) Yamaguchi, T., Kawano, Y., Kusama, Y., "Sensitivity Study of the ITER Poloidal Polarimeter," JAEA-Research 2007-078 (2008).

23) Yamauchi, M., Hori, J., Sato, S., et al., "ACT-XN; Revised Version of an Activation Calculation Code for Fusion Reactor Analysis; Supplement of the Function for the Sequential Reaction Activation by Charged Particles," JAEA-Data/Code 2007-016 (2007) (in Japanese).

24) Yokokura, K., Moriyama, S., Hasegawa, K., et al., "Development of Power Measuring Device of Transmission Type with Dielectric for High Power Millimeter Wave," JAEA-Technology 2007-045 (2007) (in Japanese).

A.1.2 List of Papers Published in Journals

1) Aiba, N., Tokuda, S., Fujita, T., et al., "Numerical Method for the Stability Analysis of Ideal MHD Modes with a Wide Range of Toroidal Mode Numbers in Tokamaks," Plasma Fusion Res., (Internet) **2**, 010 (2007).

2) Aiba, N., Tokuda, S., Takizuka, T., et al., "Effects of "Sharpness" of the Plasma Cross-Section on the MHD Stability of Tokamak Edge Plasmas," Nucl. Fusion, **47**, 297 (2007).

3) Araghy, H.P., Peterson, B.J., (Konoshima, S.), et al., "Spatial Variation of the Foil Parameters from in Situ Calibration of the JT-60U Imaging Bolometer Foil," Plasma Fusion Res., (Internet) **2**, S1116 (2007).

4) Asakura, N., ITPA SOL and Divertor Topical Group, "Understanding the SOL Flow in L-Mode Plasma on Divertor Tokamaks, and its Influence on the Plasma Transport," J. Nucl. Mater., **363-365**, 41 (2007).

5) Ashikawa, N., Kizu, K., (Miya, N.), et al., "Comparison of Boronized Wall in LHD and JT-60U," J. Nucl. Mater., **363-365**, 1352 (2007).

6) Batistoni, P., Angelone, M., (Ochiai, K.), et al., "Neutronics Experiment on a Helium Cooled pebble bed (HCPB) Breeder Blanket Mock-Up," Fusion Eng. Des., **82**, 2095 (2007).

7) Briguglio, S., Fogaccia, G., (Shinohara, K.), et al., "Particle Simulation of Bursting Alfvén Modes in JT-60U," Physics of Plasmas, **14**, 055904 (2007).

8) Callen, J.D., Anderson, J.K., (Fujita, T.), et al., "Experimental tests of paleoclassical transport," Nucl. Fusion, **47**, 1449 (2007).

9) Chankin, A.V., Coster, D.P., Asakura, N., et al., "Discrepancy Between Modelled and Measured Radial Electric Fields in the Scrape-Off Layer of Divertor Tokamaks; A Challenge for 2D Fluid Codes?," Nucl. Fusion, **47**, 479 (2007).

10) de Vries, P.C., Salmi, A., (Oyama, N.), et al., "Effect of Toroidal Field Ripple on Plasma Rotation in JET," Nucl. Fusion, **48**, 035007 (2008).

11) Donné, A.J.H., Costley, A.E., (Kawano, Y.), et al., "Progress in the ITER Physics Basis, 7; Diagnostics," Nucl. Fusion, **47**, S337 (2007).

12) Doyle, E.J., Houlberg, W.A., Kamada, Y., et al., "Progress in the ITER Physics Basis, 2; Plasma Confinement and Transport," Nucl. Fusion, **47**, S18 (2007).

13) Fasoli, A., Gormezano, C., (Shinohara, K.), et al., "Progress in the ITER Physics Basis, 5; Physics of Energetic Ions," Nucl. Fusion, **47**, S264 (2007).

14) Fujimoto, K., Nakano, T., Kubo, H., et al., "Modification of Tomography Technique for Two-Dimensional Spectroscopic Measurement in JT-60U Divertor Plasmas," Plasma Fusion Res., (Internet) **2**, S1121 (2007).

15) Fujino, I., Hatayama, A., (Inoue, T.), et al., "Analysis of Electron Energy Distribution of an Arc-Discharge H^- Ion Source with Monte Carlo Simulation," Rev. Sci. Instrum., **79**, 02A510 (2008).

16) Fujisawa, A., Ido, T., Hoshino, K., et al., "Experimental Progress on Zonal Flow Physics in Toroidal Plasmas," Nucl. Fusion, **47**, S718 (2007).

17) Fujita, T., Tamai, H., Matsukawa, M., et al., "Design Optimization for Plasma Performance and Assessment of Operation Regimes in JT-60SA," Nucl. Fusion, **47**, 1512 (2007).

18) Gormezano, C., Sips, A.C.C., (Ide, S.), et al., "Progress in the ITER Physics Basis, 6; Steady State Operation," Nucl. Fusion, **47**, S285 (2007).

19) Gribov, Y., Humphreys, D.A., (Ozeki, T.), et al., "Progress in the ITER Physics Basis, 8; Plasma Operation

and Control," Nucl. Fusion, **47**, S385 (2007).

20) Hamada, K., Nakajima, H., Kawano, K., et al., "Demonstration of Full Scale JJ1 and 316LN Fabrication for ITER TF Coil Structure," Fusion Eng. Des., **82**, 1481 (2007).

21) Hamamatsu, K., Takizuka, T., Hayashi, N., et al., "Numerical Simulation of Electron Cyclotron Current Drive in Magnetic Islands of Neo-Classical Tearing Mode," Plasma Phys. Control. Fusion, **49**, 1955 (2007).

22) Hanada, M., Ikeda, Y., Kamada, M., et al., "Correlation Between Voltage Holding Capability and Light Emission in a 500 keV Electrostatic Accelerator Utilized for Fusion Application," IEEE Trans. Dielectr. Electr. Insulat., **143**, 572 (2007).

23) Hanada, M., Inoue, T., Kashiwagi, M., et al., "R&D Progress at JAEA Towards Production of High Power and Large-Area Negative Ion Beams for ITER," Nucl. Fusion, **47**, 1142 (2007).

24) Hatae, T., Howard, J., Hirano, Y., et al., "Development of polarization interferometer based on Fourier transform spectroscopy for Thomson scattering diagnostics," Plasma Fusion Res., (Internet) **2**, S1026 (2007).

25) Hayashi, N., Takizuka, T., Aiba, N., et al., "Integrated ELM Simulation with Edge MHD Stability and Transport of SOL-Divertor Plasmas," Contrib. Plasma Phys., **48**, 196 (2008).

26) Hayashi, N., Takizuka, T., Hosokawa, M., et al., "Modeling of Dynamic Response of SOL-Divertor Plasmas to an ELM Crash," J. Nucl. Mater., **363-365**, 1044 (2007).

27) Hayashi, N., Takizuka, T., Ozeki, T., et al., "Integrated Simulation of ELM Energy Loss Determined by Pedestal MHD and SOL Transport," Nucl. Fusion, **47**, 682 (2007).

28) Hayashi, T., Kasada, R., Tobita, K., et al., "Impact of N-Isotope Composition Control of Ferritic Steel on Classification of Radioactive Materials from Fusion Reactor," Fusion Eng. Des., **82**, 2850 (2007).

29) Hayashi, T., Sakurai, S., Masaki, K., et al., "Conceptual Design of Divertor Cassette Handling by Remote Handling System of JT-60SA," Journal of Power and Energy Systems (Internet), **2**, 522 (2008).

30) Hayashi, T., Sugiyama, K., Krieger, K., et al., "Deuterium Depth Profiling in JT-60U Tiles Using the D(^{3}He, p)^{4}He Resonant Nuclear Reaction," J. Nucl. Mater., **363-365**, 904 (2007).

31) Hayashi, T., Isobe, K., Kobayashi, K., et al., "Recent Activities on Tritium Technologies for ITER and Fusion Reactors at JAEA," Fusion Sci. Tech., **52**, 651 (2007).

32) Hayashi, T., Nakamura, H., Isobe, K., et al., "Tritium Behavior on the Water-Metal Boundary for the Permeation Into Cooling Water Through Metal Piping," Fusion Sci. Tech., **52**, 687 (2007).

33) Hayashi, T., Suzuki, T., Shu, W., et al., "Isotope Effect of Hydrogen Rapidly Supplied from the Metal Storage Bed," Fusion Sci. Tech., **52**, 706 (2007).

34) Hender, T.C., Wesley, J.C., (Isayama, A.), et al., "Progress in the ITER Physics Basis, 3; MHD Stability, Operational Limits and Disruptions," Nucl. Fusion, **47**, S128 (2007).

35) Hirohata, Y., Tanabe, T., (Miya, N.), et al., "Hydrogen Isotopes Retention in JT-60U," J. Nucl. Mater., **363-365**, 854 (2007).

36) Hiroki, S., Tanzawa, S., Arai, T., et al., "Development of Water Leak Detection Method in Fusion Reactors Using Water-Soluble Gas," Fusion Eng. Des., **83**, 72 (2008).

37) Hirose, T., Tanigawa, H., Enoeda, M., et al., "Effects of Tube Drawing on Structural Material for ITER Test Blanket Module," Fusion Sci. Tech., **52**, 839 (2007).

38) Honda, M., Fukuyama, A., "Dynamic Transport Simulation Code Including Plasma Rotation and Radial Electric Field," J. Comput. Phys., **227**, 2808 (2008).

39) Hoshino, K., Suzuki, T., Isayama, A., et al., "Electron Cyclotron Heating Applied to the JT-60U Tokamak," Fusion Sci. Tech., **53**, 114 (2008).

40) Hoshino, T., Yasumoto, M., Tsuchiya, K., et al., "Non-Stoichiometory and Vaporization Characteristic of $Li_{2.1}TiO_{3.05}$ in Hydrogen Atmosphere," Fusion Eng. Des., **82**, 2269 (2007).

41) Hosogane, N., JT-60SA Design Team and Japan-Europe Satellite Tokamak Working Group, "Superconducting Tokamak JT-60SA Project for ITER and DEMO Researches," Fusion Sci. Tech., **52**, 375 (2007).

42) Ichimura, M., Higaki, H., (Moriyama, S.), et al., "Observation of Spontaneously Excited Waves in the Ion Cyclotron Frequency Range on JT-60U," Nucl. Fusion, **48**, 035012 (2008).

43) Ida, M., Nakamura, H., Sugimoto, M., "Analytical Estimation of Accessibility to the Activated Lithium Loop in IFMIF," J. Nucl. Mater., **367-370**, 1557 (2007).

44) Ida, M., Nakamura, H., Sugimoto, M., "Estimation and Control of Beryllium-7 Behavior in Liquid Lithium Loop of IFMIF," Fusion Eng. Des., **82**, 2490 (2007).

45) Ide, S., Takenaga, H., Isayama, A., et al., "Studies on Impact of Electron Cyclotron Wave Injection on the Internal Transport Barriers in JT-60U Weak Shear Plasmas," Nucl. Fusion, **47**, 1499 (2007).

46) Idomura, Y., Ida, M., Tokuda, S., "Conservative Gyrokinetic Vlasov Simulation," Commun. Nonlinear. Sci. Numer. Simulat., **13**, 227 (2008).

47) Idomura, Y., Ida, M., Tokuda, S., et al., "New conservative gyrokinetic full-f Vlasov code and its comparison to gyrokinetic δf particle-in-cell code," J. Comput. Phys., **226**, 244 (2007).

48) Ikeda, Y., Akino, N., Ebisawa, N., et al., "Technical design of NBI system for JT-60SA," Fusion Eng. Des., **82**, 791 (2007).

49) Inoue, T., Hanada, M., Kashiwagi, M., et al., "Development of Beam Source and Bushing for ITER NB System," Fusion Eng. Des., **82**, 813 (2007).

50) Inoue, T., Tobari, H., Takado, N., et al., "Negative Ion Production in Cesium Seeded High Electron Temperature Plasmas," Rev. Sci. Instrum., **79**, 02C112 (2008).

51) Ioki, K., Elio, F., Barabash, V., et al., "Six-Party Qualification Program of FW Fabrication Methods for ITER Blanket Module Procurement," Fusion Eng. Des., **82**, 1774 (2007).

52) Isayama, A., Oyama, N., Urano, H., et al., "Stabilization of Neoclassical Tearing Modes by Electron Cyclotron Current Drive in JT-60U," Nucl. Fusion, **47**, 773 (2007).

53) Ishii, Y., Azumi, M., Smolyakov, A.I., "Nonliear Evolution and Deformation of Driven Magnetic Islands in Rotating Plasmas," Nucl. Fusion, **47**, 1024 (2007).

54) Ishikawa, M., Nishitani, T., Kusama, Y., et al., "Neutron Emission Profile Measurement and Fast Charge Exchange Neutral Particle Flux Measurement for Transport Analysis of Energetic Ions in JT-60U," Plasma Fusion Res., (Internet) **2**, 019 (2007).

55) Ishikawa, M., Takechi, M., Shinohara, K., et al., "Confinement Degradation and Transport of Energetic Ions due to Alfvén Eigenmodes in JT-60U Weak Shear Plasmas," Nucl. Fusion, **47**, 849 (2007).

56) Ito, T., Hayashi, T., Isobe, K., et al., "Self-Decomposition Behavior of High Concentration Tritiated Water," Fusion Sci. Tech., **52**, 701 (2007).

57) Jolliet, S., Bottino, A., (Idomura, Y.), et al., "A Global Collisionless PIC Code in Magnetic Coordinates," Comput. Phys. Commun., **177**, 409 (2007).

58) Kajita, S., Ono, N., Takamura, S., et al., "Plasma-Assisted Laser Ablation of Tungsten; Reduction in Ablation Power Threshold due to Bursting of Holes/Bubbles," Applied Physics Letters, **91**, 261501 (2007).

59) Kamiya, K., Asakura, N., Boedo, J.A., et al., "Edge Localized Modes; Recent Experimental Findings and Related Issues," Plasma Phys. Control. Fusion, **49**, s43 (2007).

60) Kanemura, T., Kondo, H., (Ida, M.), et al., "Investigation of Free-Surface Fluctuations of Liquid Lithium Flow for IFMIF Lithium Target by Using an Electro-Contact Probe," Fusion Eng. Des., **82**, 2550 (2007).

61) Kawashima, H., Shimizu, K., Takizuka, T., "Development of Integrated SOL/Divertor Code and Simulation Study of the JT-60U/JT-60SA Tokamaks," Plasma Phys. Control. Fusion, **49**, s77 (2007).

62) Kawashima, H., Shimizu, K., Takizuka, T., et al., "Simulation of Divertor Pumping in JT-60U with SOLDOR/NEUT2D Code," J. Nucl. Mater., **363-365**, 786 (2007).

63) Kizu, K., Tsuchiya, K., Ando, T., et al., "Conceptual Design of Magnet System for JT-60 Super Advanced (JT-60SA)," IEEE Trans. Appl. Superconduct., **17**, 1348 (2007).

64) Kizu, K., Tsuchiya, K., Shimada, K., et al., "Evaluation of Bending Strain Dependence of Critical Current of Nb_3Al Conductor for Coils with React-And-Wind Method," Fusion Eng. Des., **82**, 1493 (2007).

65) Kobayashi, K., Hayashi, T., Nakamura, H., et al., "Study for the Behavior of Tritiated Water Vapor on Organic Materials," Fusion Sci. Tech., **52**, 696 (2007).

66) Kobayashi, K., Isobe, K., Iwai, Y., et al., "Studies on the Behavior of Tritium in Components and Structure Materials of Tritium Confinement and Detritiation Systems of ITER," Nucl. Fusion, **47**, 1645 (2007).

67) Kobayashi, K., Miura, H., Hayashi, T., et al., "Oxidation Performance Test of Detritiation System Under Existence of SF_6," Fusion Sci. Tech., **52**, 711 (2007).

68) Kobayashi, S., and JT-60 Team, "Development of Real-Time Measurement System of Charge Exchange Recombination Spectroscopy and its Application to Feedback Control of Ion Temperature Gradient in JT-60U," Plasma Fusion Res., (Internet) **2**, S1049 (2007).

69) Kobayashi, T., Moriyama, S., Seki, M., et al., "Achievement of 1.5 MW, 1 s Oscillation by the JT-60U Gyrotron," Plasma Fusion Res., (Internet) **3**, 014 (2008).

70) Koizumi, N., Isono, T., Hamada, K., et al., "Development of Large Current Superconductors Using High Performance Nb_3Sn Strand for ITER," Physica C, **463-465**, 1319 (2007).

71) Kojima, A., Kamiya, K., Iguchi, H., et al., "Numerical simulation of a high-brightness lithium ion gun for a Zeeman polarimetry on JT-60U," Plasma Fusion Res., (Internet) **2**, S1104 (2007).

72) Kondo, H., Kanemura, T., (Ida, M.), et al., "Measurement of Free Surface of Liquid Metal Lithium Jet for IFMIF Target," Fusion Eng. Des., **82**, 2483 (2007).

73) Kondo, K., Murata, I., Ochiai, K., et al., "Measurement and Analysis of Neutron-Induced Alpha Particle Emission Double-Differential Cross Section of Carbon at 14.2 MeV," J. Nucl. Sci. Technol., **45**, 103 (2008).

74) Kondo, K., Murata, I., Ochiai, K., et al., "Verification of Nuclear Data for DT Neutron Induced Charged-Particle Emission Reaction of Light Nuclei," Fusion Eng. Des., **82**, 2786 (2007).

75) Kubo, H., Sasaki, A., Moribayashi, K., et al., "Study of Highly Ionized Xe Spectra with 3s-3p and 3p-3d Transitions in JT-60U Reversed Shear Plasmas," J. Nucl. Mater., **363-365**, 1441 (2007).

76) Kubota, N., Kondo, K., Ochiai, K., et al., "Neutron Elastic Recoil Detection for Hydrogen Isotope Analysis in Fusion Materials," J. Nucl. Mater., **367-370**, 1596 (2007).

77) Li, Z., Tanaka, T., (Sato, S.), et al., "Spectral Effects of Activation for Liquid Blanket Relevant Materials Induced by D-T Neutron Irradiation," Fusion Sci. Tech., **52**, 817 (2007).

78) Liu, Y., Tamura, N., (Konoshima, S.), et al., "Application of Tomographic Imaging to Multi-Pixel Bolometric Measurements," Plasma Fusion Res., (Internet) **2**, S1124 (2007).

79) Loarte, A., Lipschultz, B., (Asakura, N.), et al., "Progress in the ITER Physics Basis, 4; Power and Particle Control," Nucl. Fusion, **47**, S203 (2007).

80) Maggi, C.F., Groebner, R.J., Oyama, N., et al., "Characteristics of the H-mode Pedestal in Improved Confinement Scenarios in ASDEX Upgrade, DIII-D, JET and JT-60U," Nucl. Fusion, **47**, 535 (2007).

81) Masaki, K., Tanabe, T., Hirohata, Y., et al., "Hydrogen Retention and Carbon Deposition in Plasma Facing Components and the Shadowed Area of JT-60U," Nucl. Fusion, **47**, 1577 (2007).

82) Matsumoto, T., Li, J., Kishimoto, Y., "Characteristics of ETG-Driven Turbulence Dominated by Zonal Flows," Nucl. Fusion, **47**, 880 (2007).

83) Matsushita, D., Takado, N., (Inoue, T.), et al., "Numerical Analysis of H^- Ion Transport Processes in Cs-Seeded Negative Ion Sources," Rev. Sci. Instrum., **79**, 02A527 (2008).

84) Miki, K., Kishimoto, Y., Miyato, N., et al., "Intermittent Transport Associated with the Geodesic Acoustic Mode Near the Critical Gradient Regime," Physical Review Letters, **99**, 145003 (2007).

85) Mishima, Y., Yoshida, N., (Tsuchiya, K.), et al., "Recent Results on Beryllium and Beryllides in Japan," J. Nucl. Mater., **367-370**, 1382 (2007).

86) Miyato, N., Kishimoto, Y., Li, J.Q., "Turbulence Suppression in the Neighbourhood of a Minimum-q Surface due to Zonal Flow Modification in Reversed Shear Tokamaks," Nucl. Fusion, **47**, 929 (2007).

87) Morimoto, M., Ioki, K., Terasawa, A., et al., "Design Progress of the ITER In-Wall Shielding," Fusion Sci. Tech., **52**, 834 (2007).

88) Morioka, A., Sakurai, S., Okuno, K., et al., "Development of 300°C Heat Resistant Boron-Loaded Resin for Neutron Shielding," J. Nucl. Mater., **367-370**, 1085 (2007).

89) Moriyama, S., Seki, M., Fujii, T., "Design Study of a New Antenna System for Steering Microwave Beam in Electron Cyclotron Heating/Current Drive System," Fusion Eng. Des., **82**, 785 (2007).

90) Motojima, O., Yamada, H., (Isayama, A.), et al., "Extended Steady-State and High-Beta Regimes of Net-Current Free Heliotron Plasmas in the Large Helical Device," Nucl. Fusion, **47**, S668 (2007).

91) Murakami, H., Ishiyama, A., (Koizumi, N.), et al., "Numerical Simulation of Critical Current and N-Value in Nb_3Sn Strand Subjected to Bending Strain," IEEE Trans. Appl. Superconduct., **17**, 1394 (2007).

92) Nagashima, Y., Ito, K., (Hoshino, K.), et al., "In search of Zonal Flows by Using Direct Density Fluctuation Measurements," Plasma Phys. Control. Fusion, **49**, 1611 (2007).

93) Nakajima, H., Hamada, K., Okuno, K., et al., "Development of Optimum Manufacturing Technologies of Radial Plates for the ITER Toroidal Field Coils," Fusion Eng. Des., **82**, 1473 (2007).

94) Nakamichi, M., Kulsartov, T.V., Hayashi, K., et al., "In-pile Tritium Permeation Through F82H Steel with and Without a Ceramic Coating of Cr_2O_3-SiO_2 Including $CrPO_4$," Fusion Eng. Des., **82**, 2246 (2007).

95) Nakamura, H., Kobayashi, K., Yamanishi, T., et al., "Tritium Release Behavior from Steels Irradiated by High Energy Protons," Fusion Sci. Tech., **52**, 1012 (2007).

96) Nakamura, H., Ida, M., Chida, T., et al., "Design of a Lip Seal-Replaceable Backwall for IFMIF Liquid Lithium Target," Fusion Eng. Des., **82**, 2671 (2007).

97) Nakamura, T., Sakagami, H., (Koga, J.K.), et al., "High Energy Electron Generation by Laser-Cone Interaction," Plasma Fusion Res., (Internet) **2**, 018 (2007).

98) Nakamura, T., Sakagami, H., (Koga, J.K.), et al., "Optimization of Cone Target Geometry for Fast Ignition," Physics of Plasmas, **14**, 103105 (2007).

99) Nakano, T., and JT-60 Team, "Particle Balance Under Global Wall Saturation in Long-Pulse Discharges of JT-60U," J. Nucl. Mater., **363-365**, 1315 (2007).

100) Nakano, T., Kubo, H., Asakura, N., et al., "Volume Recombination of C^{4+} in Detached Divertor Plasmas of JT-60U," Nucl. Fusion, **47**, 1458 (2007).

101) Nishimura, A., Nishijima, S., (Nishitani, T.), et al., "Change in Properties of Superconducting Magnet Materials by Fusion Neutron Irradiation," Fusion Eng. Des., **82**, 1555 (2007).

102) Nishitani, T., Enoeda, M., Akiba, M., et al., "Recent Progress in Solid Breeder Blanket Development at JAEA," Fusion Sci. Tech., **52**, 971 (2007).

103) Nishitani, T., Sato, S., Ochiai, K., et al., "Progress in Neutronics Studies for the Water Cooled Pebble Bed Blanket," Fusion Sci. Tech., **52**, 791 (2007).

104) Nishitani, T., Yamauchi, M., Izumi, M., et al., "Engineering Design of the ITER Invessel Neutron Monitor Using Micro-Fission Chambers," Fusion Eng. Des., **82**, 1192 (2007).

105) Nunoya, Y., Isono, T., Koizumi, N., et al., "Development of Strain-Applying Apparatus for Evaluation of ITER Nb_3Sn Strand," IEEE Trans. Appl. Superconduct., **17**, 2588 (2007).

106) Ochiai, K., Sato, S., Wada, M., et al., "Thin Slit Streaming Experiment for ITER by Using D-T Neutron Source," Fusion Eng. Des., **82**, 2794 (2007).

107) Ogawa, H., Sugie, T., Kasai, S., et al., "Development of Impurity Influx Monitor (Divertor) for ITER Plasma," Fusion Res., (Internet) **2**, S1054 (2007).

108) Ogawa, M., Iio, S., (Inoue, T.), et al., "Magnetic Fusion Energy Studies in Japan," Nucl. Instrum. Methods. Phys. Res., A, **577**, 30 (2007).

109) Ohira, S., Hayashi, T., Shu, W., et al., "Radiochemical Characteristics of Tritium to be Considered in Fusion Reactor Facility Design," J. Radioanal. Nucl. Chem., **272**, 575 (2007).

110) Oka, K., Onuki, S., Yamashita, S., et al., "Structure of Nano-Size Oxides in ODS Steels and its Stability Under Electron Irradiation," Materials Transactions, **48**, 2563 (2007).

111) Okuno, K., Nakajima, H., Sugimoto, M., et al., Technology Development for the Construction of the ITER Superconducting Magnet System," Nucl. Fusion, **47**, 456 (2007).

112) Onozuka, M., Shimizu, K., (Nakajima, H.), et al., "Basic Analysis of Weldability and Machinability of Structural Materials for ITER Toroidal Field Coils," Fusion Eng. Des., **82**, 1431 (2007).

113) Oshima, T., Kiyono, K., Sakata, S., et al., "Improvement of Data Processing System for Advanced Diagnostics in JT-60U," Fusion Eng. Des., **82**, 1210 (2007).

114) Oya, Y., Hirohata, Y., (Masaki, K.), et al., "Hydrogen Isotope Retentions and Erosion/Deposition Profiles in the First Wall of JT-60U," Fusion Sci. Tech., **52**, 554 (2007).

115) Oyama, N., and JT-60 Team, "Improved Performance in Long-Pulse ELMy H-mode Plasmas with Internal Transport Barrier in JT-60U," Nucl. Fusion, **47**, 689 (2007).

116) Ozeki, T., and JT-60 Team, "High-Beta Steady-State Research with Integrated Modeling in the JT-60

Upgrade,“ Physics of Plasmas, **14**, 056114 (2007).

117) Peterson, B.J., LHD Team and JT-60U Team, “Research and Development of Imaging Bolometers,” Plasma Fusion Res., (Internet) **2**, S1018 (2007).

118) Peterson, B.J., and JT-60 Team, “Observation of Divertor and Core Radiation in JT-60U by Means of Bolometric Imaging,” J. Nucl. Mater., **363-365**, 412 (2007).

119) Prater, R., La Haye, R.J., (Isayama, A.), et al., “Stabilization and Prevention of the 2/1 Neoclassical Tearing Mode for Improved Performance in DIII-D,” Nucl. Fusion, **47**, 371 (2007).

120) Rewoldt, G., Lin, Z., Idomura, Y., “Linear Comparison of Gyrokinetic Codes with Trapped Electrons,” Comput. Phys. Commun., **177**, 775 (2007).

121) Saibene, G., Oyama, N., Lönnroth, J., et al., “The H-Mode Pedestal, ELMs and TF Ripple Effects in JT-60U/JET Dimensionless Identity Experiments,” Nucl. Fusion, **47**, 969 (2007).

122) Sakamoto, K., “Progress of High-Power-Gyrotron Development for Fusion Research,” Fusion Sci. Tech., **52**, 145 (2007).

123) Sakamoto, K., Kasugai, A., Takahashi, K., et al., “Achievement of Robust High-Efficiency 1 MW Oscillation in the Hard-Self-Excitation Region by a 170 GHz Continuous-Wave Gyrotron,” Nature Physics, **3**, 411 (2007).

124) Sakamoto, Y., and JT-60 Team, “Controllability of Large Bootstrap Current Fraction Plasmas in JT-60U,” Nucl. Fusion, **47**, 1506 (2007).

125) Sakamoto, Y., and JT-60 Team, “Controllability of Large Bootstrap Current Fraction Plasmas in JT-60U,” Nucl. Fusion, **47**, 1506 (2007).

126) Sasao, M., Nishitani, T., Krasilnikov, A., et al., “Fusion Product Diagnostics,” Fusion Sci. Tech., **53**, 604 (2008).

127) Sato, K., Omori, J., Ebisawa, K., et al., “Development of ITER Diagnostic Upper Port Plug,” Plasma Fusion Res., (Internet) **2**, S1088 (2007).

128) Sato, M., Isayama, A., “Evaluation of Extended Trubnikov Emissivity to the Oblique Propagation and Application to Electron Temperature Measurement in a Reactor-Grade Tokamak,” Fusion Sci. Tech., **52**, 169 (2007).

129) Sato, M., Isayama, A., “Effects of Relativistic and Absorption on ECE Spectra in High Temperature Tokamak Plasma,” Plasma Fusion Res., (Internet) **2**, S1029 (2007).

130) Sato, S., Ochiai, K., Verzilov, Y., et al., “Measurement of Tritium Production Rate in Water Cooled Pebble Bed Multi-Layered Blanket Mockup by DT Neutron Irradiation Experiment,” Nucl. Fusion, **47**, 517 (2007).

131) Sato, S., Verzilov, Y., Ochiai, K., et al., “Neutronics Experimental Study on Tritium Production in Solid Breeder Blanket Mockup with Neutron Reflector,” J. Nucl. Sci. Technol., **44**, 657 (2007).

132) Seki, M., “ITER Activities and Fusion Technology,” Nucl. Fusion, **47**, S489 (2007).

133) Shibama, Y., Arai, T., Miyo, Y., et al., “Structural Design of Ferritic Steel Tiles for Ripple Reduction of Toroidal Magnetic Field in JT-60U,” Fusion Eng. Des., **82**, 2462 (2007).

134) Shimada, K., Ito, J., Matsukawa, M., “A Control Method of Matrix Converter for Plasma Control Coil power Supply,” Fusion Eng. Des., **82**, 1513 (2007).

135) Shimada, M., Campbell, D.J., Mukhovatov, V., et al., “Progress in the ITER Physics Basis, 1; Overview and Summary,” Nucl. Fusion, **47**, S1 (2007).

136) Shimizu, K., Takizuka, T., Kawashima, H., "A New Fast Velocity-Diffusion Modelling for Impurity Transport in Integrated Edge Plasma Simulation," J. Nucl. Mater., **363-365**, 426 (2007).

137) Shimizu, K., Takizuka, T., Kawashima, H., "Extension of IMPMC Code Toward Time Evolution Simulation," Contrib. Plasma Phys., **48**, 270 (2008).

138) Shimomura, K., Takenaga, H., Tsutsui, H., et al., "Burn Control Simulation Experiments in JT-60U," Fusion Eng. Des., **82**, 953 (2007).

139) Shinohara, K., Isobe, M., Darrow, D.S., et al., "Escaping Ion Measurement with High Time Resolution During Bursting Modes Induced by Neutral Beam Injection on CHS," Plasma Fusion Res., (Internet) **2**, 042 (2007).

140) Shinohara, K., and JT-60 Team, "Ferritic Insertion for Reduction of Toroidal Magnetic Field Ripple on JT-60U," Nucl. Fusion, **47**, 997 (2007).

141) Sueoka, M., Kawamata, Y., Kurihara, K., et al., "The Plasma Movie Database System for JT-60," Fusion Eng. Des., **82**, 1008 (2007).

142) Sugiyama, K., Hayashi, T., (Miya, N.), et al, "Ion Beam Analysis of H and D Retention in the Near Surface Layers of JT-60U Plasma Facing Wall Tiles," J. Nucl. Mater., **363-365**, 949 (2007).

143) Sukegawa, A., Sakurai, S., Masaki, K., et al., "Safety Design of Radiation Shielding for JT-60SA," Fusion Eng. Des., **82**, 2799 (2007).

144) Takado, N., Matsushita, D., (Inoue, T.), et al., "Effect of Energy Relaxation of H^0 Atoms at the Wall on the Production Profile of H^- Ions in Large Negative Ion Sources," Rev. Sci. Instrum., **79**, 02A503 (2008).

145) Takahashi, K., Kobayashi, N., Omori, J., et al., "Progress on Design and Development of ITER Equatorial Launcher; Analytical Investigation and R&D of the Launcher Components for the Design Improvement," Fusion Sci. Tech., **52**, 266 (2007).

146) Takahashi, Y., Yoshida, K., Nabara, Y., et al., "Stability and Quench Analysis of Toroidal Field Coils for ITER," IEEE Trans. Appl. Superconduct., **17**, 2426 (2007).

147) Takeda, N., Kakudate, S., Nakahira, M., et al., "Performance Test of Diamond-Like Carbon Films for Lubricating ITER Blanket Maintenance Equipment Under GPa-Level High Contact Stress," Plasma Fusion Res., (Internet) **2**, 052 (2007).

148) Takenaga, H., and JT-60 Team, "Overview of JT-60U Results for the Development of a Steady-State Advanced Tokamak Scenario," Nucl. Fusion, **47**, S563 (2007).

149) Takenaga, H., Kubo, H., Sueoka, M., et al., "Response of Fusion Gain to Density in Burning Plasma Simulation on JT-60U," Nucl. Fusion, **48**, 035011 (2008).

150) Takenaga, H., Oyama, N., Isayama, A., et al., "Observation on Decoupling of Electron Heat Transport and Long-Spatial-Scale Density Fluctuations in a JT-60U Reversed Shear Plasma," Plasma Phys. Control. Fusion, **49**, 525 (2007).

151) Takizuka, T., Oyama, N., Hosokawa, M., "Effect of Radial Transport Loss on the Asymmetry of ELM Heat Flux," Contrib. Plasma Phys., **48**, 207 (2008).

152) Tamai, H., Fujita, T., Kikuchi, M., et al., "Prospective Performances in JT-60SA Towards the ITER and DEMO Relevant Plasmas," Fusion Eng. Des., **82**, 541 (2007).

153) To, K., Shikama, T., (Yamauchi, M.), et al., "Search for Luminescent Materials Under 14 MeV Neutron Irradiation," J. Nucl. Mater., **367-370**, 1128 (2007).

154) Tobari, H., Seki, T., Takado, N., et al., "Negative Ion Production in High Electron Temperature Plasmas,"

Plasma Fusion Res., (Internet) **2**, 022 (2007).

155) Tobita, K., Nishio, S., Sato, M., et al., "SlimCS; Compact Low Aspect Ratio DEMO Reactor with Reduced-Size Central Solenoid," Nucl. Fusion, **47**, 892 (2007).

156) Tomita, Y., Smirnov, R.D., Takizuka, T., et al., "Effect of Oblieque Magnetic Field on Release Conditions of Dust Particle from Plasma-Facing Wall," Contrib. Plasma Phys., **48**, 285 (2008).

157) Tomita, Y., Smirnov, R., (Takizuka, T.), et al., "Effect of Truncation of Electron Velocity Distribution on Release of Dust Particle from Plasma-Facing Wall," J. Nucl. Mater., **363-365**, 264 (2007).

158) Tsuchiya, K., Kizu, K., Ando, T., et al., "Design of the Superconducting Coil System in JT-60SA," Fusion Eng. Des., **82**, 1519 (2007).

159) Tsuchiya, K., Hoshino, T., Kawamura, H., et al., "Development of Advanced Tritium Breeders and Neutron Multipliers for DEMO Solid Breeder Blankets," Nucl. Fusion, **47**, 1300 (2007).

160) Tsuchiya, K., Kawamura, H., Ishida, T., "Compatibility Between Be-Ti Alloys and F82H Steel," J. Nucl. Mater., **367-370**, 1018 (2007).

161) Tsuchiya, K., Kawamura, H., Ishida, T., "Effect of Ti Content on Compatibility Between Be-Ti and SS316LN," Nuclear Technology **159**, 228 (2007).

162) Tsuchiya, K., Shimizu, M., Kawamura, H., et al., "Effect of Re-Irradiation by Neutrons on Mechanical Properties of Un-Irradiated/Irradiated SS316LN Weldments," J. Nucl. Mater., **373**, 212 (2008).

163) Tsuru, D., Enoeda, M., Akiba, M., "Pressurizing Behavior on Ingress of Coolant Into Pebble Bed of Blanket of Fusion DEMO Reactor," Fusion Eng. Des., **82**, 2274 (2007).

164) Ueda, Y., Fukumoto, M., (Miya, N.), et al., "Surface Studies of Tungsten Erosion and Deposition in JT-60U," J. Nucl. Mater., **363-365**, 66 (2007).

165) Urano, H., and JT-60 Team, "H-mode Pedestal Structure in the Variation of Toroidal Rotation and Toroidal Field Ripple in JT-60U," Nucl. Fusion, **47**, 706 (2007).

166) Wakai, E., Ando, M., Sawai, T., et al., "Effect of Helium and Hydrogen Production on Irradiation Hardening of F82H Steel Irradiated by Ion Beams," Materials Transactions **48**, 1427 (2007).

167) Wakai, E., Ando, M., Sawai, T., et al., "Effect of Heat Treatments on Tensile Properties of F82H Steel Irradiated by Neutrons," J. Nucl. Mater., **367-370**, 74 (2007).

168) Watanabe, H., Nakamura, N., (Nakano, T.), et al., "X-ray Spectra from Neon-Like Tungsten Ions in the Interaction with Electrons," Plasma Fusion Res., (Internet) **2**, 027 (2007).

169) Yamada, H., Takenaga, H., Suzuki, T., et al., "Density Limit in Discharges with High Internal Inductance on JT-60U," Nucl. Fusion, **47**, 1418 (2007).

170) Yamaguchi, T., Kawano, Y., Kusama, Y., "Sensitivity Study for the Optimization of the Viewing Chord Arrangement of the ITER Poloidal Polarimeter," Plasma Fusion Res., (Internet) **2**, S1112 (2007).

171) Yamamoto, I., Nishitani, T., Sagara, A., "Overview of Recent Japanese Activities and Plans in Fusion Technology," Fusion Sci. Tech., **52**, 347 (2007).

172) Yamamoto, Y., Yamanishi, T., (Isobe, K.), et al., "Fundamental Study on Purity Control of the Liquid Metal Blanket Using Solid Electrolyte Cell," Fusion Sci. Tech., **52**, 692 (2007).

173) Yamauchi, M., Nishitani, T., Nishio, S., et al., "Activation Analysis for Sequential Reactions of a Fusion Demo-Reactor," Fusion Sci. Tech., **52**, 781 (2007).

174) Yoshida, M., and JT-60 Team, "Role of Pressure Gradient on Intrinsic Toroidal Rotation in Tokamak Plasmas," Physical Review Letters, **100**, 105002 (2008).

175) Yoshida, M., and JT-60 Team, "Momentum Transport and Plasma Rotation Profile in Toroidal Direction in JT-60U L-Mode Plasmas," Nucl. Fusion, **47**, 856 (2007).

176) Zanino, R., Astrov, M., (Takahashi, Y.), et al., "Predictive Analysis of the ITER Poloidal Field Conductor Insert (PFCI) Test Program," IEEE Trans. Appl. Superconduct., **17**, 1353 (2007).

177) Zucchetti, M., El-Guebaly, L.A., (Tobita, K.), et al., "The Feasibility of Recycling and Clearance of Active Materials from Fusion Power Plants," J. Nucl. Mater., **367-370**, 1355 (2007).

A.1.3 List of Papers Published in Conference Proceedings

1) Hayashi, T., Sakurai, S., Masaki, K., et al., "Conceptual Design of Divertor Cassette Handling by Remote Handling System for JT-60SA," Proc. 15th International Conference on Nuclear Engineering (ICONE-15) (CD-ROM), 8 (2007).

2) Isayama, A., and JT-60 Team, "Control of Current Profile and Instability by Radiofrequency Wave Injection in JT-60U and Its Applicability in JT-60SA," AIP Conference Proceedings 933, 229 (2007).

3) Isobe, K., Uzawa, M., Yamanishi, T., et al., "Development of Ceramic Electrolysis Method for Processing High-Level Tritiated Water," STI/PUB/1284 (CD-ROM), 7 (2007).

4) Kobayashi, N., Bigelow, T., Bonicelli, T., et al., "Design of Electron Cyclotron Heating and Current Drive System of ITER," AIP Conference Proceedings 933, 413 (2007).

5) Koide, Y., "Development in Diagnostics Application to Control of Advanced Tokamak Plasma," AIP Conference Proceedings 988, 413 (2008).

6) Kondoh, T., Kawano, Y., Hatae, T., et al., "Progress in Development of Collective Thomson Scattering Diagnostic with High Power CO_2 Laser," NIFS-PROC-68, 126 (2007).

7) Matsunami, N., Nakano, T., "Current Status of Chemical Sputtering of Graphite and Related Materials," Proc. International Symposium on EcoTopia Science 2007 (ISETS '07) (CD-ROM), 321 (2007).

8) Nishitani, T., Ishikawa, M., Kondoh, T., et al., "Absolute Neutron Emission Measurement in Burning Plasma Experiments," AIP Conference Proceedings 988, 267 (2008).

9) Sugie, T., Ogawa, H., Kasai, S., et al., "Spectroscopic Measurement System for ITER Divertor Plasma; Impurity Influx Monitor (Divertor)," AIP Conference Proceedings 988, 218 (2008).

10) Sukegawa, A., Oikawa, A., Miya, N., et al., "Estimation of Low Level Waste by a Regulatory Clearance in JT-60U Fusion Device," Proceedings of 15th International Conference on Nuclear Engineering (ICONE-15) (CD-ROM), 6 (2007).

11) Takahashi, K., Kajiwara, K., Kasugai, A., et al., "Investigation of Transmission Characteristic in Corrugated Waveguide Transmission Lines for Fusion Application," Proc. 8th IEEE International Vacuum Electronics Conference (IVEC 2007), 275 (2007).

12) Takato, N., Hanatani, J., (Inoue, T.), et al., "Numerical Analysis of the Hydrogen Atom Density in a Negative Ion Source," AIP Conference Proceedings 925, 38 (2007).

13) Takenaga, H., Oyama, N., Asakura, N., et al., "Divertor Density Measurements Using mm-Wave Interferometer in JT-60U," NIFS-PROC-68, 62 (2007).

A.1.4 List of other papers

1) Ando, M., Tanigawa, H., Shiba, K., et al., "Irradiation Creep Behavior of Reduced Activation Ferritic/Martensitic Steel Irradiated in HFIR," J. Jpn. Inst. Met., **71**, 559 (2007) (in Japanese).

2) Ando, M., Wakai, E., Okubo, N., et al., "Extra-Irradiation Hardening of Reduced Activation Ferritic/Martensitic Steel by Multi-Ion Irradiation," J. Jpn. Inst. Met., **71**, 1107 (2007) (in Japanese).

3) Ando, T., "Information on ITER Project, 3," J. Plasma Fusion Res., **82**, 533 (2007) (in Japanese).

4) Ando, T., "Information on ITER Project, 5," J. Plasma Fusion Res., **83**, 775 (2007) (in Japanese).

5) Ando, T., "Information on ITER Project, 7," J. Plasma Fusion Res., **84**, 69 (2008) (in Japanese).

6) Ando, T., "Information on ITER Project, 8," J. Plasma Fusion Res., **84**, 164 (2008) (in Japanese).

7) Araki, M., Kamada, Y., Mori, M., et al., "Current Status and Evolution of Nuclear Fusion Development; Aiming at the Achievement of the Nuclear Fusion Energy," Electrical Review, **92**, 38 (2007) (in Japanese).

8) Asakura, N., "Fast Plasma Flow in Tokamak Divertor and Scrape-Off Layer," J. Plasma Fusion Res., **83**, 501 (2007) (in Japanese).

9) Fujita, T., Fukuda, T., (Shinohara, K.), et al., "Report on ITPA (International Tokamak Physics Activity) Meeting, 20," J. Plasma Fusion Res., **84**, 70 (2008) (in Japanese).

10) Hayashi, T., Sakurai, S., Masaki, K., et al.,"Conceptual Design Study of Exchange of the In-Vessel Components by Remote Handling System for JT-60SA," Transactions of the American Nuclear Society, **96**, 783 (2007).

11) Higuchi, M., "Systematization of Standards," Maintenology, **6**, 73 (2007) (in Japanese).

12) Ida, M., Idomura, Y., Tokuda, S., "Gyrokinetic Simulation of Fusion Plasma Turbulence, 1; Modelling and Numerical Methods," Papers in the 2007 Annual Meeting of The Japan Society of Fluid Mechanics (CD-ROM), 5 (2007) (in Japanese).

13) Ide, S., "Present Status of Tokamak Research Towards Steady-State Operation," J. Plasma Fusion Res., **83**, 415 (2007) (in Japanese).

14) Ikeda, Y., "Recent Progress of Fusion Research," Text of The 39th Summer Seminar concerning the Reactor Physics by Atomic Energy Society of Japan, 160 (2007) (in Japanese).

15) Koide, Y., "On the JT-60 Joint Research Prize," J. Plasma Fusion Res., **84**, 230 (2008) (in Japanese).

16) Koizumi, N., Nishimura, A., "Intelligible Seminar on Fusion Reactors, 9; Superconducting Coil to Generate Magnetic Field for Plasma Confinement," J. Nucl. Sci. Tech., **47**, 703 (2007) (in Japanese).

17) Kurihara, K., "Principles of Magnetic Measurements," Handbook of the Modern Electric Power, 129 (2007) (in Japanese).

18) Maegawa, T., Yoshimatsu, K., Sato, S., "14 MeV Neutron Irradiation Test of Low-Activation Concrete with Limestone Powder," Denryoku Doboku, 86 (2008) (in Japanese).

19) Matsui, K., Koizumi, N., Nabara, Y., et al., "Evaluation of Thermal Strain Caused by Nb_3Sn Reaction Heat Treatment for the ITER Cable-in-Conduit Conductors," J. Cryo. Soc. Jpn., **42**, 311 (2007) (in Japanese).

20) Mori, M., "ITER Project in Detail," Genshiryoku eye, **53**, 11 (2007) (in Japanese).

21) Mori, M., Okuno, K., Sakamoto, K., "Information on ITER Project, 4," J. Plasma Fusion Res., **83**, 643 (2007)

(in Japanese).

22) Mori, M., Yoshida, H., "Information on ITER Project, 6," J. Plasma Fusion Res., **83**, 928 (2007) (in Japanese).

23) Ninomiya, H., "Nuclear Fusion," Thermal Power Generation and Atomic Power Generation, **58**, 1038 (2007) (in Japanese).

24) Nishitani, T., "Detail of the Broader Approach Project," Genshiryoku eye, **53**, 21 (2007) (in Japanese).

25) Ohira, S., "Information of Broader Approach Activities, 2," J. Plasma Fusion Res., **83**, 398 (2007) (in Japanese).

26) Ohira, S., "Information of Broader Approach Activity, 3," J. Plasma Fusion Res., **83**, 587 (2007) (in Japanese).

27) Ohira, S., "Information of Broader Approach Activity, 4," J. Plasma Fusion Res., **83**, 716 (2007) (in Japanese).

28) Ohira, S., "Information of Broader Approach Activity, 5," J. Plasma Fusion Res., **83**, 853 (2007) (in Japanese).

29) Ohira, S., "Information of Broader Approach Activity, 7," J. Plasma Fusion Res., **84**, 229 (2008) (in Japanese).

30) Okuno, K., "Recent Progress in the Technology Development for the ITER Superconducting Coils," Superconductivity Communications, **16**, 6 (2007) (in Japanese).

31) Ozeki, T., "Realization of a Nuclear Fusion Experiment from a Remote Place by the Advanced Security," RIST News, 3 (2007) (in Japanese).

32) Ozeki, T., "Remote Hierarchical Environment of Experiment and Simulation," Simulation, **27**, 27 (2008) (in Japanese).

33) Ozeki, T., Watanabe, K., "Avoidance and Suppression of MHD Instability," J. Plasma Fusion Res., **83**, 44 (2007) (in Japanese).

34) Sakamoto, Y., Ida, K., "Control of High Confinement Plasmas," J. Plasma Fusion Res., **83**, 439 (2007) (in Japanese).

35) Sasao, M., Kusama, Y., Kawano, Y., et al., "Report of Meetings of ITPA (International Tokamak Physics Activity), 19," J. Plasma Fusion Res., **83**, 779 (2007) (in Japanese).

36) Sawahata, A., Tanigawa, H., Enomoto, M., "Effects of Electro-Slag Remelting on Inclusion Formation and Impact Property of Reduced Activation Ferritic/Martensitic Steels," J. Jpn. Inst. Met., **72**, 176 (2008) (in Japanese).

37) Shinohara, K., Takechi, M., Ishikawa, M., "Interaction Between Alfvén Eingenmodes and Energetic Ions on Tokamaks," J. Plasma Fusion Res., **83**, 873 (2007) (in Japanese).

38) Suzuki, S., Enoeda, M., Matsuda, H., et al., "Numerical Evaluation of Crack Propagation of ITER First Wall with an Initial Interfacial Defect," Transactions of the Atomic Energy Society of Japan, **6**, 365 (2007) (in Japanese).

39) Suzuki, T., "Current profile control in advanced tokamak plasmas," J. Plasma Fusion Res., **83**, 434 (2007) (in Japanese).

40) Takahashi, Y., "How is the ITER Project Going on?," Chodendo Web 21 (Internet), 25 (2008) (in Japanese).

41) Takeda, N., Kakudate, S., Nakahira, M., et al., "Current Status of Research and Development on Remote

Maintenance for Fusion Components," J. Plasma Fusion Res., **84**, 100 (2008) (in Japanese).

42) Takemura, M., "My First stay in Provence in the South of France," FAPIG, 3 (2007) (in Japanese).

43) Takenaga, H., Morisaki, T., "Fuelling and Heat / Particle Control," J. Plasma Fusion Res., **83**, 453 (2007) (in Japanese).

44) Tobita, K., "Challenges in Technology for Attractive Fusion Energy," J. Inst. Electr. Eng. Jpn., **128**, 86 (2008) (in Japanese).

45) Urano, H., "Sun on the Earth," Enjinia Ring, 9 (2007) (in Japanese).

46) Urano, H., Matsumoto, T., Matsunaga, G., "Conference Report on "10th Plasma Research Workshop by Young Scientists" J. Plasma Fusion Res., **82**, 534 (2007) (in Japanese).

47) Ushigusa, K., Seki, M., Ninomiya, H., et al., "Research and Development of Nuclear Fusion," Genshiryoku Handbook, 906 (2007) (in Japanese).

48) Yamanishi, T., Iwai, Y., Isobe, K., et al., "Developments of Water Detritiation Systems in a Fusion Reactor," J. Plasma Fusion Res., **83**, 545 (2007) (in Japanese).

49) Yoshida, H., "The Trend of Fusion Energy Research and Development in the Participant Party and Countries in the ITER Project," Genshiryoku eye, **53**, 31 (2007) (in Japanese).

A.2 Organization of Fusion Research and Development Directorate

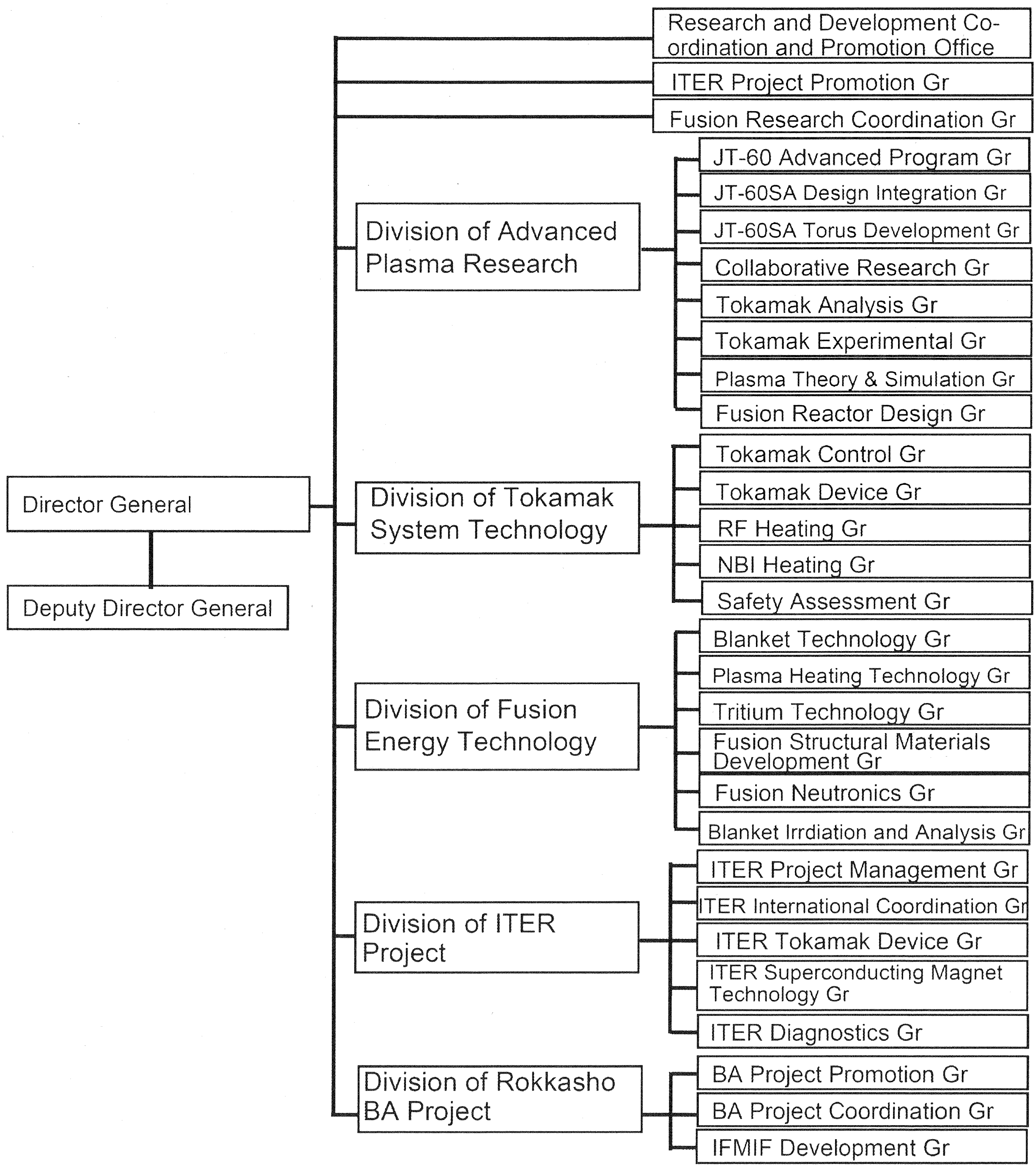

BA:Broader Approach

A.3 Personnel Data

A.3.1 Staff in Fusion Research and Development Directorate of JAEA

Fusion Research and Development Directorate

TSUNEMATSU Toshihide	(Director General)
NINOMIYA Hiromasa	(Deputy Director General)
OKUMURA Yoshikazu	(Deputy Director General)
NAGAMI Masayuki	(Supreme Researcher)
TANI Keiji	(Senior Principal Researcher)
YOSHIDA Hidetoshi	(Principal Researcher)
SEKI Masahiro	(Invited Researcher)
SEKI Shogo	(Invited Researcher)
SHIMOMURA Yasuo	(Invited Researcher)
MATSUI Hideki	(Invited Researcher)
KOHYAMA Akira	(Invited Researcher)
IDA Katsumi	(Invited Researcher)
KISHIMOTO Yasuaki	(Invited Researcher)

Research and Development Co-ordination and Promotion Office

NINOMIYA Hiromasa	(General Manager)	
WATANABE Tsutomu	(Deputy General Manager)	
GUNJI Masato	Hayashi Kazuyuki	KIMURA Shoko
KOYANAGI Daisaku	MATSUMOTO Hiroyuki	MORITA Hisao
NEMOTO Tetsuo	ONOZAKI Kazutoyo	SOGA Yoriko
TSUCHIDA Tatsuro	YOSHIDA Hiroshi	

ITER Project Promotion Group

SHIRAI Hiroshi	(Group Leader)
DOI Kenshin	OGAWA Toshihide

Fusion Research Coordination Group

USHIGUSA Kenkichi	(Group Leader)
ISEI Nobuaki	OOHARA Hiroshi

Division of Advanced Plasma Research

KIKUCHI Mitsuru	(Unit Manager)
OZEKI Takahisa	(Senior Principal Researcher)

JT-60 Advanced Program Group

KAMADA Yutaka	(Group Leader)
TAKENAGA Hidenobu	URANO Hajime

JT-60SA Design Integration Group

MATSUKAWA Makoto	(Group Leader)

YOSHIDA Kiyoshi	(Deputy Group Leader)	
KAWASHIMA Hisato	TSUCHIYA Katsuhiko	KIZU Kaname
TSUKAHARA Yoshimitsu	HOSHI Ryo (*4)	MATSUMURA Hiroshi (*4)
SUZUKI Yutaka (*17)	EDAYA Masahiro (*31)	SATO Fujio (*7)
KOMEDA Masao (*16)		

Collaborative Research Group

KOIDE Yoshihiko	(Group Leader)	
IDE Shunsuke	(Deputy Group Leader)	
HOSHINO Katsumichi	KAMIYA Kensaku	KONOSHIMA Shigeru (*1)

Tokamak Analysis Group

OZEKI Takahisa	(Group Leader)	
NAITO Osamu	(Deputy Group Leader)	
AIBA Nobuyuki (*23)	HAMAMATSU Kiyotaka	HAYASHI Nobuhiko
HONDA Mitsuru (*23)	KIYONO Kimihiro	KAMATA Isao (*24)
KOMINATO Toshiharu (*2)	SAKATA Shinya	SATO Minoru
SHIMIZU Katsuhiro	SUZUKI Mitsuhiro (*31)	TAKIZUKA Tomonori (*1)

Tokamak Experimental Group

ITAMI Kiyoshi	(Group Leader)	
ASAKURA Nobuyuki	(Deputy Group Leader)	
CHIBA Shinichi	FUJIMOTO Kayoko (*23)	HANAWA Osamu (*22)
HATAE Takaki	ISAYAMA Akihiko	KOIKE Tomonori (*22)
KITAMURA Shigeru	KOJIMA Atsushi (*23)	MATSUNAGA Go
MIYAMOTO Atsushi (*21)	NAKANO Tomohide	NUMATA Hiroyuki (*22)
OYAMA Naoyuki	SAKAMOTO Yoshiteru	SHINOHARA Kouji
SUNAOSHI Hidenori	SUZUKI Takahiro	TSUBOTA Naoaki (*21)
TSUTSUMI Kazuyoshi (*21)	UEHARA Kazuya (*1)	YOSHIDA Maiko (*25)

Plasma Theory & Simulation Group

TOKUDA Shinji	(Group Leader)	
IDOMURA Yasuhiro	ISHII Yasutomo	KAGEI Yasuhiro (*25)
LESUR Maxime (*3)	MATSUMOTO Taro	MIYATO Naoaki
SUZUKI Yoshio	TUDA Takashi (*1)	

Fusion Reactor Design Group

TOBITA Kenji	(Group Leader)	
NAKAMURA Yukiharu	KURITA Gen-ichi	NISHIO Satoshi

JT-60SA Torus Development Group

SAKASAI Akira	(Group Leader)	
HIGASHIJIMA Satoru	KASHIWA Yoshitoshi	MASAKI Kei
SAKURAI Shinji	SHIBAMA Yusuke	TAKECHI Manabu

Division of Tokamak System Technology

HOSOGANE Nobuyuki	(Unit Manager)	
YAMAMOTO Takumi	(Senior Principal Researcher)	
FUJII Tsuneyuki	(Senior Principal Researcher)	

Tokamak Control Group

KURIHARA Kenichi	(Group Leader)	
AKASAKA Hiromi	HOSOYAMA Hiromi (*8)	KAMIKAWA Masaaki (*10)
KAWAMATA Youichi	MATSUKAWA Tatsuya (*21)	OHMORI Yoshikazu
OKANO Jun	SATO Tomoki (*31)	SEIMIYA Munetaka (*1)
SHIBATA Kazuyuki (*22)	SHIMADA Katsuhiro	SUEOKA Michiharu
TERAKADO Hiroyuki (*7)	TERAKADO Tsunehisa	TOTSUKA Toshiyuki
YAMAUCHI Kunihito	WADA Kazuhiko (*22)	

Tokamak Device Group

SATO Masayasu	(Group Leader)	
ARAI Takashi	HAGA Saburo (*21)	ICHIGE Hisashi
ISHIGE Youichi (*22)	KAMINAGA Atsushi	MATSUZAWA Yukihiro (*21)
MIYO Yasuhiko	NISHIYAMA Tomokazu	OKANO Fuminori
SASAJIMA Tadayuki	SATO Yoji (*21)	SUZUKI Yozo (*4)
YAGYU Jun-ichi		

RF Heating Group

HOSOGANE Nobuyuki	(Group Leader)	
HIRANAI Shinichi	HASEGAWA Koichi	IGARASHI Koichi (*21)
KOBAYASHI Takayuki (*23)	MORIYAMA Shinichi	SATO Fumiaki (*21)
SAWAHATA Masayuki	SHIMONO Mitsugu	SUZUKI Sadaaki
SUZUKI Takashi (*22)	TERAKADO Masayuki	WADA Kenji (*21)
YOKOKURA Kenji		

NBI Heating Group

IKEDA Yoshitaka	(Group Leader)	
AKINO Noboru	EBISAWA Noboru	HANADA Masaya
HONDA Atsushi	KAMADA Masaki (*23)	KAWAI Mikito
KAZAWA Minoru	KIKUCHI Katsumi (*22)	KOBAYASHI Kaoru (*4)
KOMATA Masao	MOGAKI Kazuhiko	NOTO Katsuya (*21)
OOASA Kazumi	OSHIMA Katsumi (*21)	SASAKI Shunichi
SHIMIZU Tastuo (*21)	SHINOZAKI Shinichi	TAKENOUCHI Tadashi (*29)
TANAI Yutaka (*22)	USUI Katsutomi	

Safety Assessment Group

MIYA Naoyuki	(Group Leader)	
SUKEGAWA Atsuhiko	HAYASHI Takao	OIKAWA Akira (*1)

Division of Fusion Energy Technology

TAKATSU Hideyuki	(Unit Manager)
NISHITANI Takeo	(Senior Principal Researcher)

Blanket Technology Group

AKIBA Masato	(Group Leader)	
ENOEDA Mikio	EZATO Koichiro	HIROSE Takanori
HOMMA Takashi (*1)	MOHRI Kensuke (*12)	NISHI Hiroshi
SEKI Yohji (*23)	SUZUKI Satoshi	TANIGAWA Hisashi
TANZAWA Sadamitsu	TSURU Daigo	YOKOYAMA Kenji

Plasma Heating Group

SAKAMOTO Keishi	(Group Leader)	
INOUE Takashi	(Deputy Group Leader)	
DAIRAKU Masayuki	IKEDA Yukiharu	KASHIWAGI Mieko
KASUGAI Atsushi	KAJIWARA Ken (*25)	KOBAYASHI Noriyuki (*30)
KOMORI Shinji (*22)	OMINE Takashi (*31)	TAKAHASHI Koji
TAKESHIMA Yuichirou (*5)	TANIGUCHI Masaki	TOBARI Naoyuki (*25)
UMEDA Naotaka	WATANABE Kazuhiro	YAMAMOTO Masanori (*4)

Tritium Technology Group

YAMANISHI Toshihiko	(Group Leader)	
ARITA Tadaaki(*26)	HAYASHI Takumi	HOSHI Shuichi(*22)
INOMIYA Hiroshi(*22)	ISOBE Kanetsugu	IWAI Yasunori
KAWAMURA Yoshinori	KOBAYASHI Kazuhiro	NAKAMURA Hirofumi
SHU Wataru	SUZUKI Takumi	YAMADA Masayuki

Fusion Structural Materials Development Group

TAKATSU Hideyuki	(Group Leader)	
TANIGAWA Hiroyasu	(Deputy Group Leader)	
ANDO Masami	NOZAWA Takashi (*25)	OGIWARA Hiroyuki (*23)
SAWAHATA Atsushi (*5)	NAKATA Toshiya (*18)	

Fusion Neutronics Group

KONNO Chikara	(Group Leader))	
ABE Yuichi	IIDA Hiromasa (*1)	KAWABE Masaru (*22)
KUTSUKAKE Chuzo	OCHIAI Kentaro	OKADA Koichi (*28)
OHNISHI Seiki (*25)	SATO Satoshi	TAKAKURA Kosuke (*21)
TANAKA Shigeru		

Blanket Irradiation and Analysis Group

HAYASHI Kimio	(Group Leader)	
NAKAMICHI Masaru	HOSHINO Tsuyoshi	YONEHARA Kazuo (*9)
HASEGAWA Teiji (*22)	NAMEKAWA yoji (*22)	TSUCHIYA Kunihiko

Division of ITER Project

YOSHINO Ryuji		(Unit Manager)

ITER Project Management Group

KOIZUMI Koichi	(Group Leader)	
NEYATANI Yuzuru	(Deputy Group Leader)	
KITAZAWA Siniti	IWAMA Yasushi (*21)	SENGOKU Akio (*21)
KOIKE Kazuhisa (*21)	YAGUCHI Eiji (*13)	SATO Koichi (*31)
SATO Kazuyoshi	HIGUCHI Masahisa (*27)	

ITER International Coordination Group

MORI Masahiro	(Group Leader)	
ANDO Toshiro	(Deputy Group Leader)	
OIKAWA Toshihiro	ODAJIMA Kazuo (*1)	

ITER Tokamak Device Group

SHIBANUMA Kiyoshi	(Group Leader)	
KAKUDATE Satoshi	KOZAKA Hiroshi (*21)	MATSUMOTO Yasuhiro (*30)
TAGUCHI Kou (*22)	TAKEDA Nobukazu	

ITER Superconducting Magnet Technology Group

OKUNO Kiyoshi	(Group Leader)	
NAKAJIMA Hideo	(Deputy Group Leader)	
HAMADA Kazuya	HEMMI Tsutomu	ISONO Takaaki
KAWANO Katsumi	KOIZUMI Norikiyo	MATSUI Kunihiro
NABARA Yoshihiro	NAKAHIRA Masataka	NIIMI Kenichiro (*11)
NUNOYA Yoshihiko	OHMORI Junji (*30)	OKUI Yoshio (*14)
OSHIKIRI Masayuki (*22)	SEO Kazutaka (*19)	SHIMANE Hideo (*13)
SHIMIZU Tatuya (*13)	TAKAHASHI Yoshikazu	TAKANO Katsutoshi (*22)
TSUTSUMI Fumiaki (*31)		

ITER Diagnostics Group

KUSAMA Yoshinori	(Group Leader)	
FUJIEDA Hirobumi	HAYASHI Toshimitsu (*20)	ISHIKAWA Masao (*25)
KAJITA Shin (*25)	KAWANO Yasunori	KONDOH Takashi
OGAWA Hiroaki	SUGIE Tatsuo	TAKEI Nahoko (*23)
YAMAGUCHI Taiki (*23)	YAMAMOTO Tsuyoshi (*8)	

Division of Rokkasho BA Project

OKUMURA Yoshikazu	(Unit Manager)

BA Project Promotion Group

OHIRA Shigeru	(Group Leader)
EJIRI Shintaro	(Deputy Group Leader)

BA Project Coordination Group

OHIRA Shigeru	(Group Leader)	
TAKEMOTO Junpei (*10)		

IFMIF Development Group

OKUMURA Yoshikazu	(Group Leader)	
NAKAMURA Hiroo	(Deputy Group Leader)	
ASAHARA Hiroo(*21)	IDA Mizuho (*6)	MAEBARA Sunao
KIKUCHI Takayuki	KOJIMA Toshiyuki(*21)	KUBO Takashi (*15)
MIYASHITA Makoto (*30)	YONEMOTO Kazuhiro(*10)	

A.3.2 Staff in ITER Organization and Project Teams of the Broader Approach Activities

ITER Organization

Office of Director-General

MATSUMOTO Hiroshi	(Head)

Project Office

TADA Eisuke	(Head)

Department for Administration

IDE Toshiyuki

Department for Fusion Science & Technology

SHIMADA Michiya

Department for Central Engineering & Plant Support

MARUYAMA So

Project Teams of the Broader Approach Activities

International Fusion Energy Research Center

ARAKI Masanori	(Project Leader)

Satellite Tokamak Programme

ISHIDA Shinichi	(Project Leader)	
FUJITA Takaaki	KIMURA Haruyuki	OSHIMA Takayuki
SEKI Masami	TAMAI Hiroshi	

IFMIF EVEDA

SUGIMOTO Masayoshi	(Deputy Project Leader)
NAKAMURA Kazuyuki	SHINTO Katsuhiro(*25)

A.3.3 Collaborating Laboratories

Tokai Research and Development Center

Nuclear Science and Engineering Directorate

Irradiation Field Materials Research Group

JITSUKAWA Shiro	(Group Leader)	
FUJII Kimio	OKUBO Nariaki	TANIFUJI Takaaki
WAKAI Eiichi	YAMAKI Daiju	

Research Group for Corrosion Damage Mechanism

MIWA Yukio

Quantum Beam Science Directorate

Nanomaterials Synthesis Group

TAGUCHI Tomitsugu

Oarai Research and Development Center

Technology Development Department

MIYAKE Osamu	(Deputy Director)

Advanced Liquid Metal Technology Experiment Section

YOSHIDA Eiichi	(General Manager)
HIRAKAWA Yasushi	

Advanced Nuclear System Research and Development Directorate

Innovative Technology Group

ARA Kuniaski	(Group Leader)
OTAKE Masahiko	

*1	Contract Staff
*2	Customer System Co., Ltd.
*3	Ecole Polytechnique (France)
*4	Hitachi, Ltd.
*5	Ibaraki University
*6	Ishikawajima-Harima Heavy Industries Co., Ltd.
*7	JP HYTEC Co., Ltd.
*8	Japan EXpert Clone Corp.
*9	KAKEN Co., Ltd.
*10	Kandenko Co., Ltd.
*11	Kawasaki Heavy Industries, Ltd.
*12	Kawasaki Plant Systems, Ltd.
*13	KCS Corporation
*14	Kobe Steel, Ltd.
*15	Kumagai Gumi Co., Ltd.
*16	MAYEKAWA MFG. CO., LTD
*17	Mitsubishi Heavy Industries, Ltd.
*18	Muroran Institute of Technology
*19	National Institute for Fusion Science
*20	NEC Corporation
*21	Nippon Advanced Technology Co., Ltd.
*22	Nuclear Engineering Co., Ltd.
*23	Post-Doctoral Fellow
*25	Princeton Plasma Physics Laboratory (USA)
*24	Research Organization for Information Science & Technology
*25	Senior Post-Doctoral Fellow
*26	Sumitomo Heavy Industries, Ltd.
*27	The Japan Atomic Power Company
*28	Tohoku University
*29	Tomoe Shokai Co., Ltd.
*30	Toshiba Corporation
*31	Total Support Systems

This is a blank page.

国際単位系（SI）

表１．SI 基本単位

基本量	SI 基本単位	
	名称	記号
長さ	メートル	m
質量	キログラム	kg
時間	秒	s
電流	アンペア	A
熱力学温度	ケルビン	K
物質量	モル	mol
光度	カンデラ	cd

表２．基本単位を用いて表されるSI組立単位の例

組立量	SI 基本単位	
	名称	記号
面積	平方メートル	m^2
体積	立法メートル	m^3
速さ，速度	メートル毎秒	m/s
加速度	メートル毎秒毎秒	m/s^2
波数	毎メートル	m^{-1}
密度，質量密度	キログラム毎立方メートル	kg/m^3
面積密度	キログラム毎平方メートル	kg/m^2
比体積	立方メートル毎キログラム	m^3/kg
電流密度	アンペア毎平方メートル	A/m^2
磁界の強さ	アンペア毎メートル	A/m
量濃度 (a)，濃度	モル毎立方メートル	mol/m^3
質量濃度	キログラム毎立法メートル	kg/m^3
輝度	カンデラ毎平方メートル	cd/m^2
屈折率 (b)	（数字の）1	1
比透磁率 (b)	（数字の）1	1

(a) 量濃度（amount concentration）は臨床化学の分野では物質濃度（substance concentration）ともよばれる。
(b) これらは無次元量あるいは次元１をもつ量であるが、そのことを表す単位記号である数字の１は通常は表記しない。

表３．固有の名称と記号で表されるSI組立単位

組立量	SI 組立単位			
	名称	記号	他のSI単位による表し方	SI基本単位による表し方
平面角	ラジアン(b)	rad	1 (b)	m/m
立体角	ステラジアン(b)	sr(c)	1 (b)	m$^{2/}$m^2
周波数	ヘルツ (d)	Hz		s^{-1}
力	ニュートン	N		m kg s^{-2}
圧力，応力	パスカル	Pa	N/m^2	m^{-1} kg s^{-2}
エネルギー，仕事，熱量	ジュール	J	N m	m^2 kg s^{-2}
仕事率，工率，放射束	ワット	W	J/s	m^2 kg s^{-3}
電荷，電気量	クーロン	C		s A
電位差（電圧），起電力	ボルト	V	W/A	m^2 kg s^{-3} A^{-1}
静電容量	ファラド	F	C/V	m^{-2} kg^{-1} s^4 A^2
電気抵抗	オーム	Ω	V/A	m^2 kg s^{-3} A^{-2}
コンダクタンス	ジーメンス	S	A/V	m^{-2} kg^{-1} s^3 A^2
磁束	ウエーバ	Wb	Vs	m^2 kg s^{-2} A^{-1}
磁束密度	テスラ	T	Wb/m^2	kg s^{-2} A^{-1}
インダクタンス	ヘンリー	H	Wb/A	m^2 kg s^{-2} A^{-2}
セルシウス温度	セルシウス度(e)	℃		K
光束	ルーメン	lm	cd sr(c)	cd
照度	ルクス	lx	lm/m^2	m^{-2} cd
放射性核種の放射能 (f)	ベクレル (d)	Bq		s^{-1}
吸収線量, 比エネルギー分与, カーマ	グレイ	Gy	J/kg	m^2 s^{-2}
線量当量, 周辺線量当量, 方向性線量当量, 個人線量当量	シーベルト (g)	Sv	J/kg	m^2 s^{-2}
酸素活性	カタール	kat		s^{-1} mol

(a)SI接頭語は固有の名称と記号を持つ組立単位と組み合わせても使用できる。しかし接頭語を付した単位はもはやコヒーレントではない。
(b)ラジアンとステラジアンは数字の１に対する単位の特別な名称で、量についての情報をつたえるために使われる。実際には、使用する時には記号rad及びsrが用いられるが、習慣として組立単位としての記号である数字の１は明示されない。
(c)測光学ではステラジアンという名称と記号srを単位の表し方の中に、そのまま維持している。
(d)ヘルツは周期現象についてのみ、ベクレルは放射性核種の統計的過程についてのみ使用される。
(e)セルシウス度はケルビンの特別な名称で、セルシウス温度を表すために使用される。セルシウス度とケルビンの単位の大きさは同一である。したがって、温度差や温度間隔を表す数値はどちらの単位で表しても同じである。
(f)放射性核種の放射能（activity referred to a radionuclide）は、しばしば誤った用語で”radioactivity”と記される。
(g)単位シーベルト（PV,2002,70,205）についてはCIPM勧告2（CI-2002）を参照。

表４．単位の中に固有の名称と記号を含むSI組立単位の例

組立量	SI 組立単位		
	名称	記号	SI 基本単位による表し方
粘度	パスカル秒	Pa s	m^{-1} kg s^{-1}
力のモーメント	ニュートンメートル	N m	m^2 kg s^{-2}
表面張力	ニュートン毎メートル	N/m	kg s^{-2}
角速度	ラジアン毎秒	rad/s	m m^{-1} s^{-1}=s^{-1}
角加速度	ラジアン毎秒毎秒	rad/s^2	m m^{-1} s^{-2}=s^{-2}
熱流密度，放射照度	ワット毎平方メートル	W/m^2	kg s^{-3}
熱容量，エントロピー	ジュール毎ケルビン	J/K	m^2 kg s^{-2} K^{-1}
比熱容量，比エントロピー	ジュール毎キログラム毎ケルビン	J/(kg K)	m^2 s^{-2} K^{-1}
比エネルギー	ジュール毎キログラム	J/kg	m^2 s^{-2}
熱伝導率	ワット毎メートル毎ケルビン	W/(m K)	m kg s^{-3} K^{-1}
体積エネルギー	ジュール毎立方メートル	J/m^3	m^{-1} kg s^{-2}
電界の強さ	ボルト毎メートル	V/m	m kg s^{-3} A^{-1}
電荷密度	クーロン毎立方メートル	C/m^3	m^{-3} sA
表面電荷	クーロン毎平方メートル	C/m^2	m^{-2} sA
電束密度，電気変位	クーロン毎平方メートル	C/m^2	m^{-2} sA
誘電率	ファラド毎メートル	F/m	m^{-3} kg^{-1} s^4 A^2
透磁率	ヘンリー毎メートル	H/m	m kg s^{-2} A^{-2}
モルエネルギー	ジュール毎モル	J/mol	m^2 kg s^{-2} mol^{-1}
モルエントロピー, モル熱容量	ジュール毎モル毎ケルビン	J/(mol K)	m^2 kg s^{-2} K^{-1} mol^{-1}
照射線量（Ｘ線及びγ線）	クーロン毎キログラム	C/kg	kg^{-1} sA
吸収線量率	グレイ毎秒	Gy/s	m^2 s^{-3}
放射強度	ワット毎ステラジアン	W/sr	m^4 m^{-2} kg s^{-3}=m^2 kg s^{-3}
放射輝度	ワット毎平方メートル毎ステラジアン	W/(m^2 sr)	m^2 m^{-2} kg s^{-3}=kg s^{-3}
酵素活性濃度	カタール毎立方メートル	kat/m^3	m^{-3} s^{-1} mol

表５．SI 接頭語

乗数	接頭語	記号	乗数	接頭語	記号
10^{24}	ヨタ	Y	10^{-1}	デシ	d
10^{21}	ゼタ	Z	10^{-2}	センチ	c
10^{18}	エクサ	E	10^{-3}	ミリ	m
10^{15}	ペタ	P	10^{-6}	マイクロ	µ
10^{12}	テラ	T	10^{-9}	ナノ	n
10^{9}	ギガ	G	10^{-12}	ピコ	p
10^{6}	メガ	M	10^{-15}	フェムト	f
10^{3}	キロ	k	10^{-18}	アト	a
10^{2}	ヘクト	h	10^{-21}	ゼプト	z
10^{1}	デカ	da	10^{-24}	ヨクト	y

表６．SIに属さないが、SIと併用される単位

名称	記号	SI 単位による値
分	min	1 min=60s
時	h	1h =60 min=3600 s
日	d	1 d=24 h=86 400 s
度	°	1°=(π/180) rad
分	’	1’=(1/60)°=(π/10800) rad
秒	”	1”=(1/60)’=(π/648000) rad
ヘクタール	ha	1ha=1hm^2=10^{4}m^2
リットル	L，l	1L=11=1dm^3=10^{3}cm^3=10^{-3}m^3
トン	t	1t=10^3 kg

表７．SIに属さないが、SIと併用される単位で、SI単位で表される数値が実験的に得られるもの

名称	記号	SI 単位で表される数値
電子ボルト	eV	1eV=1.602 176 53(14)×10^{-19}J
ダルトン	Da	1Da=1.660 538 86(28)×10^{-27}kg
統一原子質量単位	u	1u=1 Da
天文単位	ua	1ua=1.495 978 706 91(6)×10^{11}m

表８．SIに属さないが、SIと併用されるその他の単位

名称	記号	SI 単位で表される数値
バール	bar	1 bar=0.1MPa=100kPa=10^{5}Pa
水銀柱ミリメートル	mmHg	1mmHg=133.322Pa
オングストローム	Å	1 Å=0.1nm=100pm=10^{-10}m
海里	M	1 M=1852m
バーン	b	1 b=100fm^2=(10^{-12}cm)2=10^{-28}m^2
ノット	kn	1 kn=(1852/3600)m/s
ネーパ	Np	SI単位との数値的な関係は、対数量の定義に依存。
ベル	B	
デジベル	dB	

表９．固有の名称をもつCGS組立単位

名称	記号	SI 単位で表される数値
エルグ	erg	1 erg=10^{-7} J
ダイン	dyn	1 dyn=10^{-5}N
ポアズ	P	1 P=1 dyn s cm^{-2}=0.1Pa s
ストークス	St	1 St =1cm^2 s^{-1}=10^{-4}m^2 s^{-1}
スチルブ	sb	1 sb =1cd cm^{-2}=10^{4}cd m^{-2}
フォト	ph	1 ph=1cd sr cm^{-2} 10^{4}lx
ガル	Gal	1 Gal =1cm s^{-2}=10^{-2}ms^{-2}
マクスウェル	Mx	1 Mx = 1G cm^2=10^{-8}Wb
ガウス	G	1 G =1Mx cm^{-2} =10^{-4}T
エルステッド (c)	Oe	1 Oe ≙ (10^3/4π)A m^{-1}

(c) ３元系のCGS単位系とSIでは直接比較できないため、等号「 ≙ 」は対応関係を示すものである。

表10．SIに属さないその他の単位の例

名称	記号	SI 単位で表される数値
キュリー	Ci	1 Ci=3.7×10^{10}Bq
レントゲン	R	1 R = 2.58×10^{-4}C/kg
ラド	rad	1 rad=1cGy=10^{-2}Gy
レム	rem	1 rem=1 cSv=10^{-2}Sv
ガンマ	γ	1 γ =1 nT=10-9T
フェルミ		1フェルミ=1 fm=10-15m
メートル系カラット		1メートル系カラット = 200 mg = 2×10-4kg
トル	Torr	1 Torr = (101 325/760) Pa
標準大気圧	atm	1 atm = 101 325 Pa
カロリー	cal	1cal=4.1858J（「15℃」カロリー），4.1868J（「IT」カロリー）4.184J（「熱化学」カロリー）
ミクロン	µ	1 µ =1µm=10^{-6}m

（第8版，2006年改訂）